SMHI

REPORT METEOROLOGY AND CLIMATOLOGY No. 114, 2011

Assessing and improving the Swedish forecast and information capabilities for ground-level ozone

Thomas Klein[1], Per-Erik Karlsson[2], Stefan Andersson[1], Magnuz Engardt[1], Karin Sjöberg[2]

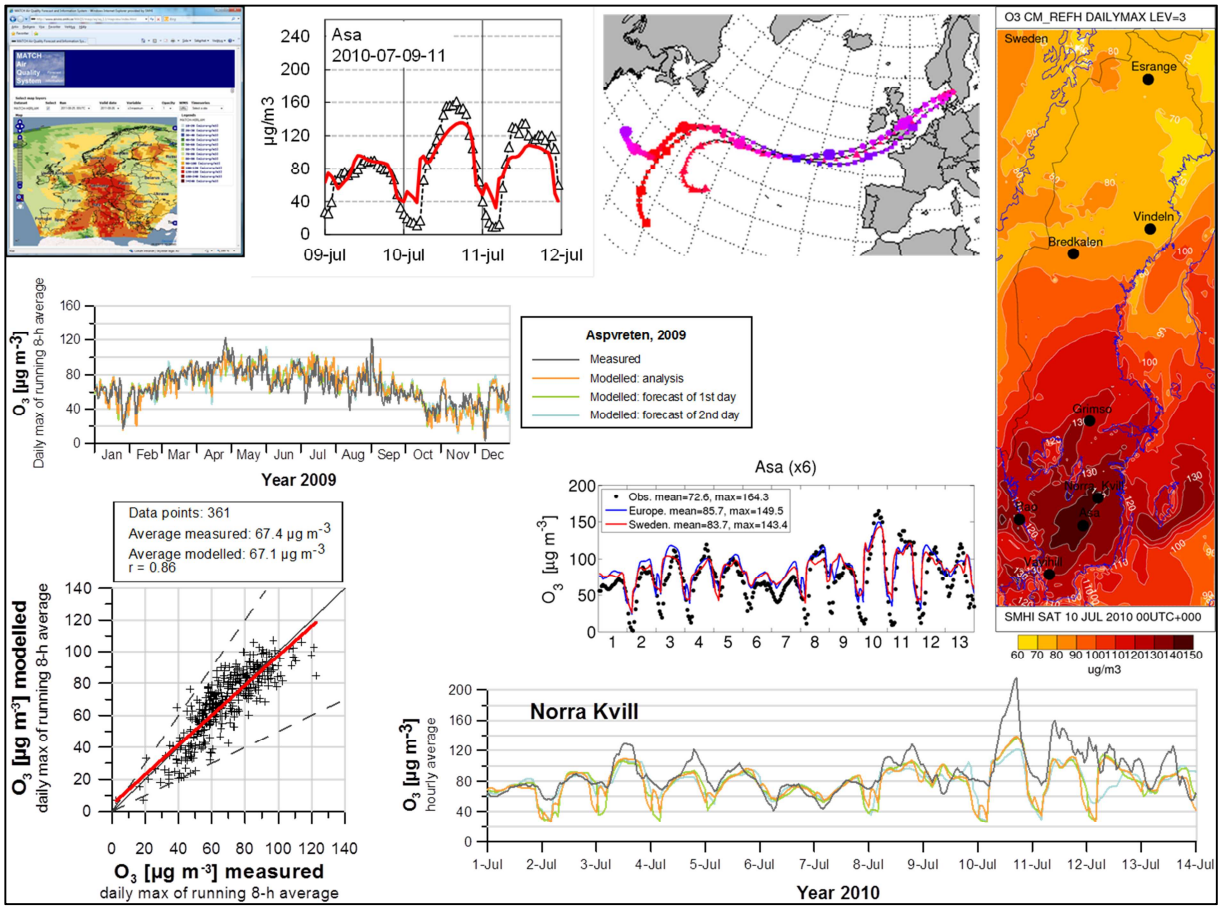

[1] Swedish Meteorological and Hydrological Institute
SE 601 76 Norrköping
Sweden

[2] IVL Swedish Environmental Research Institute
P.O. Box 5302
SE-400 14 Gothenburg
Sweden

Front:
The front picture is a collage of figures, representing different parts of the work carried out in this study.

ISSN: 0347-2116

REPORT METEOROLOGY AND CLIMATOLOGY No. 114, 2011

Assessing and improving the Swedish forecast and information capabilities for ground-level ozone

Thomas Klein[1], Per-Erik Karlsson[2], Stefan Andersson[1], Magnuz Engardt[1], Karin Sjöberg[2]

[1] Swedish Meteorological and Hydrological Institute
SE 601 76 Norrköping
Sweden

[2] IVL Swedish Environmental Research Institute
P.O. Box 5302
SE-400 14 Gothenburg
Sweden

Empty page

SUMMARY

This study aims to assess and improve the Swedish forecast and information capabilities for ground-level ozone concentrations in ambient air. The assessment is based on a set of archived results from the Swedish operational chemical transport model MATCH and Swedish in-situ measurements of ozone covering the period of May 2008 to November 2010. The evaluation comprises two major activities: The first activity is an analysis of the overall model performance using standard statistical metrics suitable for longer time series. The second evaluation activity comprises in-detail analyses of the specific ozone episodes occurring in Sweden during the study period. In addition, trajectory modelling is used to investigate the meteorological conditions and transport patterns associated with those episodes. The evaluation of the model results shows that the model scores well according to standard evaluation criteria and confirms results of other studies in that the model easily meets the data quality requirements of the EU air quality directive 2008/50/EC. However, from an operational forecasting and information perspective it would be desirable to further improve the prediction of, in particular, high-level ozone episodes. Two different activities in our study are dedicated to the task of improving the forecast and information capabilities: The first activity tests the usefulness of statistical post-processing of model results using regression techniques. The tests show promising results although the model performance during high-level ozone episodes is not improved. A limitation of our study is the relatively small archive of model data available for calibration and evaluation. Adaptive post-processing methods have not been tested in our study. The second activity aimed to improve ozone forecasting is a high-resolution model run for the year 2010. The higher resolution run gives slightly better results than the coarser operational model, which can be attributed to a better resolution of the physiography and thus certain physical and chemical processes. In particular, high-resolution simulations provide a more realistic representation of the spatial ozone variation which is desirable for environmental assessments with a longer time horizon. However, from the perspective of operational ozone forecasting the increase in resolution cannot correct systematic problems such as an under-prediction of ozone if the source of ozone is non-local and the long-range transboundary transport is not correctly described by the European-scale model used as boundaries. Other potential sources of error are incomplete or erroneous emissions, representativeness issues, oversimplifications in the model's physical or chemical processes, lacking data assimilation and initialization and oversimplified boundary conditions. While several of these issues are already addressed in current initiatives such as the EU FP7-project MACC, it is clear that further work will be needed during the coming years. Further work should also be invested in a better exploitation of the international developments within MACC and in the establishment of operational high-resolution air quality forecasts for Sweden, using boundary values from European-scale forecasts provided by the MACC-ensemble of regional air quality models.

Table of contents

1 Introduction

1.1 Background

Elevated concentrations of ground-level ozone (O_3) adversely affect public health. In addition, ground-level ozone can have negative effects on vegetation, ecosystems and the environment as a whole. According to an assessment of air pollution in Europe for the period of 1990-2004, the main air pollution human health issues in Europe are impacts of exposure to particulate matter and ozone, and to a lesser extent nitrogen dioxide (NO_2), sulphur dioxide (SO_2), lead and benzene and impacts of heavy metals and persistent organic pollutants (EEA, 2007). Considering ground level ozone, there is a multitude of short-term effects, comprising lung inflammatory reactions, adverse effects on respiratory symptoms, increase in medication usage, increase in hospital admissions and an increase in mortality as well as a long-term reduction in lung function development (WHO, 2004).

Substantial impacts of ambient ozone concentrations have been demonstrated for agricultural crops, trees and semi-natural vegetation for southern Sweden (Karlsson et al., 2009). Impacts range between 2% and 10% reductions for trees (leaf chlorophyll, tree growth) and up to 15% reductions for agricultural crops (yield, wheat/potato).

The occurrence of ozone concentrations in Sweden above northern hemispheric background concentrations depends strongly on the synoptic weather conditions. Connections between episodic high ozone concentrations over southern Sweden and synoptic weather conditions over the period 1990 – 2005 and air mass trajectories have been analysed by Tang et al. (2009a) and by Tang et al. (2009b), respectively. For the Swedish sites Rörvik/Råö, Norra Kvill and Vavihill about 75% to 85% of the ozone episode days (characterized as days with an 8-h moving average >60 ppb[1]) were observed under three so called Lamb weather type circulation patterns: anti-cyclonic flow, directional flow from east/southeast and directional flow from southwest/south. In their study, the authors find a probability of almost 20% for the occurrence of an ozone episode at Rörvik/Råö and Vavihill for a SE/E directional flow and probabilities of 10-15% for Rörvik/Råö, Vavihill and Norra Kvill under anti-cyclonic flow. The total vorticity index ζ, reflecting the intensity of synoptic circulation, is found to play a key role for the variation of ground-level ozone.

In Tang et al. (2009b) the long-range transport patterns associated with high-ozone events were classified into trajectories from WE (Western Europe), EE (Eastern Europe) and VIC (in the vicinity of southern Sweden), based on trajectory analysis by the FLEXTRA model (EMEP/NILU). Cluster VIC occurred more frequently during high-ozone events compared with cluster EE and WE: 43% at Rörvik/Råö, 45% at Vavihill and 42% at Aspvreten. The short and whirling trajectories in cluster VIC indicate a stagnant atmospheric situation with a stable air mass parking over the same region for a long time, usually associated with a persistent high-pressure system. In particular, the sub-cluster VIC_{we}, with air masses stagnating over Western Europe, was related to the highest ozone levels, both in terms of means and maxima. The influences of synoptic circulation on high-ozone events during spring seemed to be disturbed by perturbations from other processes. One of these perturbations might be stratospheric injection, which may become significant due to springtime maximum in upper level cyclogenesis (the development of mid-latitudes cyclone) and tropopause folding events.

Current EU legislation (EC, 2002; 2008) addresses the short-term effects of O_3 by defining a public information threshold (180 $\mu g/m^3$) and an alert threshold (240 $\mu g/m^3$) for the hourly average O_3 concentration in ambient air, advising national authorities to inform the public and give advice immediately after an exceedance of these thresholds. In addition, countries should report monthly on all exceedances. Another threshold explicitly stated in the ozone directive 2002/3/EC (EC, 2002) and

[1] In this report we use both ppb and $\mu g/m^3$ as units for atmospheric concentrations. The conversion between these units can be approximated as 2 $\mu g/m^3 \approx$ 1 ppb.

confirmed in the air quality directive 2008/50/EC (EC, 2008) is related to the limitation of long-term exposure and human health concerns. By 2010, the 8-hour average O_3 concentration should not exceed 120 $\mu g/m^3$ on more than 25 days per year. According to the ozone directive 2002/3/EC and the air quality directive 2008/50/EC, "up-to-date information on concentrations of O_3 in ambient air should be routinely made available to the public". In addition to measurements, which are mandatory in zones with exceedances of the long-term air quality objectives, three-dimensional chemical transport modelling provides a powerful complementary tool for both assessing and forecasting pollutant concentrations at larger scales. The ability to model atmospheric source and sink processes, transport and chemical conversions in a consistent way is especially useful for describing and forecasting pollutants such as O_3 which are subject to long-range transboundary transport. As a consequence, the existing Swedish forecasting and information capabilities are designed to respond to the above needs by means of two essential components: in-situ measurements of ozone, provided in near-realtime to the public by IVL on behalf of the Swedish Environmental Protection Agency, and operational model simulations using the SMHI chemical transport model MATCH ("Multiscale Atmospheric Transport and CHemistry model).

1.2 Objective of the study

The present study aims to assess and improve the existing Swedish forecast and information capabilities for ground-level ozone. Other pollutants, e.g. particulate matter, are not explicitly considered in the present study. In order to reach the objective of assessing and improving the forecast and information capabilities for ozone, four key tasks have been carried out:

- Evaluation of the overall model performance during May 2008 to November 2010: Using the available IVL in-situ measurements and archived model data from operational MATCH runs, the forecast capability of the model is thoroughly assessed. The evaluation uses standard statistical metrics (e.g., bias, correlation, RMSE) as well as performance criteria for the prediction of specific thresholds.
- Analyses of episodes with high ozone values in Sweden: The study comprises in-detail evaluations of the model performance during all episodes occurring during the above study period. In addition, trajectory calculations are used to assess the meteorological conditions and transport patterns leading to the specific episodes and to explain the MATCH-model's performance.
- Statistical post-processing of model results: This activity aims to test the usefulness of statistical post-processing methods for the improvement of the dynamical model products generated by MATCH. Standard output from model runs is combined with in-situ measurements to derive tailored predictions for the sites of the measurements. In addition, the use of other (mainly meteorological) predictors is tested.
- Assessment of the importance of high-resolution modelling: Too coarse resolution is often quoted as an explanation for underperformance of air quality models. This activity is aimed to investigate to what extent high-resolution modelling can improve the prediction of ozone episodes. For this study, a high-resolution model run with a four times better resolution than the operational model runs has been performed for the complete period of 2010.

1.3 Outline of this report

Section 2 of this report provides a short description of the available ozone monitoring sites and the MATCH-model and its operational setup. The methods for trajectory analyses, verification, statistical post-processing and dynamical downscaling are described in Section 3. In Section 4 the results of the four key activities are presented and discussed. Section 5 comprises a summary of our key findings, conclusions and suggestions for further work. For reference, we include most of the material produced and analysed in our study as appendix.

2 Swedish Ozone Forecast and Information Capabilities

2.1 In-situ measurements

Ozone concentrations over Sweden are routinely measured on an hourly basis at 5 m above ground within the national ozone monitoring network. These monitoring sites are also part of the European Monitoring and Evaluation Programme (EMEP). In this study, we also use ozone monitoring data from the EMEP site Prestebakke in south-east Norway, close to the Swedish border. In addition, hourly ozone concentrations are measured by IVL at Östad Säteri and by SLU at Asa experimental forest. The routines for these measurements are similar to those used within the national ozone monitoring network. Furthermore, ozone concentrations are measured by Stockholm and Uppsala county administrations at Norr Malma, approximately 50 km northeast of Stockholm. Ozone measurements in Gothenburg at "Femman" are positioned approximately 30 m above ground and operated by the Environmental Administration in the City of Gothenburg. The positions of the different monitoring sites used in this study are indicated in Figure 2.1.

Figure 2.1: *A map illustrating the positions for the monitoring sites with hourly ozone concentration measurements with instruments. Blue symbols indicate monitoring sites within the Swedish national ozone monitoring network and are part of the European Monitoring and Evaluation Programme (EMEP, data available at www.ivl.se). Prestebakke is part of the Norwegian national ozone monitoring network and also part of EMEP. Norr Malma (yellow symbol) is part of Stockholm and Uppsala County air quality management association (data available at slb.nu/lvf) and Asa (red) is an experimental forest and research station of the Swedish University of Agricultural Sciences in co-operation with the regional air quality protection associations in Kronoberg and Jönköping County (asa.esf.slu.se). Östad (red) is operated during Apr – Sept by IVL and supported by the County administration of Västra Götaland as well as the Swedish Environmental Protection Agency. Ozone measurements at Gothenburg at "Femman" (grey) are positioned approximately 30 m above ground and operated by the Environmental Administration in the City of Gothenburg.*

The legends used in the presentation of hourly ozone concentrations in different parts of Sweden during the episodes are shown in Figure 2.2. To enable comparison, the ozone concentrations for Vavihill are shown in the diagrams for all parts of Sweden.

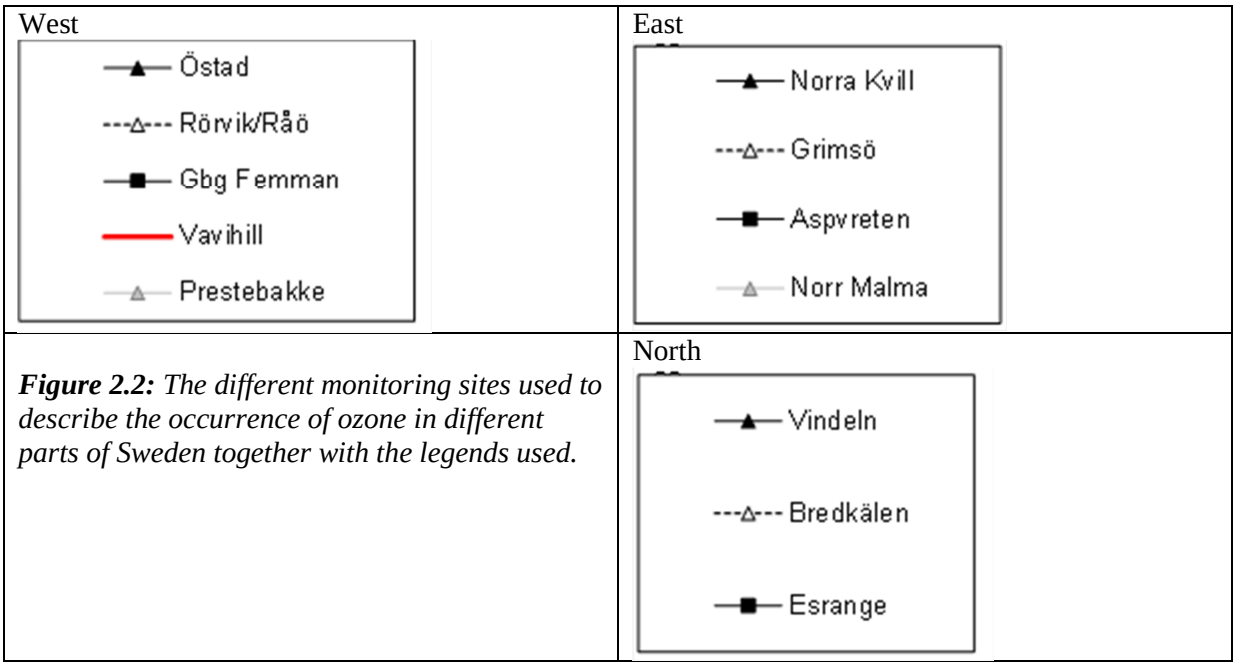

Figure 2.2: *The different monitoring sites used to describe the occurrence of ozone in different parts of Sweden together with the legends used.*

2.2 The MATCH Air Quality Forecast and Information System

2.2.1 The MATCH-model

MATCH (Multiple-scale Atmospheric Transport and Chemistry modelling system) is an Eulerian three-dimensional chemical transport model. It is a flexible system aimed at describing the distribution of air pollution given relevant meteorology and emission inventory. The meteorology can consist of meteorological analyses, utilizing observations to reproduce a historical (or the present) situation, or forecasted meteorology, simulating the likely evolution of the weather over the next few days. At SMHI, weather forecasts from the global ECMWF model and from the SMHI limited area model HIRLAM are operationally available for MATCH (see also Section 2.2.2). The emission inventory used by MATCH, contains information on the magnitude and distribution of the atmospheric emissions of species relevant for the air quality simulations.

MATCH includes modules to handle the emission, chemical and physical transformation, transport, mixing and deposition of a number of species. A thorough description of the core system can be found in e.g. Robertson et al. (1999) while more recent features such as the photochemical scheme used in MATCH can be found in e.g., Andersson et al. (2007) and van Loon et al. (2007). The advection-scheme is based on Bott (1989), using fourth-order scheme in the horizontal and a second-order scheme in the vertical. MATCH has been used extensively to study ozone in Europe and elsewhere, but also for the simulation of many other species at a broad range of scales [e.g. Langner et al. (1998a), Gidhagen et al. (2005), Langner et al. (2005); Engardt et al. (2005); Persson and Kahnert (2006)].

2.2.2 Operational system

SMHI currently operates two European-scale air quality forecast systems that produce forecasts of tropospheric ozone for two or three days, respectively. Both systems use very similar versions of MATCH, with nearly identical chemical and deposition schemes, and operate at comparable spatial resolutions. The main difference between the configurations lies in the driving meteorological data, the emission inventory and the boundary concentrations utilized for the simulations. A summary of the two systems' key features is given in Table 2.1.

Table 2.1: *The two operational MATCH-configurations currently used for SMHI's air quality forecasting systems.*

	MATCH-HIRLAM	MATCH-ECMWF
Meteorological driver	HIRLAM-22	ECMWF global model
Horizontal resolution	0.4°×0.4°	0.5°×0.5°, 0.2°×0.2°[2]
Vertical resolution	22 layers up to ca. 450 hPa	40 layers up to ca. 220 hPa
Emissions	EMEP	MACC
Boundary concentrations	Static climatological values with monthly variation	From a global CTM; values are updated every 6 hours
Data assimilation, initial conditions	No	Under development
Forecast length	+48 hours	+72 hours

Further information can be found at the MATCH Air Quality Forecast and Information (MAQS) site (MAQS, 2011) or in the final report of a previous SMHI-IVL collaboration project on ozone (Engardt et al., 2009). The MATCH-ECMWF system is run operationally at the European Centre for Medium Range Weather Forecast (ECMWF) as part of the ensemble of regional air quality models in the framework of the EU FP7-project MACC (Monitoring Atmospheric Composition and Climate). The MACC-project aims specifically at the implementation of Global and European-scale atmospheric core services for the joint EU/ESA-initiative GMES (Global Monitoring for Environment and Security), see MACC (2011) and GMES (2011) for further information. While MATCH-HIRLAM already had been in semi-operational mode for several years, it was decided to build the independent system MATCH-ECMWF specifically for the MACC-project in order to benefit from collaborative research and development on data assimilation, model initializations and emissions, including satellite-based compilations of near real-time of emissions from forest fires. Until the MACC-services are fully developed, the MATCH-HIRLAM system will be operated in its current setup, i.e. as a stand-alone system for the area of Europe with a resolution comparable to MATCH-ECMWF. In the longer term, these two systems should be integrated to deliver a full chain of operational services from the global down to the national and potentially sub-national scale. MATCH-HIRLAM could be run operationally at high resolution for the area of Sweden (see also Section 3.4 and Section 4.4 of the present report), using boundary values from the European-scale system MATCH-ECMWF which in turn is driven by a global chemical transport model operated within the GMES-initiative. However, nesting MATCH-HIRLAM into MATCH-ECMWF will require some development work. Furthermore, the operation of a high-resolution MATCH-HIRLAM will result in the need for additional computational resources. As of today, the (less resource-intensive) operational MATCH-HIRLAM simulations lack a robust long-term funding and are mainly a result of a suite of different research projects. As a consequence, the migration to an even more resource-intensive configuration has been postponed several times. However, a major upgrade of the system is scheduled for 2011-2013 in connection with a new project aimed at the development of an operational Swedish warning capability for heat waves and air pollution episodes, funded by the Swedish Civil Contingencies Agency (MSB).

For the present study we use archived operational forecasts performed by MATCH-HIRLAM and evaluate and further improve the forecasts for Sweden. The following text describes specific features of MATCH-HIRLAM in more detail.

MATCH-HIRLAM uses anthropogenic emissions of ammonia (NH_3), NO_x, SO_x, non-methane volatile organic compounds (NMVOC) and CO (and natural emissions of SO_x) taken from the EMEP web-page (50km x 50km resolution; valid for 2003) and regridded to the MATCH domain (0.4°x0.4° resolution, rotated lat-lon grid). Biogenic emissions of isoprene are calculated internally according to the E-94 methodology proposed by Simpson et al. (1995). MATCH-HIRLAM uses dry

[2] The resolution of MATCH-ECMWF was increased to 0.2°×0.2° in early 2011. The previous version with the coarser resolution of 0.5°×0.5° is still maintained for comparison but will be phased out in the near future.

deposition of gaseous and particulate matter based on a resistance approach depending on land-use (Water, Forest, Low vegetation and "No vegetation"). The dry deposition flux is proportional to the concentration of each component and the inverse of the sum of the aerodynamic resistance and a species specific surface resistance. For species with stomatal uptake as a significant deposition route (such as ozone), surface resistance is calculated taking into account soil moisture, soil type, vegetation type, leaf area index, photosynthetic active radiation and temperature. For other species a simpler approach is used with only monthly varying surface resistances. For O_3, NO_2, SO_2 and NH_3 the surface resistances are decreased when snow cover occurs (given by the meteorological model HIRLAM).

For most species, wet scavenging is assumed to be proportional to the precipitation intensity at the surface and a species-specific scavenging coefficient. For O_3, hydrogen peroxide (H_2O_2) and SO_2, in-cloud scavenging is calculated by assuming Henry's law equilibrium; subcloud scavenging is neglected for these species. All particulate sulphate inside clouds is assumed to be dissolved in cloud droplets; in-cloud scavenging is proportional to the fraction of the cloud water that hits the ground as precipitation. Sub-cloud scavenging for sulphate is calculated as in Berge (1993).

The photochemistry scheme proposed by Simpson et al. (1993) is used with some modifications and updates; the most notable being a modified production mechanism for isoprene chemistry, based on the so-called Carter-1 scheme (Carter, 1996; Langner et al., 1998b). The photochemical scheme includes 60 chemical components. The lateral boundary concentrations are deduced from a combination of observations at background locations and large-scale model calculations. The boundaries are changed seasonally or monthly. The values are largely as in Andersson et al. (2007).

In MATCH-HIRLAM, the air quality model is driven by three-dimensional meteorological data from SMHI's operational numerical weather forecast model (HIRLAM), which runs 4 times a day. The MATCH-HIRLAM simulations are performed on a daily basis, starting ca. 03.00 each night. The model runs consist of a hindcast of the previous day and forecasts for the present and next day. Weather data from the analysis (based on meteorological observations; available every 6 hours) and 6 hour HIRLAM-forecasts are used for the hindcast. The two air quality forecast days are calculated from the operational 48 hour HIRLAM-forecasts starting at 00 UTC, see Figure 2.3. Since each air quality simulation is stored, each day is covered three times, i.e. by the analysis (An), the one-day forecast (d1) and the two-day forecast (d2), see Figure 2.3. In Section 4.1 we will study the difference between An, d1 and d1, which mainly emanates from whether the meteorology used is from the analysis or the one- or two-day weather forecast.

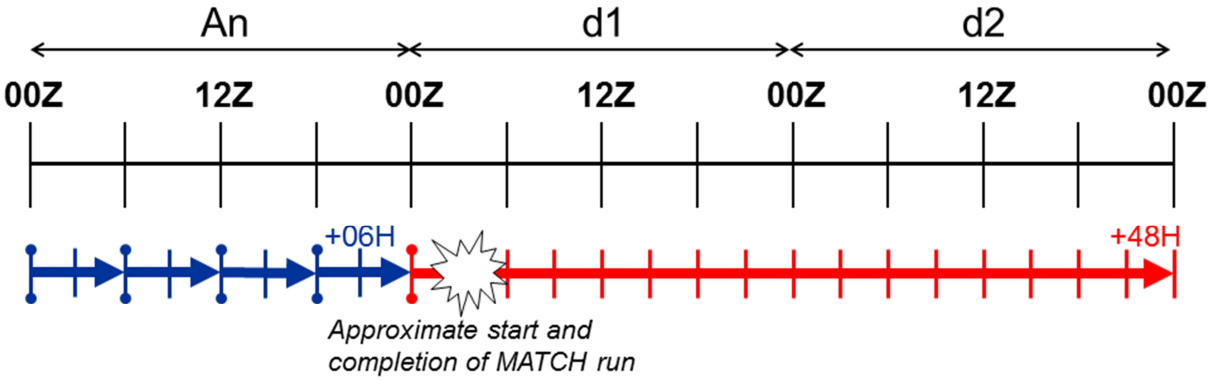

Figure 2.3: *Time period covered by each MAQS simulation (a 24h hindcast plus a 48h forecast). The hindcast is driven by analyses every 6 hours together with 6h HIRLAM forecasts. The MATCH forecast is based on the complete 48h forecasted initiated 00Z.*

3 Methods

3.1 Trajectory analysis

Backward trajectory analysis is a valuable tool for determining the transport patterns of air parcels arriving at particular locations at a specific time and provides a useful means of establishing source-receptor relationships of air pollutants. In this study, the backward trajectories were calculated by the FLEXTRA trajectory model (e.g. FLEXPART, 2011; Stohl et al., 1999).

FLEXTRA trajectory plots are created operationally by the Norwegian Institute for Air Research (NILU) four times a day for each location. Each trajectory spans 7 days in time. There are 3 trajectories in each plot with three different heights at arrival. Height above sea level at arrival is indicated by the legends in the upper right corner of each plot. Height along the trajectories is indicated by colour (colour/height scale in the lower left corner of the plot). Each 3-hour interval along the trajectory path is indicated by a small legend, each 24-hour interval by a big legend (see Figure 3.1).

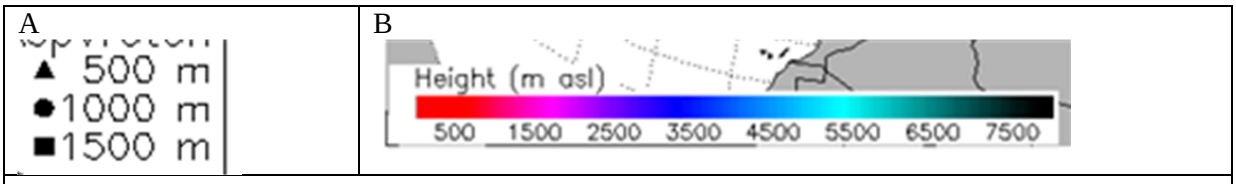

Figure 3.1: *Specification for the different legend used in the illustrations of trajectories calculated by the FLEXTRA model. A, Symbols specifying the height of the specific air mass upon arrival to the site; B, Color identification of the elevation of a certain air mass during transport.*

In addition to the FLEXTRA-trajectories computed operationally by NILU specific trajectory-simulations have been performed for the current project with the NOAA HYSPLIT-model (HYSPLIT, 2011). The comparison of HYSPLIT-trajectories and FLEXTRA-trajectories showed a good agreement between the two trajectory models. In our discussion we thus concentrate on the operational FLEXTRA-trajectories and provide examples of HYSPLIT-simulations only where they provide additional value.

3.2 Verification statistics

Comparing modelled and measured concentrations requires the use of appropriate verification statistics. Traditional statistics like correlation coefficient, bias and root mean square error will be used in this study, as well as evaluation of the model's ability to reproduce concentrations in terms of annual average, daily maximum of 8h-running average and AOT40 (in accordance with the standards). The requirements of model calculations according to the EU air quality directive (EC, 2008; Denby et al., 2010) will not be evaluated in detail within this study. In a previous study it was concluded that the MATCH model meets these demands for ozone in regional background (Engardt et al., 2010a).

There are, however, other useful verification statistic and scores to be used when validating model calculations and forecasts (US-EPA, 2003; Wilks, 2006). One simple and effective method is a two category forecast. The first step is to create a contingency table (frequency table), see Figure 3.2. For a given threshold value there are four possible options; a, b, c and d, where a and d indicate correct "hits".

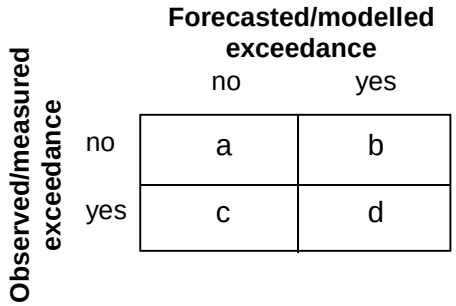

Figure 3.2: *Contingency table for a two-category forecast for a certain given threshold value.*

From this contingency table it is possible to create scores, each one evaluating the model performance in a unique way. The scores that will be used within this study are summarized in Table 3.1.

Table 3.1: *Verification statistics (scores) used to evaluate two-category forecasts (after US-EPA, 2003).*

Statistics name	What it measures	Equation	How to interpret
(A) Accuracy	Percent of forecast that correctly predicted the event or non-event	A = (a + d) /N * 100	Higher values are better
(B) Bias	Indicates, on average, if the forecast are under- or overpredicted	B = (b + d)/(c + d)	Values closer to 1 are best
(FAR) False Alarm Rate	The percent of times a forecast of high pollution did not actually occur	FAR = b/(b + d) * 100	Smaller values are best
(CSI) Critical Success Index	How well the high-pollution events were predicted. Useful for rarer events like high-pollution days. It is not affected by a large number of correctly forecasted, low-pollution events	CSI = d/(b+c+d) * 100	Higher values are best
(POD) Probability of Detection	Ability to predict high-pollution events (i.e., the percentage of forecasted high-pollution events that actually occurred)	POD = d/(c + d) * 100	Higher values are best

3.3 Statistical post-processing at sites

In order to improve the modelled concentrations of ozone, two approaches are applied in this study; post-processing of model results by multiple linear regression and improvements by performing high-resolution modelling (see Section 3.4). For this study we choose multiple linear regression because it is a well-approved methodology in traditional Numerical Weather Prediction, but also a useful tool in air quality modelling.

Model Output Statistics (MOS) is basically multiple linear regression, which is the more general situation of linear regression. Multiple linear regression has, in consistence with simple regression,

only one predictand (y), but in distinction there is more than one predictor (x). In our case the predictor variables are ozone measurements and other parameters including meteorology (for example temperature, humidity, wind etc.).

Let *J* donate the number of predictor variables. The multiple linear regression formula becomes:

$$\hat{y} = \sum_{j=0}^{J} b_j x_j = b_0 + b_1 x_1 + b_2 x_2 + ... + b_J x_J \quad (1)$$

The linear regression coefficients b_j in equation (1) are determined by minimizing the sum of square of the errors. This minimization is usually done using matrix algebra, in practice often using statistical software. In this study we use the R tool for statistical computing (http://www.r-project.org) and the measurement dataset, i.e. ozone 1h-mean concentrations during 2008-2010, are divided into two parts; one part which is used for the regression as a training dataset (i.e. dependent dataset) and another part which is used as a validation dataset (i.e. independent dataset).

There are some conditions which have to be achieved in order for a MOS system to run optimally (Kalney, 2003):

- Training period should be as long as possible (at least several years).
- The model-based forecasting system should be kept unchanged to the maximum extent as possible during the training period.
- After training, the MOS system should be applied to future model forecasts that also use the same unchanged model system.

If the conditions above are satisfied, MOS has many advantages since it objectively interprets the model output and produces the best site-specific linear prediction, thus improves the correlation and removes systematic biases. For the MATCH-model ozone forecasting system in this study most of the conditions above are fulfilled. However, measurements covering only 1-2 years are used as training data set, in order to have a large enough portion of data for evaluation. It is likely that a longer record with consistent model data and measurements would improve the performance of the statistical post-processing technique.

Other methods such as classification and regression tree (CART) or iterative methods such as Kalman-filtering may be tested in potential follow-up projects. For more details regarding MOS and multiple linear regression, see, for example, Kalney (2003) and Wilks (2006).

3.4 Downscaling of European-scale MATCH-simulations

To further investigate whether it is possible to improve the modelling results over Sweden, we employ a chain of nested air quality models. This enables us to run on higher resolution, use a more detailed emission inventory and a more precise land-surface classification over Sweden (see Figure 3.3).

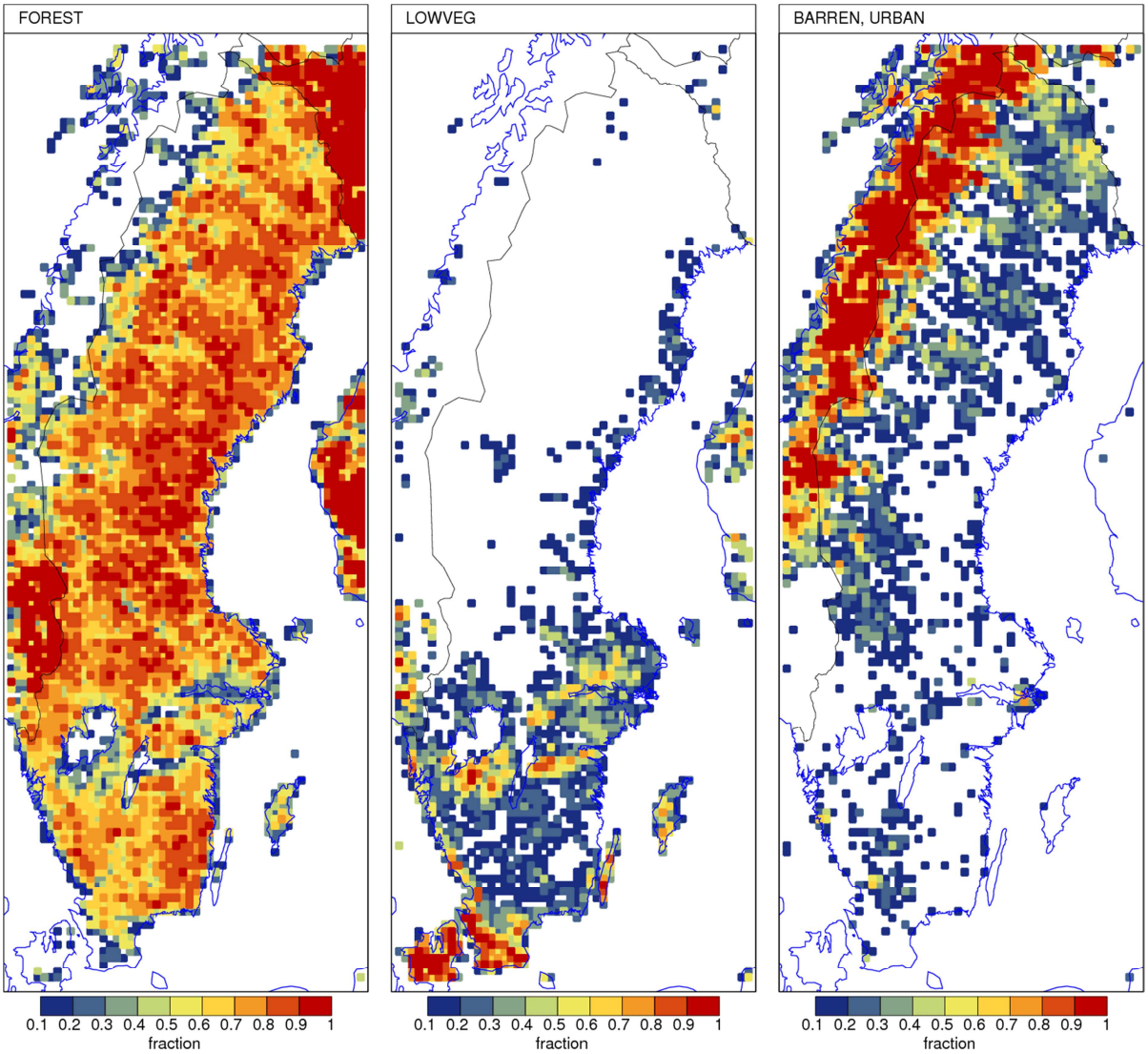

Figure 3.3: *MATCH-SWE modelling domain. The panels show fractions of forest, low vegetation and barren land (including urban areas).*

The inner model (MATCH-SWE) runs on 11 km horizontal resolution while the vertical configuration is kept identical as in the outer model to enable straightforward passing of concentrations from one model to the next. For the outer model we use archived model runs from the operational MATCH-HIRLAM system described in Section 2.2.2. The boundary concentrations of the inner model are taken from the outer model at regular intervals. Depending on the tracer's chemical lifetime, and importance for O_3 chemistry, different species are updated with different intervals. O_3 is updated hourly, which means that ozone generated outside the inner domain will flow into the high resolution domain at the right time and location. Other species are updated every 6 hours or every 24 hour, some species are only updated monthly, yielding quasi-static boundary concentrations.

The European and the Swedish setup both use the same meteorological driver, namely the analyses from HIRLAM-22 (see Section 2.2.2). While higher resolution meteorological data are available at SMHI (e.g. HIRLAM runs with 11km or 5km grid spacing), it was decided to use the same meteorology for this study and to focus on the impact of physiography and emission data for the simulations. For both the standard MATCH-HIRLAM runs (in our comparison in the present section called MATCH-EU) and MATCH-SWE, the meteorology is interpolated from the 22 km HIRLAM horizontal resolution to the resolution of the respective air quality model. The high-resolution Swedish simulation utilizes an emission inventory taken from SMED (Swedish Environmental Emissions Data)

for Sweden and MACC/GEMS for areas outside Sweden (including shipping). The annual totals in Sweden represent the emissions in 2007.

For this study we run MATCH-SWE for one year (2010) and compare whether the statistical scores are improved compared to the coarse resolution simulations (MATCH-EU), and if the ozone episodes during the summer of 2010 are reproduced better than in the European-scale model setup. The high resolution simulation runs in a continuous mode from 1 January 2010 to 1 January 2011, while the coarse resolution simulations are restarted every day. However, as all concentrations in the European-scale run are loaded from the previous day's model run; this data series also represents a consistent series of air quality data and the difference should not affect our comparison (this was also tested in previous intercomparisons, e.g. Engardt et al. 2009). As the high-resolution study is performed in a continuous mode based on meteorological analyses we will only evaluate the performance of the European-scale and Sweden-specific setups for the analyses. A discussion of the forecast quality of MATCH-analysis compared to the day 1 and day 2 forecasts is given in Section 4.1.

In this setup we use MATCH-HIRLAM as the large scale model, which works with climatological tracer boundaries far away from Europe. As pointed out in Section 2.2.2, a long-term goal is to establish a full chain of nested air quality models through the use of MATCH-ECMWF as boundary conditions for the high-resolution Swedish application. As MATCH-ECMWF uses boundaries from a global tracer model this would complete the chain of nested models.

The SMHI-IVL expert-team tasked with the present project also had a joint seminar with scientists from Gothenburg University (Håkan Plejel and Jenny Klingberg) in order to discuss the possibility to use predictors such as orography or relative orography (e.g. based on the Aster or SRTM digital elevation models) in further downscaling steps. As this is still an ongoing work, it was not possible to directly include the method proposed by Klingberg et al. (2011) within the scope of the present project and it is thus recommended that future projects further explore this idea.

4 Results

4.1 MATCH model evaluation for June 2008 to November 2010

The temporal variation of the daily maximum of the running 8h-mean concentrations of ground-level ozone for 2008, 2009 and January-September 2010 is shown in Figure 4.1 for the sites Vavihill (southern Sweden) and Norra Kvill (south eastern Sweden). Both measured and modelled concentrations are included in the plots. Additional figures with measured and simulated ozone concentrations for all monitoring stations included in the study (Table 4.1) are provided in Appendix 8.1.

The concentrations of ozone show a distinct seasonal variation. In general, the concentrations are highest in spring and summer mainly due to the importance of solar radiation for the production of ozone. During the evaluated time period, a few episodes occurred with concentrations exceeding 140 $\mu g\ m^{-3}$; these occasions are analysed in more detail in Section 4.2. From Figure 4.1 it can be concluded that 2010 is the year with the highest concentrations of ozone due to some episodes in June and July (with the highest concentrations at Norra Kvill on July 10). However, these episodes can only be observed at the sites Grimsö, Norra Kvill, Asa and Vavihill (see Appendix 8.1), i.e. in the southern and south eastern part of Sweden.

The comparison of measured and modelled daily maximum of running 8h-mean concentrations of ozone in Figure 4.1 and Appendix 8.1 shows that the model performance is good. Overall, the magnitude and the seasonal variation of concentrations are reproduced well. Hence, the correlation of modelled and measured concentrations is strong (especially for 2008 and 2009), regarding both northern and southern Sweden. However, during the ozone episodes with the highest concentrations, the MATCH-model somewhat underestimates the concentrations (for instance, during the episode on July 10 2010 at Norra Kvill the model calculations give a maximum of hourly concentrations of 133 $\mu g\ m^{-3}$ whereas the measurements indicate a maximum of 187 $\mu g\ m^{-3}$). The reason for this might be that some emissions of ozone producing compounds are not included in the calculations, for example biomass burning as well as some anthropogenic emissions in Eastern Europe.

Modelled concentrations in Figure 4.1 are provided for analysis as well as forecasts of 1st day and 2nd day, respectively. The forecast skill decreases only marginally with time during the first two days, and the differences between analysis and the forecasts are generally small.

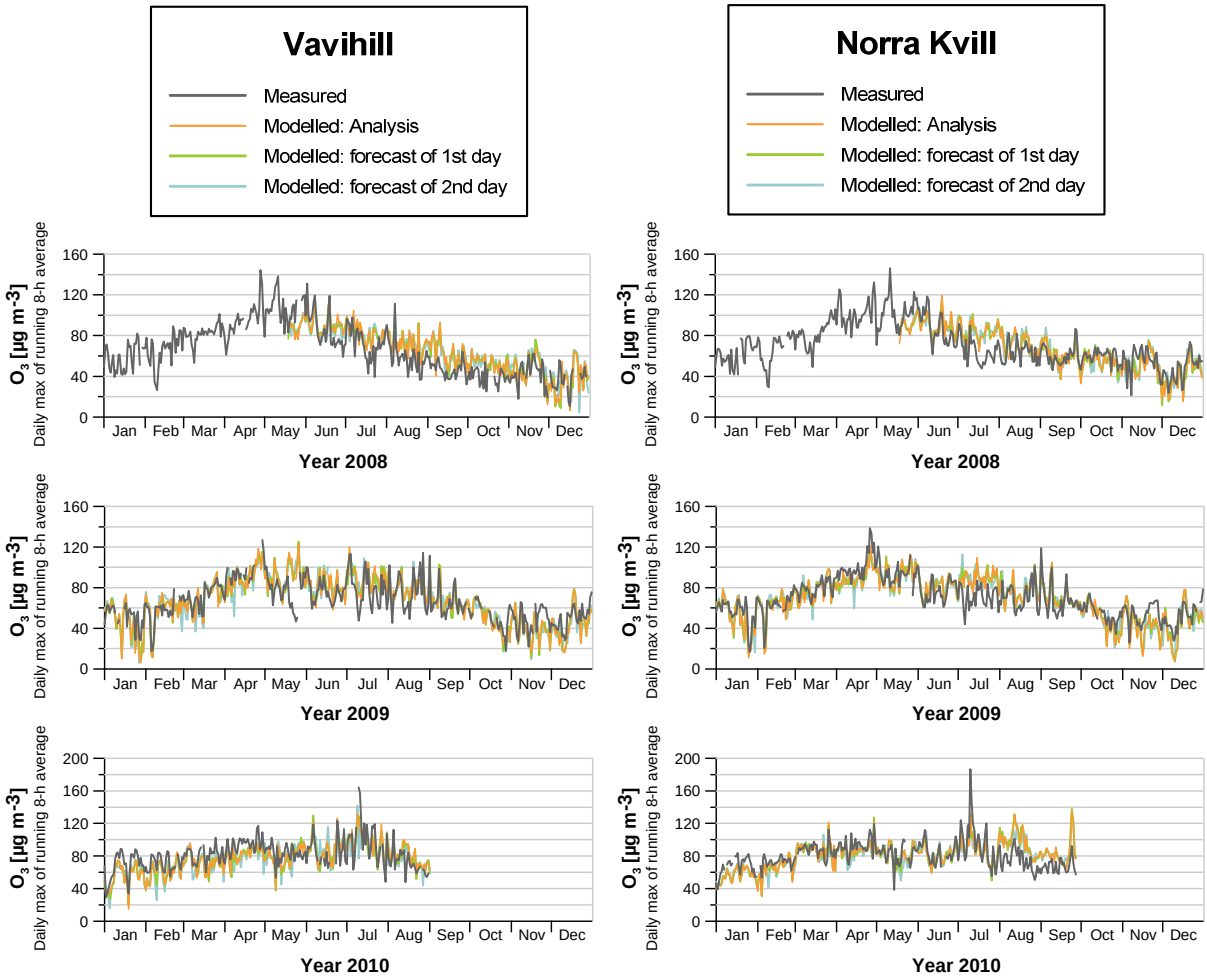

Figure 4.1: *Comparison between measured and modelled daily maximum of 8h-mean concentration of ozone for the years 2008, 2009 and 2010 at two sites; Vavihill in southern Sweden (left hand side) and Norra Kvill in south eastern Sweden (right hand side). For modelled concentrations, the results are shown, respectively, for analysis, forecast of 1st day and forecast of 2nd day.*

In Figures 4.2 and 4.3, time series of measured and calculated concentrations of ozone are shown for the period June to July 2010 at Vavihill and Norra Kvill. This is the time period with the highest concentrations within this study. As can be observed in the figures, the correlation between the calculations and measurements is generally high and the model is able to reproduce the main features of the spatial and temporal variations in concentrations.

However, the figures also show that the MATCH-model is not able to reproduce the highest concentrations occurring 10 – 12 July 2010. These episodes are analysed in more detail in Section 4.2. In general, the difference between the analysis and the forecasts is small, however, it can also be concluded that the calculations for the analysis, to some extent, are better than the forecasts during these episodes (see for instance Norra Kvill July 10 in Figure 4.3).

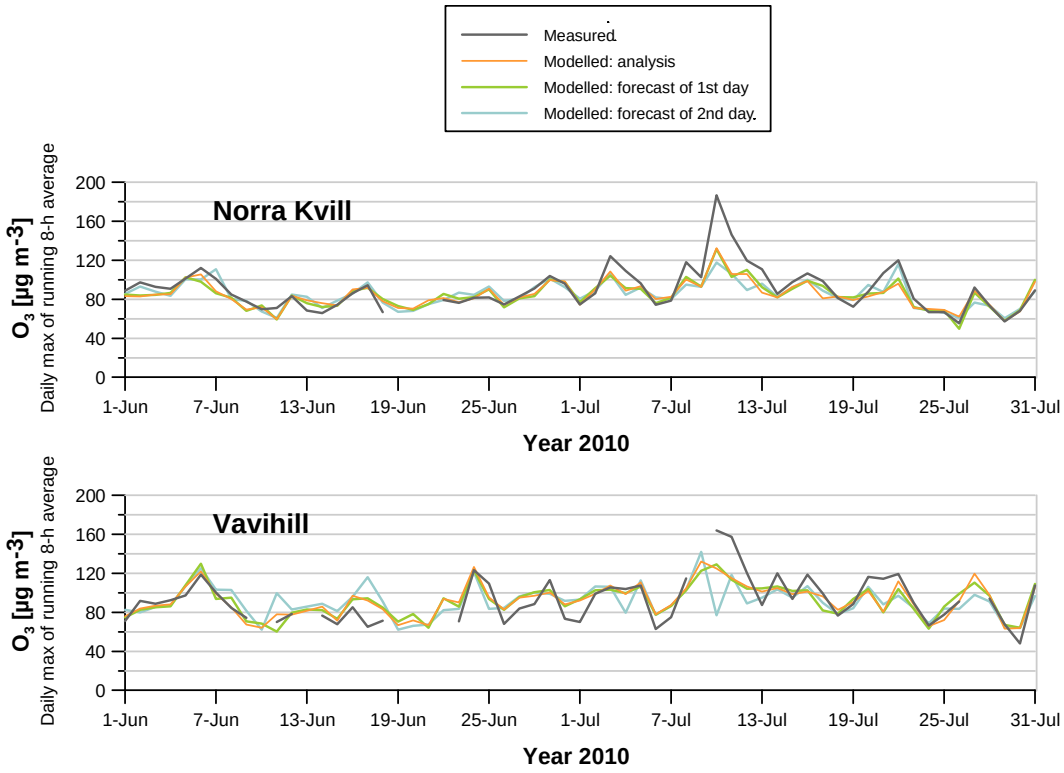

Figure 4.2: *Comparison between measured and modelled daily maximum of 8h-mean concentration of ozone for June – July 2010 at two sites; Vavihill in southern Sweden and Norra Kvill in south eastern Sweden. For modelled concentrations, the results are shown, respectively, for analysis, forecast of 1st day and forecast of 2nd day.*

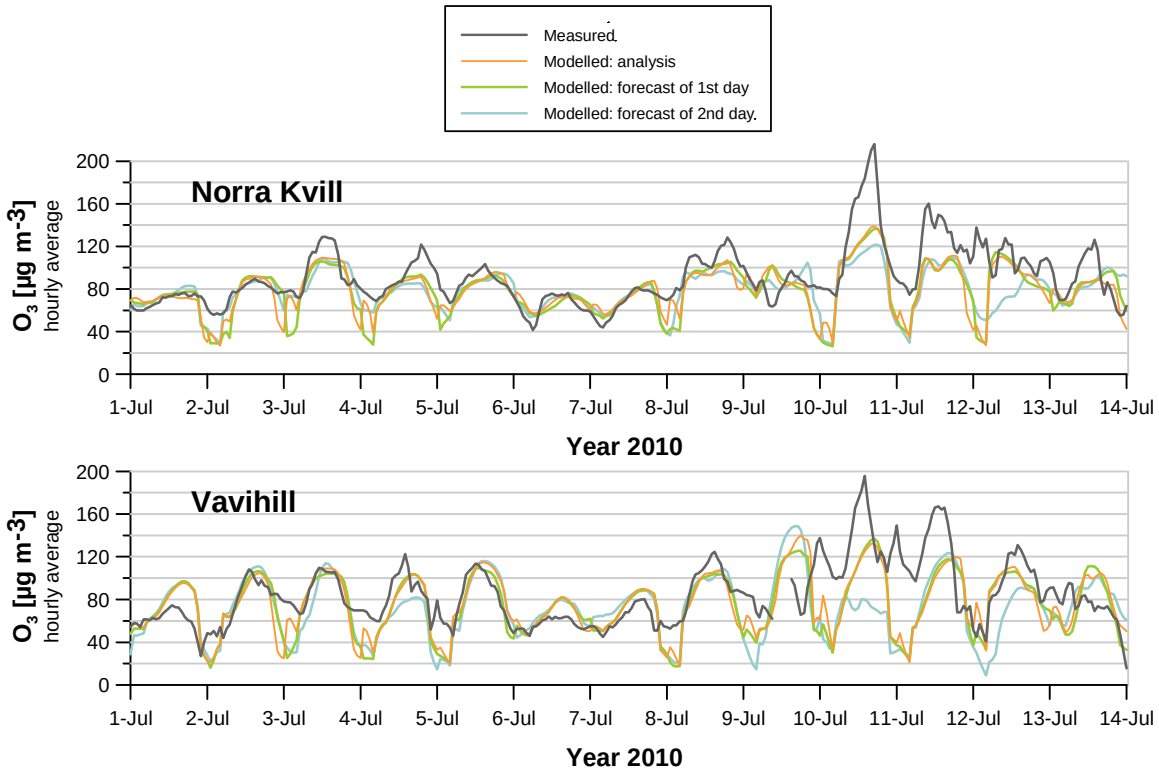

Figure 4.3: *Comparison between measured and modelled hourly concentration of ozone for July 1 – July 14 2010 at two sites; Vavihill in southern Sweden and Norra Kvill in south eastern Sweden. For modelled concentrations, the results are shown, respectively, for analysis, forecast of 1st day and forecast of 2nd day.*

A summary of the validation of the MATCH-model against the measurements is visualized in Figure 4.4. In these scatterplots, modelled ozone concentrations (analysis) are plotted against measurements in terms of annual average, annual maximum of running 8h-average and AOT40[3], in accordance with the targets in the EU air quality directive 2008/50/EC. Each point is representing a station for a certain year.

Calculated yearly mean concentrations of ozone generally show good agreement with measured concentration and thus the bias is small. Furthermore, for most stations, the calculated annual maximum of the running 8h-mean concentration corresponds well with the measurements, however, there is a systematical underestimation of this statistical measure especially for the year 2010, reflecting the model's difficulties in simulating the highest concentrations.

For all stations, RPE and RDE[4] for yearly average and the annual maximum of running 8h-average are well below 50 % which is the model quality requirement according to the EU air quality directive 2008/50/EC (Denby et al., 2010).

AOT40 varies greatly between the different stations (Figure 4.4); from 11 000 µg m^{-3} h at Råö 2008 to 650 µg m^{-3} h at Bredkälen 2010. A particular problem with AOT40 is the high sensitivity of this index (e.g., Tuovinen, 2000). The model validation results are also varying substantially between the different stations and years, but no systematic under- or overestimation can be observed (the scatter in the figure is, however, large).

More verification statistics from the validation of the MATCH-model are shown in Tables 4.1-4.4, where measured and calculated concentrations of ozone are listed (annual average, annual maximum of running 8h-average, AOT40, correlation coefficient, bias and root mean square error). Further statistics are available in Appendix 8.1. Note that the monitoring data for Grimsö 2010 are under revision. Concentrations simulated for Gothenburg approximately 40 km southwest of Östad have been used in the comparison to measurements at Östad since modelled concentrations for Östad were not available in the archive of simulations. In analogy, model results for Växjö approximately 30 km south of Asa have been used for the comparison with measurements at Asa. Since the spatial resolution of the modelled concentrations is relatively low (44 km x 44 km), this basically results in choosing a neighbouring grid point instead of the closest one.

[3] AOT40 is defined as the sum of all 1-hourly ozone concentrations exceeding the value of 40 ppb(v) during the period of 1 May until 31 July. The sum is calculated for Swedish daytime (assumed as 08:00-20:00 local time). The correction method proposed by Engardt et al. (2010a) is used to account for missing data in the observations.

[4] See Denby et al. (2010) for the definitions of RDE (Relative Directive Error) and RPE (Relative Percentile Error).

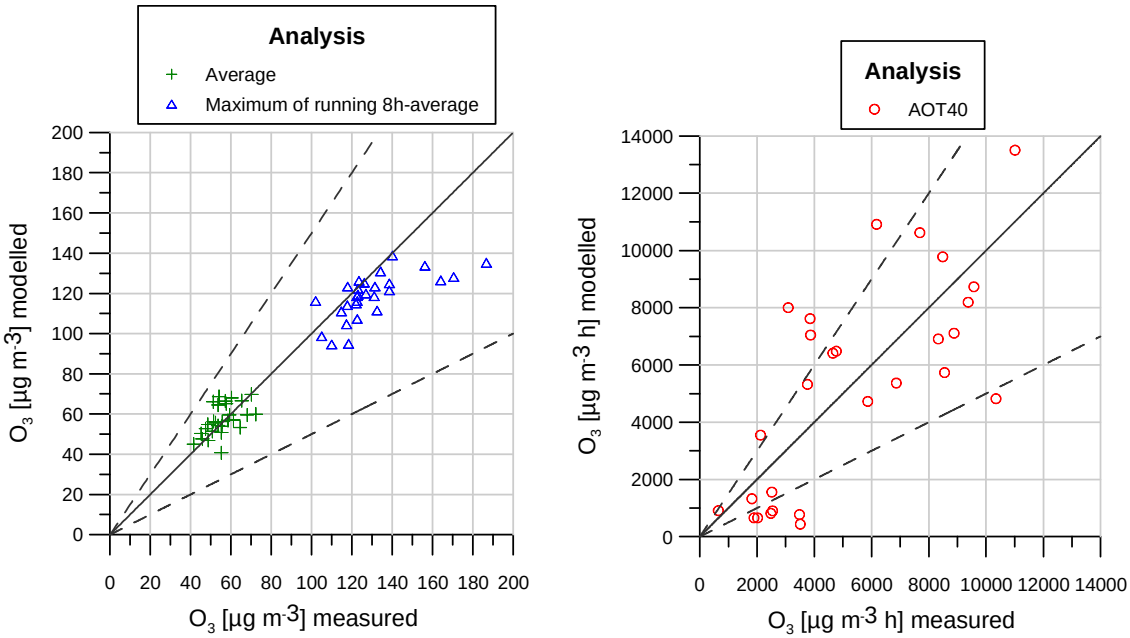

Figure 4.4: *Scatterplots with summary of the comparison between measured and modelled concentration of ozone; annual mean values (green), annual maximum of running 8h-mean concentration (blue) and AOT40 (red). Each point is representing a station and a certain year. The continuous line represents 1:1 and dashed lines represent ±50 %. Numerical values are given in Table 4.1.*

Correlation coefficients (Table 4.2) for 2008 and 2009 are generally high and vary between 0.6 and 0.8 for 1-h mean concentrations and 0.7-0.9 for running 8h-mean concentrations. The correlation between calculations and measurements is strongest for Asa, Aspvreten, Råö and Vindeln. For some sites (Asa, Bredkälen, Esrange, Grimsö, Norra Kvill and Vindeln) the correlation is lower for the year 2010 (0.4-0.7). At this stage it is not clear if this is a systematic error in the model or measurements; for several stations, the available data did not cover the whole of 2010. Further work will be needed to locate more specific problems.

Concerning bias and root mean square error (RMSE), shown in Table 4.3 and 4.4, these statistical metrics are relatively low for most sites. Hence, the MATCH-model is able to reproduce satisfying spatial variability in Sweden. However, the bias and RMSE regarding annual maximum of running 8h-average for 2010 are higher than 2008 and 2009, which likely can be explained by the difficulties for the model to reproduce the high-level ozone episode events during year 2010.

Note that the results for Östad and Asa might be affected by the inconsistence when using a neighbouring grid point in the calculations.

In accordance with the previous conclusions, the results for the 1st and 2nd day forecast (d1 and d2) are similar to the analysis (An), even though the calculations for the analysis in general show a slightly better agreement with the measurements.

Table 4.1: *Measured (obs) and modelled (an, d1 and d2) concentration of ozone (annual mean values, annual maximum of running 8h-mean concentration and AOT40) for different sites and years included in the study. Modelled concentrations are shown both for analysis (an), forecast of 1st day (d1) and forecast of 2nd day (d2).*

	O_3 [µg m^{-3}] annual average				**O_3 [µg m^{-3}] annual max of running 8h-average**				**AOT40 [µg m^{-3} h]**			
	obs	An	d1	d2	obs	An	D1	d2	obs	An	d1	d2
Asa, 2008[1]	47.5	52.7	52.3	53.5	126.2	125.3	115.6	113.8	9573	8732	8282	8172
Asa, 2009[1]	51.4	56.3	55.4	55.8	138.6	125.0	118.3	121.1	3852	7620	7815	6721
Asa, 2010[1]	53.7	64.5	63.3	63.1	156.2	133.8	130.8	122.6	4768	6483	6789	7060
Aspvreten, 2008	50.8	51.4	51.5	52.2	117.7	114.2	112.4	110.0	6864	5367	5026	4601
Aspvreten, 2009	53.6	54.3	54.0	54.4	122.6	107.3	110.5	112.0	3761	5319	5736	5827
Bredkälen, 2008	48.7	46.9	46.9	47.7	105.0	98.7	96.4	101.3	1893	657	582	1001
Bredkälen, 2009	55.7	56.2	55.2	55.5	131.4	123.4	116.6	115.9	1819	1324	1427	1348
Bredkälen, 2010	57.2	66.5	65.7	65.6	102.0	116.3	117.3	110.9	648	910	1011	1153
Esrange, 2008	55.2	40.7	40.4	42.2	110.0	94.6	86.6	87.9	3509	436	290	307
Esrange, 2009	64.5	53.3	52.6	53.2	122.6	116.3	121.2	119.0	2515	1555	1595	1309
Esrange, 2010	72.4	59.9	59.2	60.2	117.4	104.7	104.5	113.8	2018	655	810	1278
Grimsö, 2008	45.2	50.3	50.0	51.2	114.8	111.1	111.7	107.7	5867	4724	4357	4632
Grimsö, 2009	48.6	54.8	53.7	53.6	122.1	115.0	115.0	112.9	2121	3548	3888	3655
Grimsö, 2010	60.3	68.1	66.9	66.7	170.5	128.2	127.3	120.0	10345	4819	4722	4998
N. Kvill, 2008	55.5	53.9	53.7	55.0	123.0	119.3	114.7	111.3	8330	6907	6684	6935
N. Kvill, 2009	61.2	57.1	56.5	56.7	138.6	121.5	118.9	117.2	4647	6409	6943	6303
N. Kvill, 2010	70.2	69.8	68.9	68.6	186.7	135.3	138.0	131.7	8550	5733	5989	6056
Råö, 2008	59.3	59.5	59.2	59.1	123.0	122.3	120.3	118.6	11010	13506	12949	11195
Råö, 2009	58.5	56.8	56.2	57.0	134.2	131.0	132.8	131.0	6175	10914	11033	10730
Råö, 2010	65.4	66.6	65.5	66.1	140.1	138.8	140.7	131.1	7687	10623	10527	10035
Vavihill, 2008	45.8	47.6	47.5	48.8	131.1	118.7	111.3	108.9	8880	7108	6484	6098
Vavihill, 2009	55.3	50.8	50.5	50.6	126.9	119.9	115.3	115.2	3869	7046	6796	6206
Vavihill, 2010	68.0	59.5	58.4	58.1	164.1	126.5	129.7	125.1	9374	8191	8110	7749
Vindeln, 2008	41.6	45.0	44.8	45.9	118.4	95.0	93.4	96.8	3482	772	634	893
Vindeln, 2009	52.3	55.6	54.9	54.7	117.9	123.4	115.2	105.9	2542	902	989	879
Vindeln, 2010	57.7	65.1	64.2	64.3	132.5	111.5	109.3	108.4	2483	813	898	1201
Östad, 2008[2]	51.2	66.1	65.6	66.0	122.5	118.7	116.7	113.9	8485	9778	9539	8840
Östad, 2009[2]	54.0	68.7	68.2	68.5	123.5	126.3	128.8	123.5	3088	8002	8332	8002

[1] Calculations for Växjö used.
[2] Calculations for Göteborg used.

Table 4.2: *Correlation coefficient (r) between measured and modelled concentration of ozone, regarding 1-h average concentration and daily maximum of running 8h-average, for different sites and years included in the study. Results are shown both for analysis (an), forecast of 1st day (d1) and forecast of 2nd day (d2).*

	r 1-h average			**r daily max of running 8h-average**		
	An	d1	d2	An	d1	d2
Asa, 2008[1]	0.80	0.80	0.78	0.86	0.86	0.86
Asa, 2009[1]	0.75	0.76	0.73	0.87	0.86	0.84
Asa, 2010[1]	0.57	0.60	0.57	0.66	0.67	0.61
Aspvreten, 2008	0.82	0.81	0.78	0.90	0.89	0.88
Aspvreten, 2009	0.75	0.76	0.73	0.86	0.85	0.84
Bredkälen, 2008	0.71	0.70	0.67	0.76	0.75	0.75
Bredkälen, 2009	0.75	0.73	0.70	0.83	0.82	0.80
Bredkälen, 2010	0.40	0.38	0.35	0.44	0.43	0.41
Esrange, 2008	0.67	0.65	0.62	0.75	0.72	0.69
Esrange, 2009	0.73	0.72	0.70	0.79	0.78	0.76
Esrange, 2010	0.55	0.54	0.52	0.62	0.61	0.58
Grimsö, 2008	0.80	0.81	0.78	0.88	0.88	0.87
Grimsö, 2009	0.74	0.75	0.72	0.83	0.83	0.79
Grimsö, 2010	0.47	0.46	0.46	0.58	0.56	0.55
N. Kvill, 2008	0.68	0.67	0.67	0.79	0.79	0.79
N. Kvill, 2009	0.74	0.72	0.69	0.85	0.84	0.81
N. Kvill, 2010	0.52	0.50	0.47	0.64	0.63	0.60
Råö, 2008	0.84	0.83	0.82	0.91	0.90	0.90
Råö, 2009	0.81	0.80	0.77	0.86	0.86	0.84
Råö, 2010	0.72	0.71	0.67	0.81	0.81	0.78
Vavihill, 2008	0.72	0.71	0.70	0.83	0.83	0.83
Vavihill, 2009	0.72	0.71	0.67	0.83	0.83	0.79
Vavihill, 2010	0.65	0.64	0.57	0.76	0.76	0.64
Vindeln, 2008	0.75	0.74	0.72	0.84	0.83	0.80
Vindeln, 2009	0.76	0.77	0.75	0.85	0.85	0.82
Vindeln, 2010	0.39	0.39	0.35	0.51	0.50	0.47
Östad, 2008[2]	0.79	0.77	0.76	0.82	0.79	0.82
Östad, 2009[2]	0.72	0.74	0.70	0.74	0.71	0.72

[1] Calculations for Växjö used.
[2] Calculations for Göteborg used.

Table 4.3: *Bias between modelled and measured concentration of ozone, regarding annual average concentration and annual maximum of running 8h-average, for different sites and years included in the study. Results are shown both for analysis (an), forecast of 1st day (d1) and forecast of 2nd day (d2).*

	Bias [µg m^{-3}] annual 1-h average			**Bias [µg m^{-3}] annual max of running 8h-average**		
	An	d1	d2	An	D1	d2
Asa, 2008[1]	5.2	4.8	6.0	-0.9	-10.6	-12.5
Asa, 2009[1]	4.9	4.1	4.4	-13.5	-20.3	-17.4
Asa, 2010[1]	10.9	9.6	9.4	-22.4	-25.4	-33.6
Aspvreten, 2008	0.6	0.7	1.5	-3.5	-5.3	-7.8
Aspvreten, 2009	0.7	0.5	0.8	-15.3	-12.1	-10.6
Bredkälen, 2008	-1.7	-1.8	-1.0	-6.3	-8.6	-3.6
Bredkälen, 2009	0.5	-0.5	-0.2	-8.0	-14.8	-15.5
Bredkälen, 2010	9.3	8.4	8.4	14.3	15.4	8.9
Esrange, 2008	-14.4	-14.7	-13.0	-15.5	-23.4	-22.1
Esrange, 2009	-11.2	-11.8	-11.3	-6.3	-1.4	-3.6
Esrange, 2010	-12.5	-13.2	-12.2	-12.7	-12.9	-3.6
Grimsö, 2008	5.0	4.8	5.9	-3.7	-3.1	-7.1
Grimsö, 2009	6.2	5.1	5.0	-7.2	-7.2	-9.2
Grimsö, 2010	7.8	6.7	6.4	-42.3	-43.2	-50.5
N. Kvill, 2008	-1.6	-1.8	-0.5	-3.7	-8.4	-11.8
N. Kvill, 2009	-4.1	-4.7	-4.5	-17.1	-19.7	-21.4
N. Kvill, 2010	-0.4	-1.3	-1.7	-51.4	-48.7	-55.0
Råö, 2008	0.2	-0.2	-0.2	-0.6	-2.7	-4.4
Råö, 2009	-1.7	-2.3	-1.5	-3.2	-1.4	-3.2
Råö, 2010	1.2	0.1	0.7	-1.3	0.6	-8.9
Vavihill, 2008	1.8	1.7	3.0	-12.3	-19.8	-22.1
Vavihill, 2009	-4.5	-4.8	-4.7	-7.0	-11.7	-11.8
Vavihill, 2010	-8.5	-9.6	-9.9	-37.6	-34.5	-39.0
Vindeln, 2008	3.4	3.2	4.4	-23.4	-25.0	-21.6
Vindeln, 2009	3.4	2.6	2.4	5.5	-2.7	-12.0
Vindeln, 2010	7.4	6.5	6.6	-21.0	-23.2	-24.1
Östad, 2008[2]	14.9	14.3	14.8	-3.8	-5.7	-8.6
Östad, 2009[2]	14.7	14.2	14.4	2.8	5.3	0.0

[1] Calculations for Växjö used.
[2] Calculations for Göteborg used.

Table 4.4: *Root mean square error (RMSE) between modelled and measures concentration of ozone, regarding 1-h average concentration and daily maximum of running 8h-average, for different sites and years included in the study. Results are shown both for analysis (an), forecast of 1st day (d1) and forecast of 2nd day (d2).*

	RMSE [µg m^{-3}] 1-h average			**RMSE [µg m^{-3}] running 8h-average**		
	An	d1	d2	An	D1	d2
Asa, 2008[1]	16.2	16.1	16.9	15.6	16.3	15.3
Asa, 2009[1]	17.9	17.4	18.3	11.7	11.8	12.0
Asa, 2010[1]	23.4	22.5	23.0	15.9	15.8	16.6
Aspvreten, 2008	14.5	14.7	15.7	9.3	9.5	10.1
Aspvreten, 2009	16.4	16.1	17.1	10.9	10.9	11.1
Bredkälen, 2008	14.0	14.1	14.8	10.7	10.7	11.1
Bredkälen, 2009	14.9	15.5	16.3	11.4	11.7	12.3
Bredkälen, 2010	20.5	20.6	20.9	17.2	17.3	17.4
Esrange, 2008	20.4	20.9	20.1	11.9	11.8	11.8
Esrange, 2009	19.1	19.9	19.7	15.0	15.4	15.6
Esrange, 2010	20.5	21.4	21.2	17.2	17.2	17.1
Grimsö, 2008	15.0	14.8	15.9	10.7	10.4	11.2
Grimsö, 2009	17.0	16.5	17.4	12.4	12.4	13.4
Grimsö, 2010	24.0	24.0	24.1	18.5	18.9	18.9
N. Kvill, 2008	17.0	17.4	17.2	12.8	12.8	12.5
N. Kvill, 2009	16.3	17.0	17.6	11.7	11.7	12.4
N. Kvill, 2010	18.2	19.0	19.1	14.2	14.4	14.5
Råö, 2008	13.7	14.2	14.4	10.1	10.3	9.6
Råö, 2009	15.8	16.4	17.2	12.8	13.2	13.6
Råö, 2010	15.8	16.7	17.1	11.6	11.7	12.0
Vavihill, 2008	18.5	18.9	19.2	15.2	15.2	15.2
Vavihill, 2009	18.8	19.2	20.1	12.8	12.6	14.0
Vavihill, 2010	20.2	21.4	22.9	13.5	13.8	16.5
Vindeln, 2008	15.6	15.8	16.7	9.4	9.7	10.5
Vindeln, 2009	15.9	15.5	15.8	10.5	10.5	11.2
Vindeln, 2010	23.3	23.4	24.1	16.2	16.3	16.9
Östad, 2008[2]	22.8	22.8	23.2	15.7	16.2	15.0
Östad, 2009[2]	23.6	23.0	24.1	14.2	15.0	14.6

[1] Calculations for Växjö used.
[2] Calculations for Göteborg used.

4.2 Analysis of ozone episodes in Sweden

4.2.1 Strategies for the evaluation of episodes and predicted ozone concentrations

One of the aims of this study is to forecast ozone concentrations over Sweden. It will be of particular importance to be able to forecast ozone episodes, i.e. very high ozone concentrations during a few days.

The analysis of ozone episodes in Sweden during the considered time period (18 May 2008 – 31 Dec 2010) has been carried out with a specific focus on the geographical areas of Sweden affected by a particular episode, the governing synoptic weather conditions and the origin of air masses.

In our study we use the following definition: A Swedish ozone episode is present when the hourly ozone concentrations anywhere over Sweden exceeded 140 $\mu g\ m^{-3}$ (70 ppb). This value was chosen to reflect conditions when ozone concentrations were substantially elevated above normal concentrations in southern Sweden during a sunny summer day.

Altogether eight ozone episodes were identified for the period 18 May 2008 until the end of 2010. In the following we provide two detailed analyses of Swedish ozone episodes: The first example is an episode with the highest ozone concentrations in the eastern part of south Sweden while the second example has highest ozone concentrations in the western part. We then summarize the analyses for all ozone episodes with regard to the specific conditions for the ozone episodes and the MATCH model's ability to forecast the ozone concentrations during those episodes. The complete analysis of all episodes is provided in the Appendix.

In order to allow for the intercomparison of different ozone episodes we needed to harmonize the time periods used for the evaluation. The ozone concentrations and the relevant meteorological parameters are thus analysed in a three day time window. The window of analysis was generally centered around the day with the highest concentration, but if high ozone concentrations lasted for several days, days with high concentrations were included as far as possible. The analysis was made separately for the measuring sites western (Skåne län, Hallands län, Västra Götalands län) and eastern (Kronobergs län, Östergötlands län, Södermanlands län, Stockholms län, Örebro län) parts of south Sweden, as well as for northern Sweden (Norrland), see also Figures 2.1 and 2.2 above.

4.2.2 The ozone episode of 2010-07-09 to 2010-07-11

In the first part of July 2010, there was an ozone episode with very high ozone concentrations mainly in the eastern parts of south Sweden and in Skåne (Figure 4.5). The information level of 180 $\mu g/m^3$ (~90 ppb), was exceeded at Vavihill and Norra Kvill. The highest concentrations at Vavihill and Norra Kvill were evident mainly on 2010-07-10 but also on 2010-07-11.

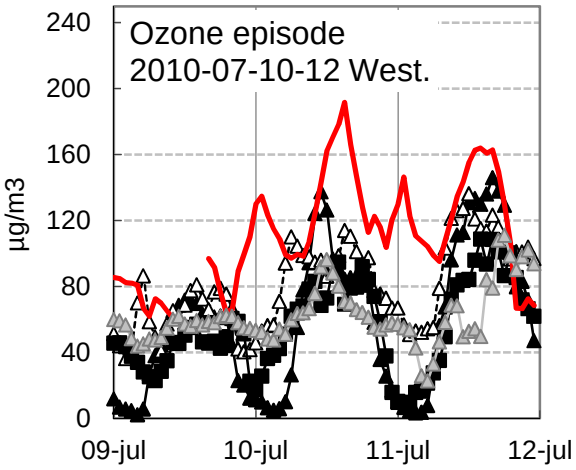

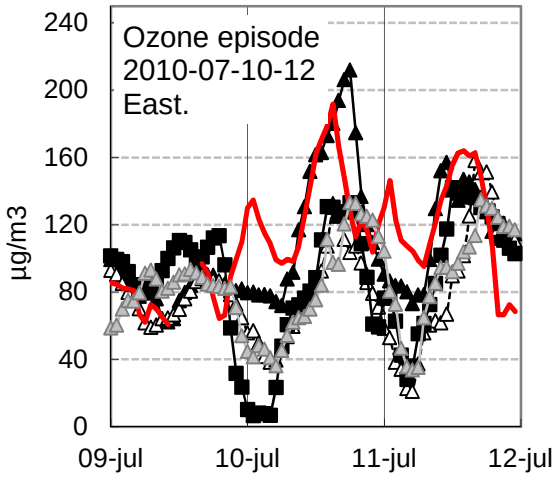

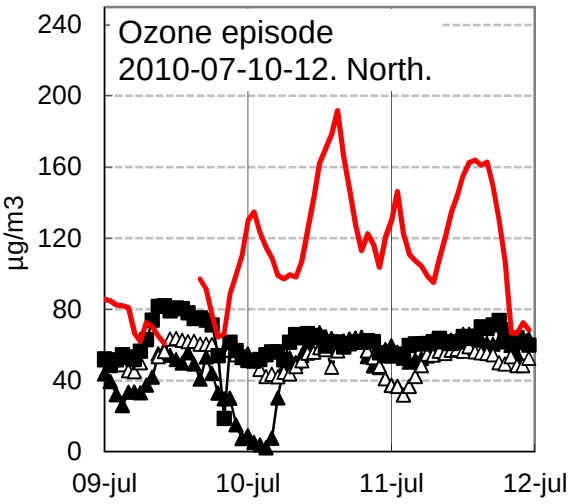

Figure 4.5: *Hourly ozone concentrations measured with instruments in different parts of Sweden during the ozone episode 2010-07-09 to 2010-07-11. For legends and locations see Figures 2.1 and 2.2. The red line included in all diagrams represents ozone concentrations at Vavihill, Skåne, for comparison.*

The operational trajectory analysis made by NILU with the FLEXTRA model (Figure 4.6) indicates that the air arriving in the afternoon at Vavihill and Norra Kvill (trajectories are not available for Norra Kvill, instead trajectories for the nearby site Aspvreten are used) on 2010-07-10 originated from northern and former eastern Germany and to some extent from Poland. The air arriving at Aspvreten in fact first passed over Vavihill. However, ozone measurements show that increases in ozone concentrations at Vavihill and Norra Kvill occur almost simultaneously. It is somewhat difficult to resolve from the trajectory illustrations, but it seems that the air masses spent quite some time above Germany before arriving at Vavihill and Aspvreten.

Air arriving at the western parts of south Sweden this day originated from a completely different area, namely from the Atlantic via UK, North Sea and Denmark. This explains the low ozone concentrations over the western parts of Sweden this day.

On 2010-07-11, the air arriving at Vavihill still originated from northern Germany, while the air arriving at Norra Kvill (Aspvreten) came from northern-central Poland, resulting in somewhat lower ozone concentrations. Air arriving at Grimsö in the afternoon 2010-07-11 originated from western Poland and resulted in high concentrations. It is somewhat difficult to distinguish the differences in air mass origins between air arriving at Aspvreten and Grimsö, respectively, in relation to the resulting ozone concentrations.

Vavihill 2010-07-10 18:00.

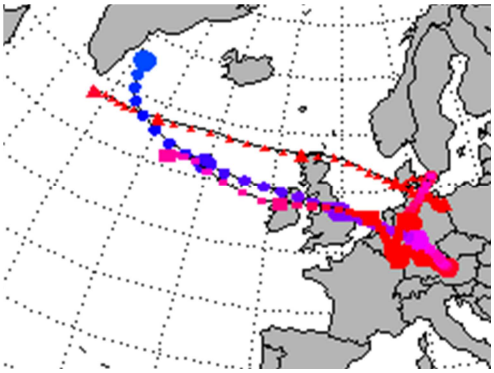

Vavihill 2010-07-11 18:00

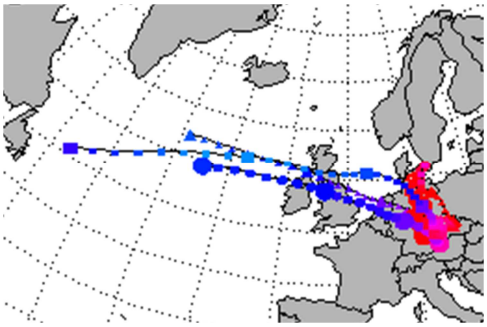

Råö 2010-07-10 18:00

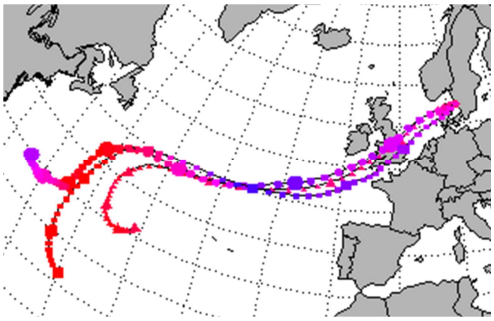

Råö 2010-07-11 18:00

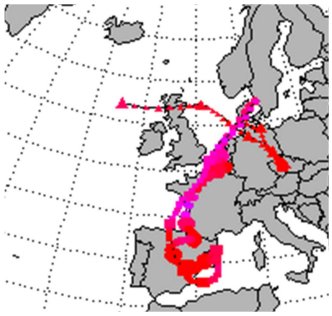

Aspvreten 2010-07-10 18:00.

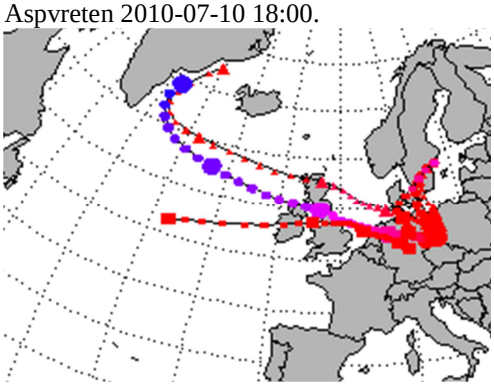

Aspvreten 2010-07-11 18:00.

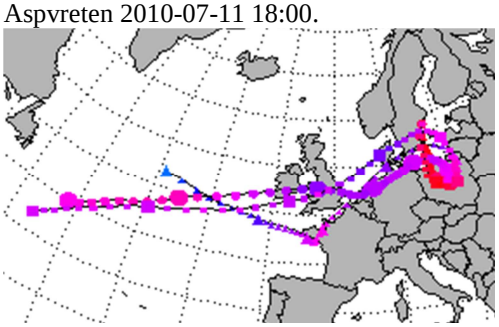

Grimsö 2010-07-10 18:00.

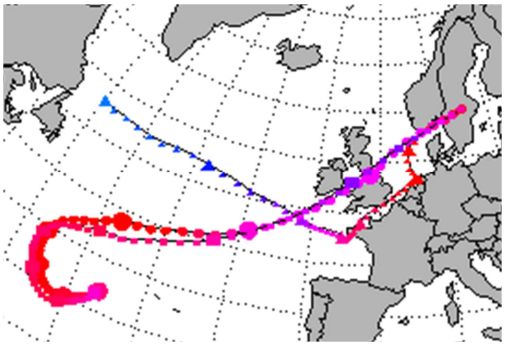

Grimsö 2010-07-11 18:00.

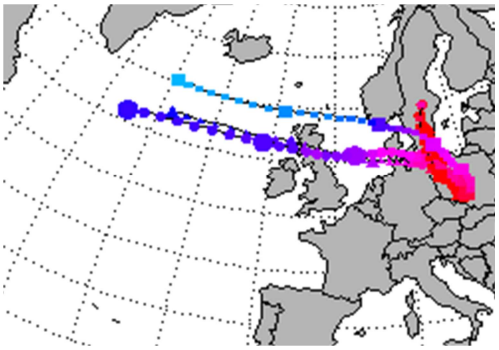

Figure 4.6: *Trajectories for air masses arriving at Vavihill, Råö, Aspvreten and Grimsö during an ozone episode from 2010-07-10 to 2010-07-12, as estimated with the FLEXTRA model available at NILU. The time for arrival is indicated close to each diagram.*

Table 4.5 summarizes the comparison of the modelled and observed extreme values during the episode. The highest ozone concentration during this episode was 216 µg/m^3 (108 ppb) and was measured at Norra Kvill in the afternoon of 2010-07-10. The somewhat lower concentration of 196 µg/m^3 (98 ppb) was measured at Vavihill on the same day. In the north of Sweden, the ozone concentrations reached a maximum of only 84 µg/m^3 (42 ppb). High ozone concentrations were also measured at Norra Kvill (168 µg/m^3 / 84 ppb) and at Grimsö (162 µg/m^3 / 81 ppb) on 2010-07-11.

Table 4.5: *Highest concentrations of ozone observed and modelled during the ozone episode 2010-07-09 to 2010-07-11.*

	West part of southern Sweden	East part of southern Sweden	Northern Sweden
Highest measured one-hour ozone concentration ($\mu g/m^3$)	195.6	216.1	83.6
No of days with ozone concentrations >140 $\mu g/m^3$	2	2	0
Highest modelled one-hour ozone concentration ($\mu g/m^3$)	137.3	136.1	81.4
Ratio modelled vs measured	0.72	0.64	0.99

Modelled ozone concentrations for the eastern parts, including Vavihill, Asa and Norra Kvill, during 2010-07-10 matched relatively poorly with the measured concentration. There was a 36% underestimation at Norra Kvill. In the western parts, with low ozone concentrations in air originating from the Atlantic passing over UK, as well as in the north, the agreement of modelled and measured values was excellent (Table 4.5 and Figure 4.7).

It is interesting that simultaneous measurements of ozone concentrations at "Bjärehalvön", only 50 km northwest of Vavihill, did not show ozone concentrations exceeding 146 $\mu g/m^3$ (73 ppb) on 2010-07-10. Thus, there was a very sharp border between the polluted and unpolluted air masses. The difference in maximum ozone concentrations over this border was 50 $\mu g/m^3$ (25 ppb).

Also for 2010-07-11 the agreement between model and measurements values was poor for Vavihill and Norra Kvill, in particular when considering the highest ozone concentrations.

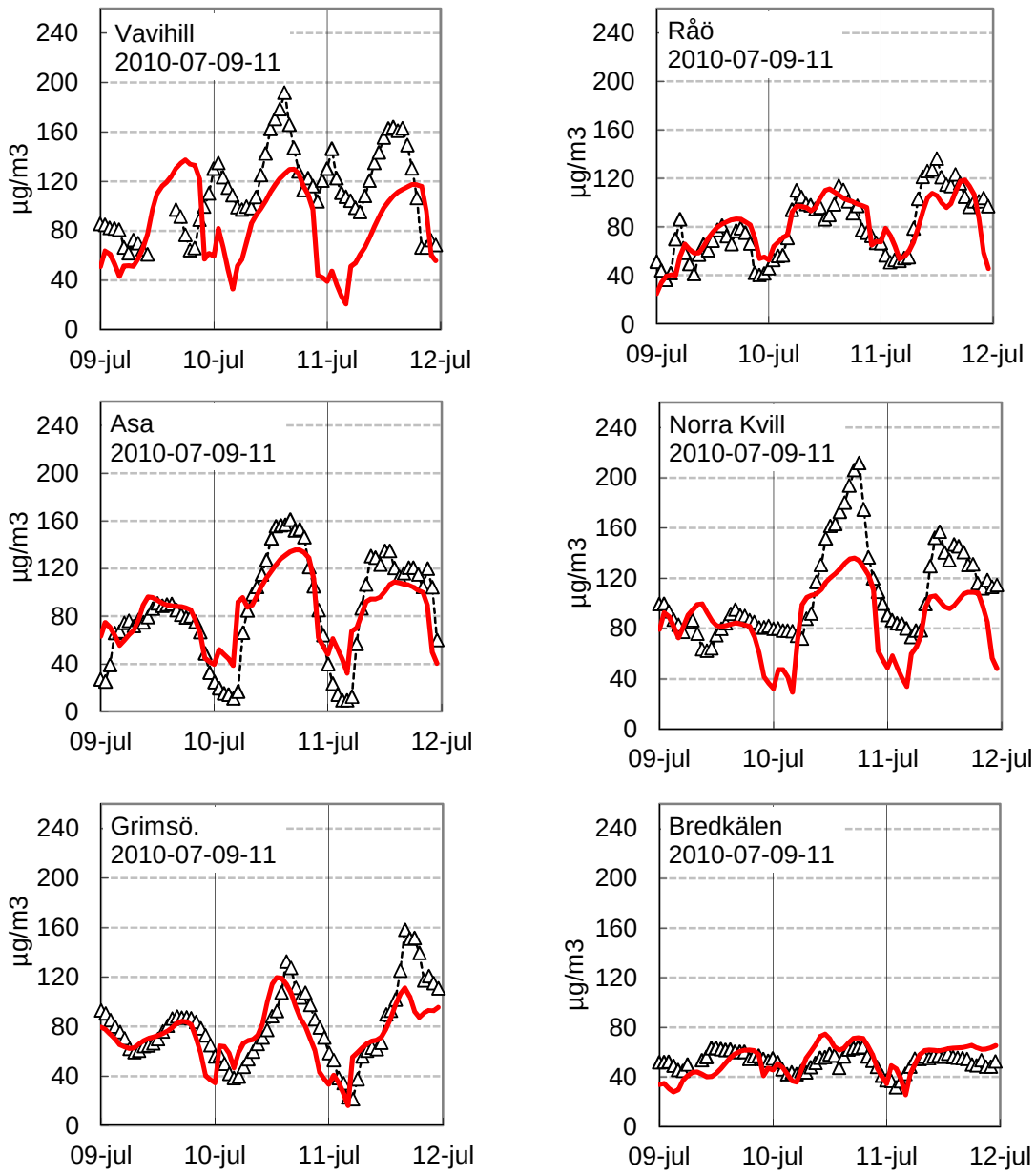

Figure 4.7: *Comparison between modelled and measured hourly ozone concentrations at three sites in different parts of Sweden during the ozone episode of 2010-07-09 to 2010-07-11. Black open triangles represent measured values, red line modelled values.*

4.2.3 The ozone episode of 2010-07-20 to 2010-07-22

In late July 2010, there was a moderate ozone episode with high ozone concentrations mainly in the western parts of south Sweden but also to some extent in Skåne and in the eastern parts of south Sweden (Figure 4.8). High concentrations in the west were evident mainly on 2010-07-20 while high concentrations in the south and east were most evident on 2010-07-22.

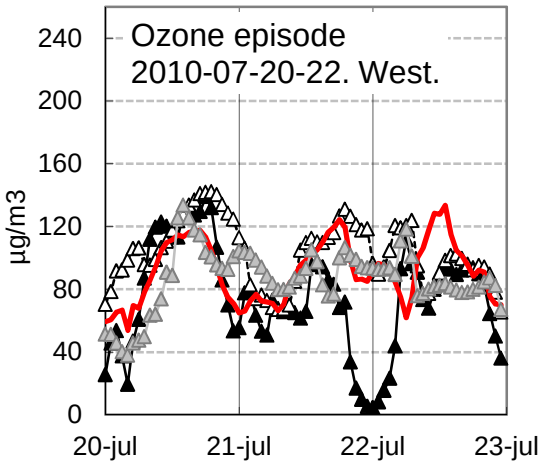

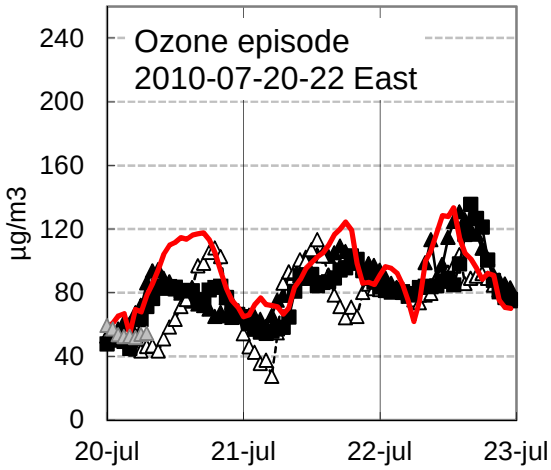

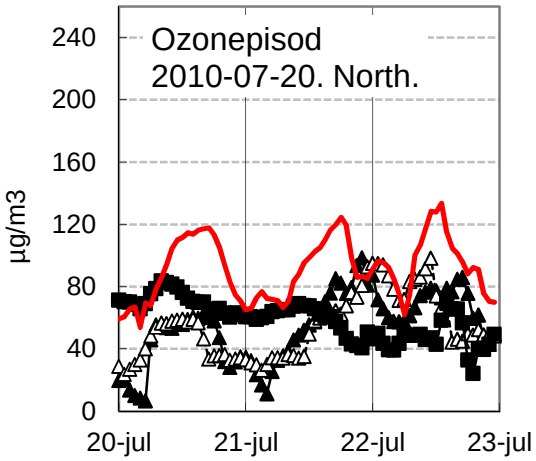

Figure 4.8: *Hourly ozone concentrations measured with instruments in different parts of Sweden during the ozone episode 2010-07-20 to 2010-07-22. For site locations and legends see Figures 2.1 and 2.2 above. The red line included in all diagrams represents ozone concentrations at Vavihill, Skåne, for comparison.*

Trajectory analysis made by NILU with the FLEXTRA model (Figure 4.9) indicated that the air arriving in the afternoon at Råö on 2010-07-20 originated from relatively deep into northern and former eastern Germany and that the air had been transported at a relatively low elevation, 500 m. The air arriving at the same time to Aspvreten in the eastern part of south Sweden originated more to the west of Europe, coming from Denmark, Netherlands, Belgium and UK. These differences might explain differences in measured ozone concentrations during 2010-07-20, with higher concentrations in the western part of southern Sweden.

On 2010-07-22, the air arriving at Råö came over the North Sea from the UK and then from the Atlantic, explaining the relatively low concentrations in western parts of southern Sweden. The air arriving at Vavihill on this day came over the English channel, Netherlands and Denmark and seemed to have slowed down over northern Germany. This air mass also resulted in relatively high ozone concentrations at Vavihill.

The air arriving at Aspvreten on 2010-07-22 seemed to have been transported along almost the same track as for Vavihill, but seemed to have also passed over northern France. This air mass seemed to have moved at a much higher elevation and resulted in relatively high ozone concentrations at Aspvreten upon arrival.

Vavihill 2010-07-20 18:00.

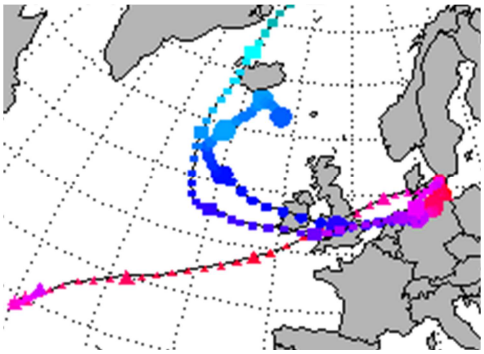

Vavihill 2010-07-22 18:00

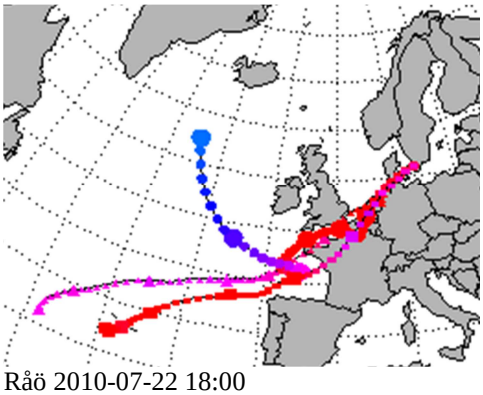

Råö 2010-07-20 18:00

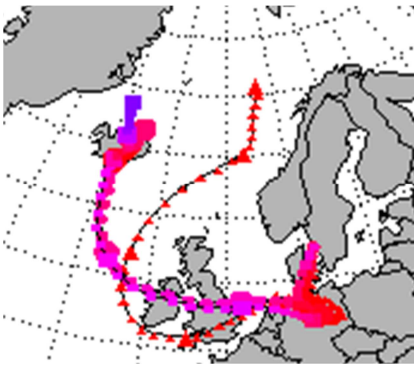

Råö 2010-07-22 18:00

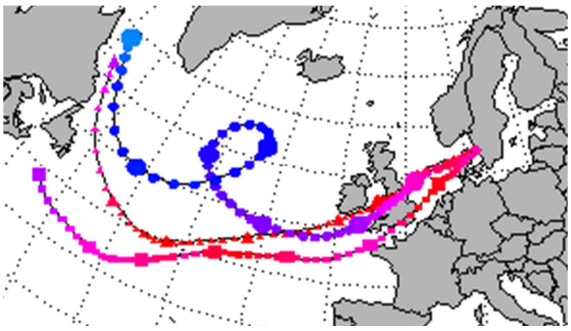

Aspvreten 2010-07-20 18:00.

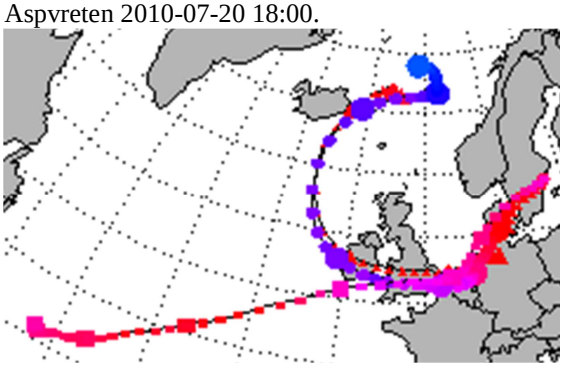

Aspvreten 2010-07-22 18:00.

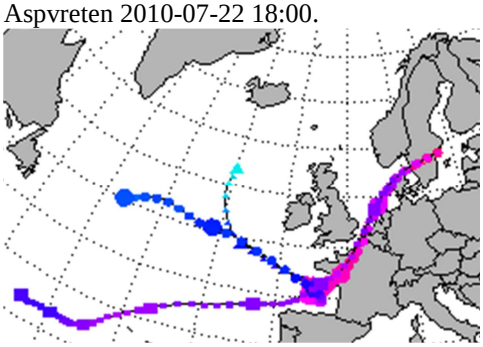

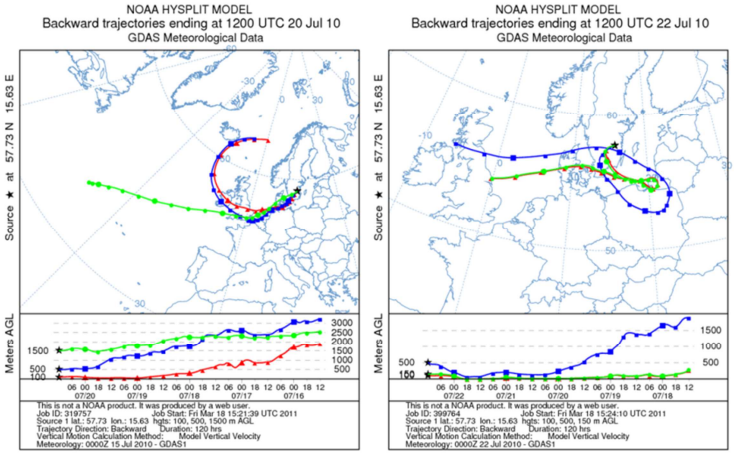

Figure 4.9: *Trajectories for air masses arriving at Vavihill, Råö and Aspvreten during an ozone episode 2010-07-20 to 2010-07-22, as estimated with the FLEXTRA model. The time of arrival is indicated close to each diagram. The lowest panel shows HYSPLIT-trajectories arriving at Norra Kvill on 2010-07-20 and 2010-07-22 at 12:00.*

The highest ozone concentration during this episode was measured at Råö in the afternoon 2010-07-20 (145 µg/m^3 / 73 ppb). Slightly lower concentrations were measured at Aspvreten on 2010-07-22 (138 µg/m^3 / 69 ppb). In the north of Sweden, the ozone concentrations reached a maximum of 100 µg/m^3 (50 ppb).

Table 4.6: *Highest ozone concentrations observed and modelled during the ozone episode 2010-07-20 to 2010-07-22.*

	West part of southern Sweden	East part of southern Sweden	Northern Sweden
Highest measured one-hour ozone concentration (µg/m^3)	145.1	138.1	100.3
No of days with ozone concentrations >140 µg/m^3	1	0	0
Highest modelled one-hour ozone concentration (µg/m^3)	130.5	105.2	93.2
Ratio modelled vs measured	0.90	0.76	0.93

Modelled ozone concentrations for western parts, Råö, during 2010-07-20 agreed relatively well with measured concentrations with only a 10% underestimation (Table 4.6 and Figure 4.10). The modelled ozone concentrations during 2010-07-22 matched less well with the high ozone concentrations measured in eastern parts, Asa and Norra Kvill (25% underestimation for Norra Kvill). Trajectory analysis with HYSPLIT for Norra Kvill 2010-07-22 12:00 indicates that the air mass originated from southeast and passed Denmark and northern Poland before arriving to Norra Kill. The air was transported mainly within the boundary layer.

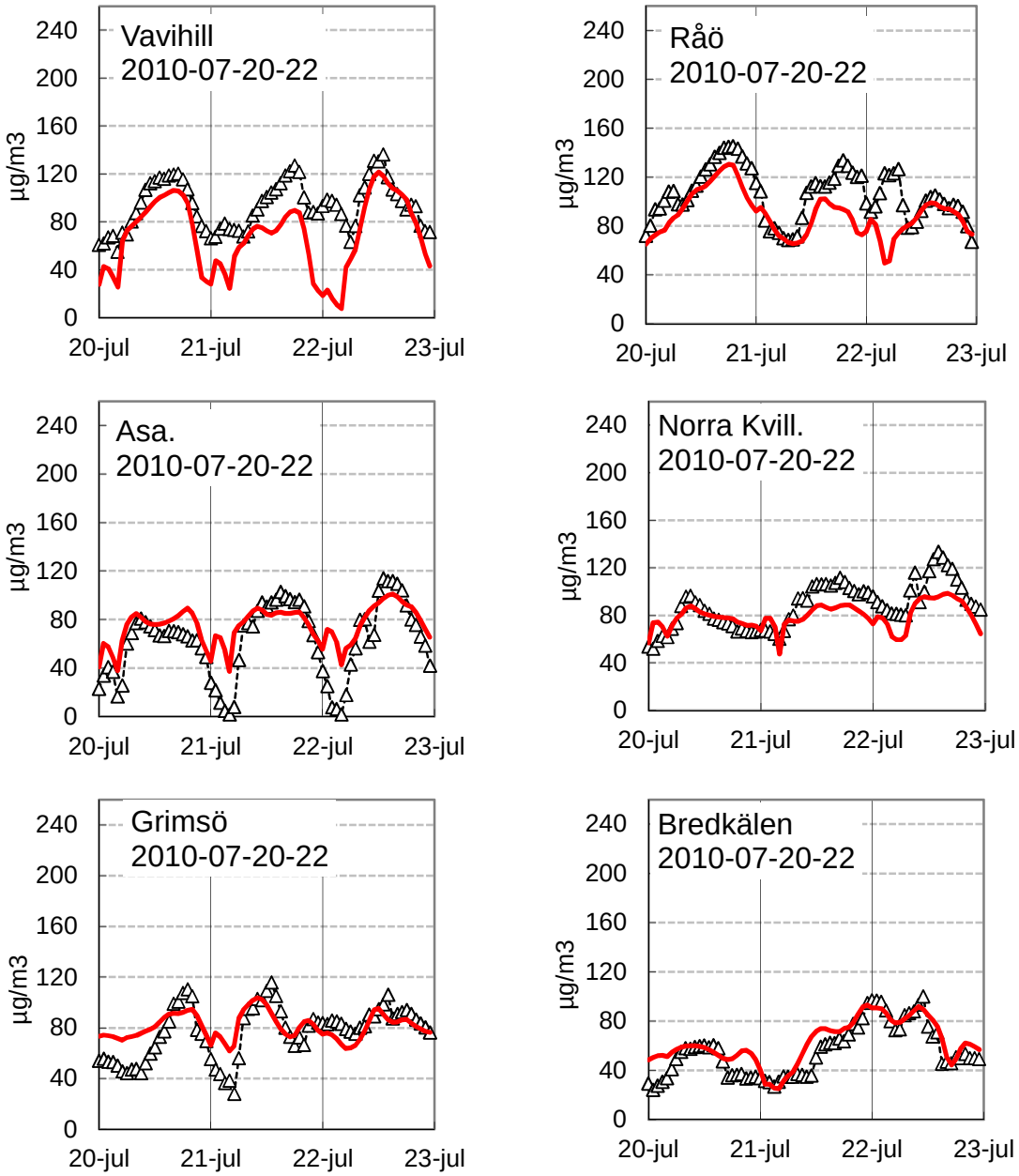

Figure 4.10: *Comparison between modelled and measured hourly ozone concentrations at six sites in different parts of Sweden during an ozone episode 2010-07-20-22. Black open triangles represents measured values, red line modelled values.*

4.2.4 Summary of the analysis of all episodes

Altogether eight ozone episodes were identified for the period 18 May 2008 until the end of 2010 (the period where archived ozone concentrations from MATCH were available), with measured ozone concentrations exceeding 140 µg/m^3 (Table 4.7). Four of the episodes resulted in the highest ozone concentrations in the western parts of south Sweden, three in the eastern part of southern Sweden and one in northern Sweden.

The highest ozone concentration measured during the analysed period was 216 µg/m^3 at Norra Kvill in the eastern part of southern Sweden on 2010-07-10.

For all episodes except one, the air masses causing the highest ozone concentrations originated from northern Germany, and countries beyond. The exception was one ozone episode with high concentration in the north of Sweden, 2010-05-15, where the air masses originated from Russia. Four of the episodes were connected with a synoptic weather situation with substantially decreasing air pressure over the three-day period, while for the remaining episodes the air pressure dynamics were variable during the episode.

The MATCH model managed to simulate the highest ozone concentrations during the episodes relatively well (Table 4.8). However, the model performed best when maximum ozone concentration occurred in the western part of southern Sweden, with a mean ratio between maximum simulated and measured concentrations of 0.89. The corresponding value when the maximum ozone concentrations occurred in the eastern part of southern Sweden was 0.77. The MATCH model performed less well during the ozone episode when the highest ozone concentrations were measured, 2010-07-10. The highest ozone concentration simulated was only 64 % of the highest measured. Even during this episode the polluted air masses originated from northern Germany. Based on the trajectory analysis it appears that the air was moving relatively slowly in an anti-cyclonic weather situation. This is the typical weather situation connected with very high ozone concentrations over southern Sweden (i.e. sub-cluster VIC_{we} suggested by Tang et al., 2009b).

In addition to the ozone episodes described above, one more period was investigated, aiming at analysing the relatively high ozone concentrations that occur over Sweden during spring, when air was transported from far northern latitudes. It has been suggested that these high ozone concentrations either are caused by ozone intrusion from the stratosphere or are the result of accumulation of ozone precursors over the Artic during wintertime. In any case, the MATCH model managed to simulate the ozone concentrations during the spring period relatively well, implying that any mechanisms needed to simulate these high spring ozone concentrations are present in the MATCH model formulations.

It can be concluded that the MATCH model can simulate high ozone concentrations relatively well but that some problems still remain when simulating the highest hourly mean ozone concentrations. This result is in line with the experiences of other modelling communities: The Danish THOR-system, e.g., had similar problems in capturing the major ozone episode of 2010 (personal communication Jörgen Brandt, Aarhus Universitet).

Table 4.7: Selected characteristics for the analysed ozone episodes: Bold indicates the highest ozone concentrations during each episode, regions are referred to as: n, north; Ge, Germany; Pol, Poland; BeNeLux, Belgium, Netherlands, Luxemburg; N Sea, North Sea; UK, United Kingdom.

Episode days	Month	Highest measured hourly ozone concentration (µg/m^3)			Air mass origin*			Air pressure dynamics over three days		
		West	East	North	West	East	North	West	East	North
2010-07-20 - 22	July	**145**	138	100	**n Ge**	BeNeLux s UK	Atlantic	**decreasing 12 mbar**	decreasing 9 mbar	-
2010-07-10 - 12	July	196	**216**	84	UK, Atlantic	**n Ge, Pol**	UK, Atlantic	variable	**variable**	-
2010-07-02 - 04	July	146	**160**	101	n Ge, BeNeLux	**n Ge, BeNeLux**	Norway,UK, Atlantic	variable	**variable**	-
2010-06-28 - 30	June	**145**	127	104	**n Ge, N Sea**	n Ge, N Sea	UK, Atlantic	**decreasing 9 mbar**	decreasing 10 mbar	-
2010-05-14 - 16	May	96	128	**148**	Baltic, Ukrain	Baltic, Belarus	**Finland, Russia**	variable	variable	**-**
2009-07-03 - 05	July	**141**	109	72	**n Ge, Poland**	Finland, north Atlantic	Arctic	**decreasing 12 mbar**	decreasing 12 mbar	-
2009-04-25 - 27	April	131	**145**	127	Ge, Tjeckien	**Ge, Tjeckien**	Norway, n GE, n Pol	decreasing 20 mbar	**decreasing 18 mbar**	-
2008-06-01 - 03	June	**141**	133	122	**n Ge, Pol, Baltic states**	Atlantic	Atlantic	**variable**	variable	-

Table 4.8: Measured and simulated maximum ozone concentrations during analysed ozone episodes for different parts of Sweden. Highest values during each episode are marked bold.

Episode days	Month	Highest measured hourly ozone concentration ($\mu g/m^3$)			Highest simulated hourly ozone concentration ($\mu g/m^3$)			Ratio simulated vs measured		
		West	East	North	West	East	North	West	East	North
2010-07-20 – 22	July	**145**	138	100	**130**	105	93	**0.90**	0.76	0.93
2010-07-10 – 12	July	196	**216**	84	140	**139**	83	0.72	**0.64**	0.99
2010-07-02 – 04	July	146	**160**	101	145	**124**	89	0.99	**0.77**	0.89
2010-06-28 – 30	June	**145**	127	104	**130**	119	91	**0.90**	0.94	0.87
2010-05-14 – 16	May	96	128	**148**	96	99	**102**	1.00	0.78	**0.69**
2009-07-03 – 05	July	**141**	109	72	**124**	117	85	**0.88**	1.08	1.18
2009-04-25 - 27	April	131	**145**	127	129	**128**	128	0.98	**0.89**	1.00
2008-06-01 - 03	June	**141**	133	122	**124**	108	96	**0.88**	0.81	0.79
Mean		143	144	107	127	117	96	0.90	0.83	0.92
Mean when highest		143	174		127	130		0.89	0.77	

4.3 Statistical post-processing study

In order to improve the modelled ozone concentrations, two approaches are applied within this study; statistical post-processing of concentrations and high-resolution modelling. In this section, a showcase from the statistical post-processing with multiple linear regression (MOS) is presented, divided into two subsections; bias correction (only measurements as predictor) and correction using measurements and other predictors.

4.3.1 Bias correction

The most basic application of MOS (Model Output Statistics, explained in more detail in Section 3.3) is simple linear regression by using measured ozone concentrations as the only predictor, i.e. correction of bias.

The results of applying this method are shown in Table 4.9. For each station, one half of the measuring period is used as training dataset, in order to calibrate the coefficients in the regression equation ($y = ax + b$). Data for the second half of the measuring period are used as a validation dataset, i.e. the post-processed concentrations from the linear regression are applied and the results are then validated against the reserved portion of the measurements.

For almost all stations the linear regression implies smaller bias than before when validated against the validation dataset. The improvements are largest for Esrange, Grimsö and Vindeln, since the systematic under-/overestimation is corrected by the regression. However, for some sites these systematic errors are not eliminated, probably due to large differences between the two datasets.

Note that the correlation coefficient is equal before and after the regression, since data only are shifted in accordance with the linear regression.

Table 4.9: *Linear regression coefficients a and b ($y = ax + b$) used in the simple linear regression (bias correction) of modelled ozone concentrations (analysis). Bias (for the validation dataset) is shown before (MATCH) and after (Reg) the linear regression. Green colour indicates improvements by MOS, red colour the reverse.*

	a	b	Bias [µg m^{-3}] 1-h average	
			MATCH	Reg
Aspvreten	0.80	10.9	2.1	1.7
Bredkälen	0.68	18.9	6.5	6.6
Esrange	0.62	31.1	-13.2	-2.2
Grimsö	0.82	4.5	5.4	0.0
Norra Kvill	0.66	22.9	-2.0	-0.2
Råö	0.69	19.5	-0.3	0.5
Vavihill	0.64	19.9	-6.6	-5.5
Vindeln	0.88	3.0	6.0	2.3

4.3.2 Correction using multiple linear regression including meteorological parameters as predictors

Another application of MOS is multiple linear regression, where more than one predictor is included in the linear regression. In this study, which can be interpreted as a showcase, the focus is on the impacts of meteorological parameters on the concentrations of ozone at the different sites.

In Table 4.10 the correlation coefficient between measured ozone concentrations and different parameters is shown for the sites included in this study (Asa and Östad are excluded since corresponding modelled concentrations are valid for other adjacent locations). According to the table, the correlation coefficient is relatively high for some meteorological parameters; temperature T_{2m} (0-0.5), wind speed ff_{10m} (0.1-0.3), relative humidity RH_{2m} (0.2-0.6) and total cloud cover tcc (0.1-0.4). In addition, there are some other parameters that correlate to the ozone concentration; concentration of nitrogen dioxide NO_2 (0.2-0.5), month (0.2-0.5) and to some extent the hour (0.1-0.2).

The importance of season and hour may reflect the impacts of solar radiation for production of ozone. The same for total cloud cover and relative humidity which likely correlates well with incoming radiation. However, an interesting fact is that the wind direction only to a smaller extent affects the concentrations of ozone (even if using trigonometric transformation) in contrast to the results in Section 4.2 which point out the importance of different source regions for the episodes of ozone. Thus, it would likely be beneficial to include wind information for levels higher than 10 meter above ground (not available from the archive analysed in our study) to appropriately capture long-range transportation in the statistical post-processing.

Table 4.10: *Correlation coefficient (r) between measured concentrations of ozone in respect to different parameters.*

	Aspvreten	Bredkälen	Esrange	Grimsö	Norra Kvill	Råö	Vavihill	Vindeln
T_{2m}	0.26	-0.05	-0.11	0.29	0.33	0.52	0.35	0.04
$Prec_{1h}$	0.01	-0.07	-0.05	-0.01	-0.06	0.01	-0.01	0.02
ff_{10m}	0.22	0.17	0.18	0.30	0.07	0.11	0.18	0.28
dd_{10m}	-0.06	0.18	0.21	0.02	-0.06	0.22	-0.03	0.06
RH_{2m}	-0.50	-0.25	-0.15	-0.56	-0.56	-0.55	-0.65	-0.36
tcc	-0.23	-0.17	-0.16	-0.23	-0.38	-0.24	-0.38	-0.11
NO_2	-0.40	-0.26	-0.19	-0.35	-0.50	-0.54	-0.48	-0.34
weekday	0.03	0.03	0.04	0.02	0.00	0.03	0.00	0.00
month	-0.27	-0.48	-0.51	-0.37	-0.36	-0.18	-0.41	-0.44
day	0.00	0.05	0.03	0.07	0.08	0.05	-0.02	0.05
hour	0.15	0.06	0.09	0.15	0.10	0.13	0.08	0.06

The chosen predictors for the multiple linear regression are presented in equation (2). In this showcase we have chosen to include wind direction as well, since it is likely that it affects the ozone concentrations, especially during high-level ozone episodes, which is the most important part to improve.

$$\begin{aligned} MATCH\_stat = {} & \mathrm{A}\cdot \mathrm{MATCH\_org} + \mathrm{B}\cdot \mathrm{T}_{2\mathrm{m}} + \mathrm{C}\cdot \mathrm{RH}_{2\mathrm{m}} + \mathrm{D}\cdot \mathrm{ff}_{10\mathrm{m}} + \mathrm{E}\cdot \mathrm{tcc} + \\ & \mathrm{F}\cdot \mathrm{NO}_2 + \mathrm{G}\cdot \sin\left(\frac{2\pi}{12}\cdot \mathrm{month}\right) + \mathrm{H}\cdot \cos\left(\frac{2\pi}{12}\cdot \mathrm{month}\right) + \mathrm{I}\cdot \sin\left(\frac{2\pi}{24}\cdot \mathrm{hour}\right) + \mathrm{J}\cdot \cos\left(\frac{2\pi}{24}\cdot \mathrm{hour}\right) + \\ & \mathrm{K}\cdot \cos\left(\frac{2\pi}{360}\cdot \mathrm{dd}_{10\mathrm{m}}\right) + \mathrm{L}\cdot \sin\left(\frac{2\pi}{360}\cdot \mathrm{dd}_{10\mathrm{m}}\right) + \mathrm{M} \end{aligned} \tag{2}$$

The regression coefficients used for each monitoring stations, respectively, are listed in Table 4.11. The same pattern can be observed for most sites regarding the signs of the coefficients, however, the magnitude varies. Thus, no general regression formula can be found which means that the regressions are site-dependent.

Table 4.11: *Multiple linear regression coefficients corresponding to equation (2), valid for different sites. MATCH_org means MATCH modelled ozone concentrations (µg m-3) for the analysis.*

	Asp-vreten	Bred-kälen	Esrange	Grimsö	Norra Kvill	Råö	Vavihill	Vindeln
A (MATCH_org)	0.67	0.38	0.42	0.55	0.28	0.59	0.42	0.56
B (T_{2m})	0.65	0.35	0.21	0.70	0.57	1.09	0.90	0.29
C (RH_{2m})	-0,20	-0.09	0.006	-0.20	-0.20	-0.21	-0.16	-0.11
D (ff_{10m})	1,63	0.03	-1.46	2.31	0.65	0.043	0.41	1.88
E (tcc)	-2,46	-4.08	-2.95	-2.53	-7.27	-1.89	-8.00	-1.70
F (NO_2)	0,63	0.89	0.45	0.24	-1.20	0.23	0.33	-0.79
G (sin month)	10,4	16.1	13.1	12.9	14.3	9.54	15.4	13.1
H (cos month)	1,74	4.49	1.06	5.40	0.60	5.19	-1.68	1.24
I (sin hour)	-0,86	1.42	-0.90	0.48	0.33	1.33	2.46	1.82
J (cos hour)	-1,35	-0.24	-0.20	-1.32	2.79	1.56	0.27	-4.26
K (cos dd10m)	0,11	0.95	1.86	0.73	-1.87	-2.51	3.34	1.65
L (sin dd10m)	2,48	-2.20	-4.10	2.10	0.45	-1.78	2.80	2.01
M	-157	-51.9	-9.45	-164	-94.1	-268	-208	-54.0

The effects of applying the regression formula are shown in Tables 4.12 and 4.13, where the post-processed calculated ozone concentrations are compared with measurements for the validation dataset (as well as modelled concentrations without applying MOS).

In general, MOS yields improved calculations, especially in terms of correlation with measurements; for all sites the correlation coefficient (regarding 1h-mean concentrations) increases to approximately 0.8. Thus, for stations with lower correlation coefficients (for instance Bredkälen, Esrange, Grimö and Vindeln) the improvements are large.

Even though the correlation increases, the results regarding other verification statistics differ substantially between the measuring sites. For Aspvreten, Esrange, Grimsö and Vindeln the overall performance improves, but for the other stations multiple linear regression might imply worse result than MATCH original concentrations. For all stations, AOT40 is underestimated by MOS. An explanation for this could be the lower range of variability of the statistically post-processed time series which is also evident from Figure 4.11. This may be a first indication of overfitting but it is also likely a result of the choice of predictors based on their correlation with the 1-hourly measurements only. While MOS gives the expected improvements for the correlation of the 1-hourly statistically post-processed values with the measurements for the validation period, it does not automatically improve other characteristics of the time series which might be more relevant for short-term forecasting of air quality. We assume that this would require a selection of predictors based on other criteria than just the linear correlation coefficient and, potentially, the inclusion of specific break points for the application of specific regression relations. Hence, it should be possible to tune the statistical post-processing method for the detection of high ozone episodes, e.g. through the calibration of a subset of the data consisting of high ozone concentrations only. It could also be interesting to test other methods such as CART analysis but this is beyond the scope of our showcase. Tuning the statistical post-processing method specifically for the detection of episodes would probably also require a longer record of predictors and measurements (in our data set there were only 8 episodes with concentrations above 140 µg m^{-3}).

Table 4.12: *Measured (obs), modelled (mod) and post-processed modelled (MOS) concentration of ozone (annual mean values, annual maximum of running 8h-mean concentration and AOT40) for different sites and years included in the study.*

	O_3 [µg m^{-3}] annual average			**O_3 [µg m^{-3}] annual max of running 8h-average**			**AOT40 [µg m^{-3} h]**		
	obs	mod	MOS	obs	mod	MOS	obs	mod	MOS
Aspvreten	53.8	56.0	54.7	129.9	111.1	109.3	3681	5244	3405
Bredkälen	51.9	58.3	55.7	110.0	117.8	95.8	348	385	6
Esrange	66.7	53.5	62.3	103.6	99.5	93.9	1217	506	333
Grimsö	51.6	59.0	50.7	183.8	132.0	105.7	9973	5000	1587
Norra Kvill	63.5	61.5	59.1	216.1	139.5	105.2	5687	4292	1759
Råö	60.1	59.8	57.6	148.6	144.9	120.3	2475	2059	572
Vavihill	59.7	53.0	50.7	195.6	140.1	102.8	4644	3046	876
Vindeln	51.8	57.8	51.6	148.1	112.9	103.5	1461	1711	113

Table 4.13: *Correlation coefficient (r), bias and root mean square error (RMSE) of the validation data set. Results are shown both for modelled ozone concentrations (mod) and post-processed modelled ozone concentrations (MOS). Green colour indicates improvements by MOS, red colour the reverse.*

	r 1h-average		**Bias [µg m^{-3}] 1-h average**		**RMSE [µg m^{-3}] 1-h average**	
	mod	MOS	mod	MOS	mod	MOS
Aspvreten	0.75	0.80	2.2	0.9	17.1	14.4
Bredkälen	0.60	0.75	6.5	3.8	13.1	9.4
Esrange	0.65	0.78	-13.2	-4.4	20.8	11.9
Grimsö	0.63	0.80	7.4	-0.9	17.5	11.4
Norra Kvill	0.68	0.80	-2.0	-4.4	14.7	11.7
Råö	0.77	0.79	-0.3	-2.5	16.1	11.7
Vavihill	0.72	0.79	-6.6	-8.9	16.6	15.7
Vindeln	0.56	0.78	6.0	-0.2	15.6	13.2

Figure 4.11 shows a time series with a comparison of measured and modelled concentrations of ozone (for both MOS and original MATCH). As illustrated in the figure, the temporal correlation increases with MOS and the lowest concentrations correlates better with measurements. However, it can also be concluded that MOS (in the present configuration) tends to decrease the highest concentrations, thus decreases the performance during ozone episodes. Using a longer training dataset that includes more ozone episode events could probably improve the results.

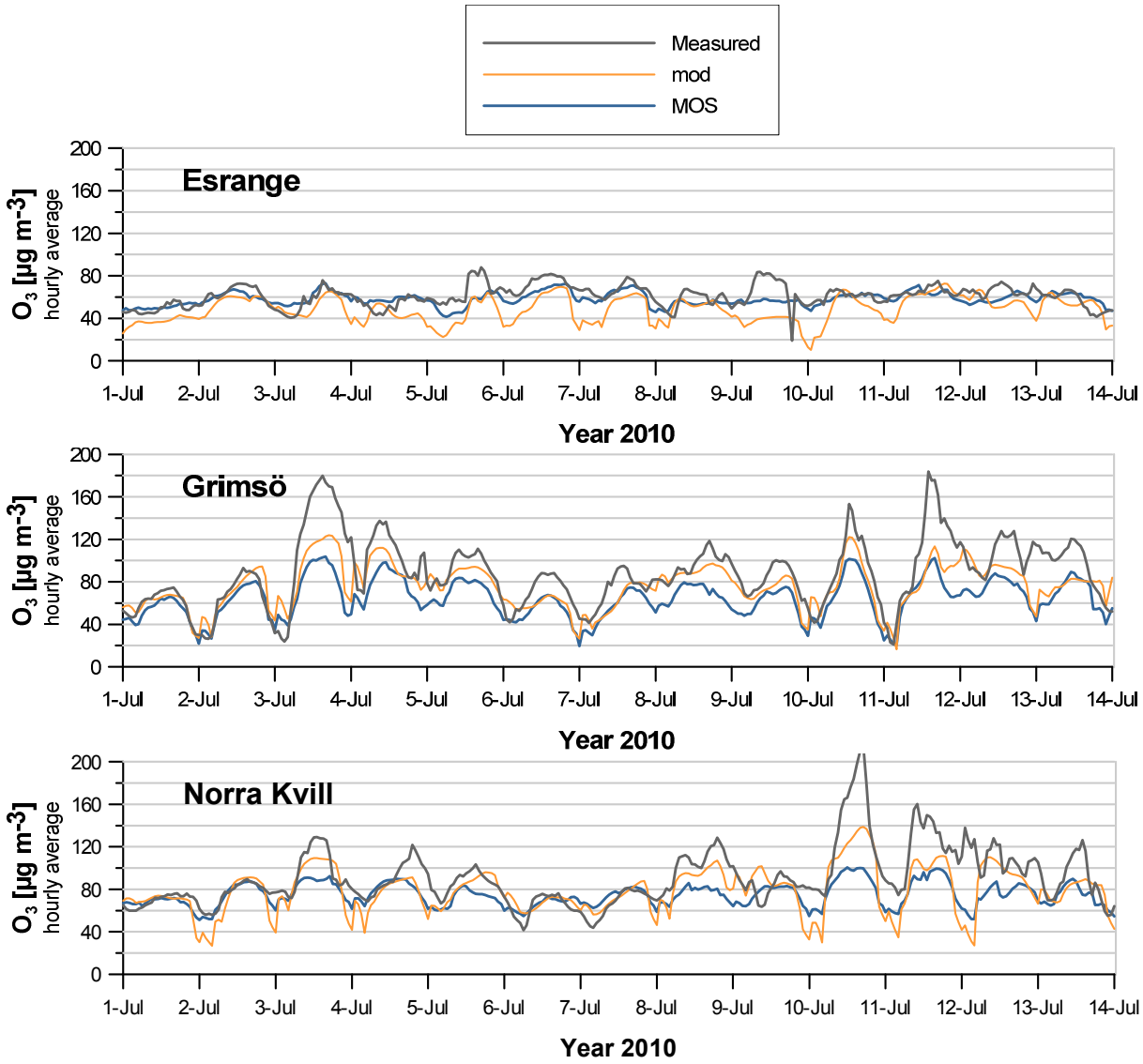

Figure 4.11: *Time series with comparison of measured and modelled concentrations of ozone during July 1 – July 14, 2010. The model results are divided into original data from MATCH (mod) and post-processed data (MOS). The evaluated period is part of the validation time window (independent data).*

A more detailed validation of the model calculations (before and after MOS) is presented in Table 4.14, where different scores are evaluated in accordance with the verification methods described in Section 3.2. Some threshold values are evaluated (60, 80 and 100 µg m-3). The reason why higher values have not been chosen is that there are too few events to give a representative score.

Most of the scores are improved by the multiple linear regression regarding the lowest threshold value. The scores of most interest are CSI and POD, since they reflect how well the high-pollution events are predicted. Higher values of these scores are better. For lower threshold levels, MOS tends to increase (i.e. improve) the values, but for higher concentrations the situation is reverse.

Table 4.14: *Scores (defined in Section 3.2) for MATCH modelled (mod) and post-processed modelled (MOS) concentrations of ozone. Green color indicates improvements by MOS, red colour the reverse. The scores analysed are: Acurracy (A), Bias (B), False Alarm Rate (FAR), Critical Success Index (CSI) and Probability of Detection (POD).*

	A	B	FAR	CSI	POD
Threshold = 60 µg m^{-3}					
Aspvreten, mod	79.5	1.2	30.4	62.3	85.5
Aspvreten, MOS	83.3	1.1	22.8	66.1	82.1
Bredkälen, mod	69.6	1.5	46.8	46.5	78.8
Bredkälen, MOS	82.3	1.1	28.1	59.4	77.2
Esrange, mod	63.9	0.6	11.6	47.6	50.7
Esrange, MOS	73.5	0.7	10.2	61.9	66.6
Grimsö, mod	72.8	1.5	43.4	51.3	84.7
Grimsö, MOS	83.7	0.9	22.1	60	72.4
N. Kvill, mod	73.0	1.0	23.7	61.1	75.5
N. Kvill, MOS	79.1	0.8	12.5	66.3	73.3
Råö, mod	78.7	1.0	21.5	66.4	81.2
Råö, MOS	78.8	0.9	16.5	64.5	73.9
Vavihill, mod	76.3	0.8	19.6	58.3	67.9
Vavihill, MOS	76.2	0.6	8.9	53.7	56.7
Vindeln, mod	72.1	1.3	40.6	51.1	78.4
Vindeln, MOS	84.1	0.9	17.2	62.8	72.2
Threshold = 80 µg m^{-3}					
Aspvreten, mod	87.4	1.1	42.2	44.1	65.1
Aspvreten, MOS	90.4	0.8	27.0	48.2	58.7
Bredkälen, mod	87.4	4.0	80.2	18.8	78.5
Bredkälen, MOS	92.6	2.2	72.3	23.7	62.0
Esrange, mod	82.2	0.5	20.8	32.7	35.8
Esrange, MOS	87.3	0.7	13.7	51.8	56.5
Grimsö, mod	86.0	1.4	51.2	39.7	67.9
Grimsö, MOS	90.6	0.5	16.5	35.5	38.2
N. Kvill, mod	84.9	1.1	41.2	45.3	66.4
N. Kvill, MOS	87.9	0.5	15.7	40.8	44.2
Råö, mod	87.1	1.5	47.4	46.1	78.9
Råö, MOS	90.9	0.8	27.6	45.9	55.6
Vavihill, mod	84.8	0.7	38.5	35.2	45.1
Vavihill, MOS	85.7	0.3	16.7	25.7	27.1
Vindeln, mod	89.0	1.2	46.6	40.0	61.5
Vindeln, MOS	91.8	0.6	23.3	39.8	45.3
Threshold = 100 µg m^{-3}					
Aspvreten, mod	97.3	0.7	71.4	13	19.2
Aspvreten, MOS	97.7	0.2	70.6	5.9	6.8
Bredkälen, mod	98.9	18.7	96.4	3.5	66.7
Bredkälen, MOS	99.9	-	-	-	-
Esrange, mod	98.1	0.2	50.0	7.8	8.4
Esrange, MOS	98.0	-	-	-	-
Grimsö, mod	96.8	0.9	72.0	15.5	25.9
Grimsö, MOS	97.9	0.1	0	7.9	7.9
N. Kvill, mod	95.8	1.2	69.1	20.3	37.2
N. Kvill, MOS	97.2	-	-	-	-
Råö, mod	96.8	1.5	56.6	35.2	65.1
Råö, MOS	97.8	0.3	13	21.6	22.3
Vavihill, mod	96.9	0.7	45.9	29.1	38.6
Vavihill, MOS	96.7	-	-	-	-
Vindeln, mod	99.1	1.6	96.6	2.1	5.3
Vindeln, MOS	99.5	0.2	-	-	-

It is important to note that our study is just a first showcase; a more thorough analysis would require a longer consistent time series. Here we a priori choose regression as method because it is the gold standard (according to Kalney, 2003) and because it is used in operational weather forecasting. Other methods (e.g. adaptive methods such as Kalman filtering) could be tested in a follow-up study. In a future study, it could also be interesting to investigate differences between seasons, i.e. using different regression formulas for winter and summer conditions or other specific characteristics (break points). Furthermore, it should be interesting for future projects to look at results from, in particular, the MACC reanalysis once a longer time slice of MACC-reanalyses has been produced.

4.4 High-resolution modelling study

As discussed in Sections 4.1 and 4.2, the performance of MATCH is generally quite good although a particular challenge lies in the correct simulation of high ozone concentrations. Running MATCH on higher resolution, with a more detailed land-surface classification and more detailed emissions, yields similar or improved statistical scores, see Tables 4.15 and 4.16. For both the European-scale version (in the comparison here called MATCH-EU) and the high-resolution version of MATCH (here called MATCH-SWE) the scores are better for the daily maximum of running 8h-mean concentrations than for the hourly concentrations. This is related to the meteorological model's and the chemical transport model's disability to realistically describe the stable, low mixing situations during night-time. The daily maximum of running 8h-mean concentrations are related to the well mixed boundary layer, which occurs during day-time. However, the night-time ozone concentrations are typically lower and thus not as relevant from the perspective of human health impacts or vegetation damage.

Running MATCH at a higher horizontal resolution generally results in improved temporal correlation both for the hourly values as well as the daily maximum of running 8h-mean concentrations. An obvious exception is the station Råö. Bias and RMSE are slightly improved in MATCH-SWE compared to MATCH-EU.

While the overall statistics are slightly better in MATCH-SWE, the ability to reproduce high-ozone episodes is not improved. Figure 4.12 shows time-series of observed and modelled ozone during early July 2010, when the information threshold of 180 $\mu g\ m^{-3}$ was exceeded at several stations in southern Sweden. MATCH-EU produces slightly higher ozone values than MATCH-SWE, but both model configurations severely underestimate the highest ozone concentrations at Norra Kvill and Vavihill on 10 July. Figure 4.13 shows the spatial distribution of the calculated daily maximum of 1-hour concentration over Sweden during 10 July 2010 and 11 July 2010 for MATCH-EU and MATCH-SWE. Although the two simulations use very different emission and different land-surface classification the results are not significantly different for this particular case. While the simulation with lower resolution provides less spatial detail it manages to produce slightly higher ozone concentrations in southern Sweden during the investigated episode.

Table 4.15: *Observed and modelled annual average of hourly mean, annual average of daily maximum of running 8h-mean and day-time AOT40 at selected Swedish monitoring stations during 2010. Model results are from the "analyses" in the European scale simulation (EU) and the high- resolution configuration (SWE). For some stations measurements for the last months of 2010 were not available and these periods are thus excluded in the analysis.*

	O_3, 1h-mean [µg m^{-3}]			**O_3, daily max of running 8h-mean [µg m^{-3}]**			**AOT40 (May – July) [µg m^{-3} h]**		
	Obs	EU	SWE	Obs	EU	SWE	Obs	EU	SWE
Asa. 2010	53.6	64.5	66.1	69.8	76.4	76.9	4768	6483	7502
Bredkälen.2010	57.2	66.5	62.5	65.4	74.8	72.3	648	910	2630
Esrange. 2010	72.4	59.9	60.8	79.1	68.0	69.5	2018	655	1935
Grimsö. 2010	60.3	68.1	65.4	74.9	79.0	76.5	10345	4819	5409
N. Kvill. 2010	70.2	69.8	69.2	80.6	81.1	79.8	8550	5733	6698
Råö. 2010	65.4	66.6	72.1	77.6	80.7	82.6	7687	10623	8857
Vavihill. 2010	68.0	59.5	69.6	81.5	76.2	81.7	9374	8191	9677
Vindeln. 2010	57.7	65.1	63.5	69.3	73.4	72.0	2483	813	2469

Table 4.16: *Summarizing statistics of the hourly values and the daily maximum of running 8h-mean for all hours or days with observations during 2010. Green colour indicates improvements by high resolution modelling, red colour the reverse.*

	Hourly values						**Daily maximum of running 8h-mean**					
	correlation coefficient		**Bias [µg m^{-3}]**		**RMSE [µg m^{-3}]**		**correlation coefficient**		**bias [µg m^{-3}]**		**RMSE [µg m^{-3}]**	
	EU	SWE	EU	SWE	EU	SWE	EU	SWE	EU	SWE	EU	SWE
Asa. 2010	0.57	0.68	10.8	12.5	23.4	18.2	0.66	0.77	6.5	7.1	15.9	13.9
Bredkälen.2010	0.40	0.55	9.3	5.3	20.5	18.2	0.44	0.52	9.4	6.9	17.2	16.3
Esrange. 2010	0.55	0.61	-12.5	-11.6	20.5	20.1	0.62	0.63	-11.1	-9.6	17.2	16.6
Grimsö. 2010	0.47	0.74	7.8	5.2	24.0	17.1	0.58	0.78	4.1	1.6	18.5	13.6
N. Kvill. 2010	0.52	0.68	-0.4	-1.0	18.2	14.2	0.64	0.78	0.6	-0.8	14.2	11.0
Råö. 2010	0.72	0.46	1.2	6.7	15.8	21.2	0.81	0.66	3.1	5.0	11.6	15.3
Vavihill. 2010	0.65	0.65	-8.5	1.6	20.2	16.7	0.76	0.73	-5.2	0.2	13.5	12.7
Vindeln. 2010	0.39	0.71	7.4	5.8	23.3	17.0	0.51	0.75	4.1	2.8	16.2	12.0

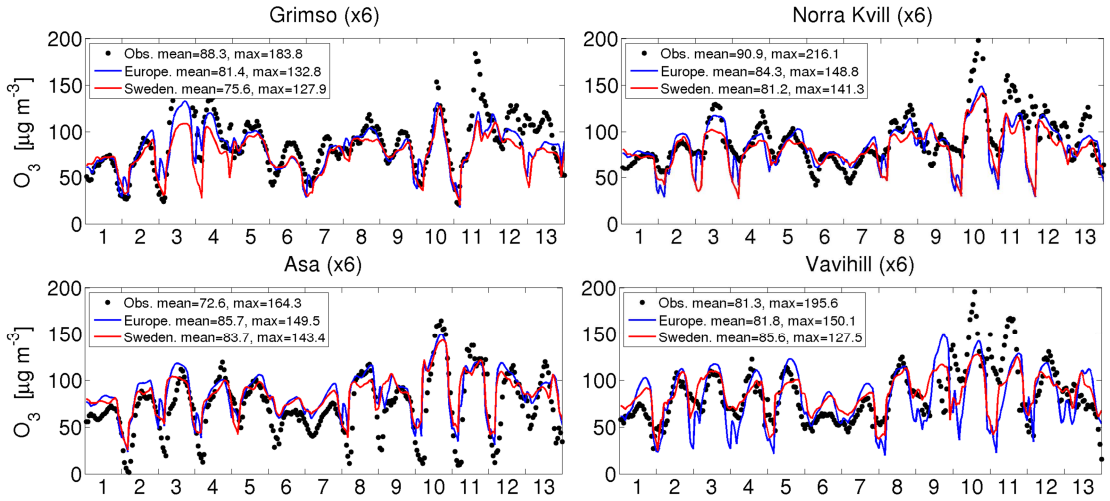

Figure 4.12: *Time-series of observed and modelled near-surface concentration of ozone at Grimsö, Norra Kvill, Asa and Vavihill 1-13 July, 2010. Europe and Sweden refer to the Europan and Swedish configuration of MATCH, respectively. Mean and max in the legend indicate the average and maximum concentration for the period displayed.*

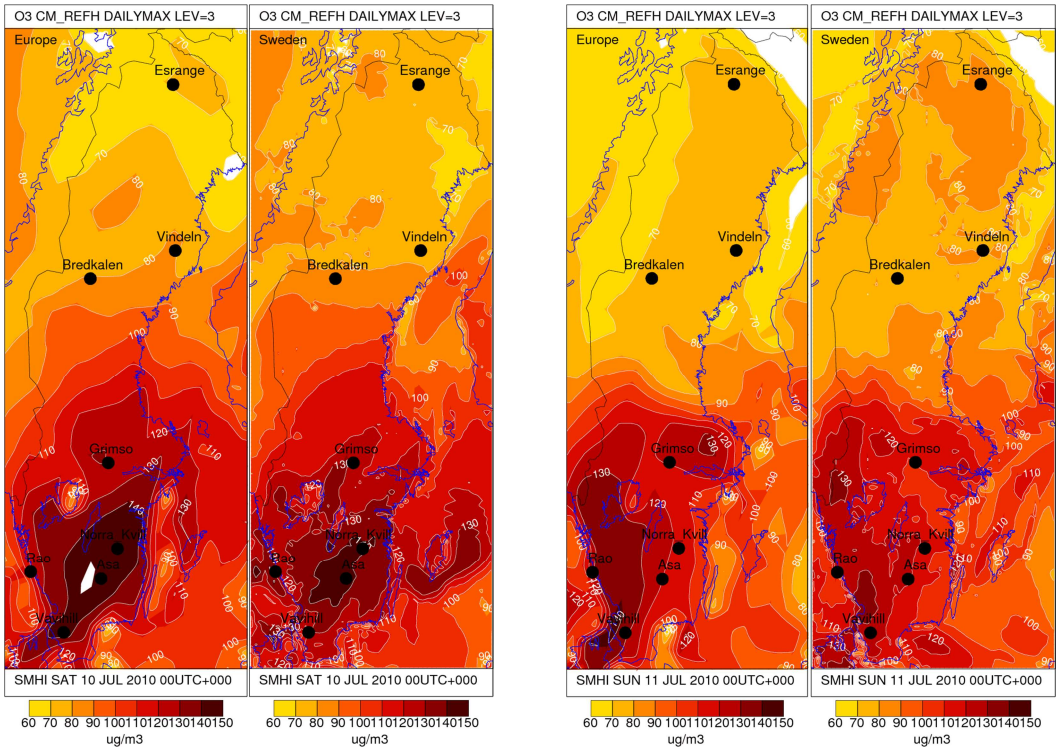

Figure 4.13: *Calculated daily maximum (of 1h-mean) near-surface ozone concentration in the European-scale (left panels) and high-resolution Swedish (right panels) MATCH setup. Left pair is 10 July 2010; right pair is 11 July 2010.*

The higher temporal correlation in the finer-resolution version of MATCH reflects the model's ability to describe smaller scale features occurring on finer temporal and spatial scales. The fact that the very high values during the episode for 10 to 11 July at, e.g., Norra Kvill, are not reproduced in any of the modelling systems suggests that these high ozone concentrations emanate from ozone precursors emitted outside Sweden and probably not included in the European-scale emissions inventory used for MATCH-EU.

5 Conclusions

- ***Overall performance of MATCH for ozone very good***

High concentrations of ground-level O_3 such as exceedances of the public information threshold occur less frequently in Sweden than in, e.g., central and southern Europe. Nevertheless, ozone is an issue even for Sweden, affecting both human health and vegetation. In our study we assess the existing capabilities for forecasting and informing on ground-level ozone in Sweden. The evaluation of the operational chemical transport model MATCH shows overall very good results, and it is obvious that the model already in its present configuration easily meets the data quality objectives regarding modelling uncertainty as required in the EU air quality directive 2008/50/EC (see also Engardt et al., 2010a, Sjöberg et al., 2010). Overall, the results of our evaluation are in line with previous model evaluations in different intercomparison studies [e.g., van Loon et al. (2007 and 2004), Hass et al. (2003), Tilmes et al., (2002)] and in international projects such as MACC and its precursor GEMS (e.g. Agnew et al., 2007, GEMS, 2010 as well as personal communication within the modelling communities).

- ***High-resolution model setup needs thorough calibration***

From an operational forecasting perspective it is clearly desirable to further improve the prediction of ozone episodes. Like most other European models, the current operational MATCH-versions at SMHI still run at relatively coarse resolutions (0.4°, 0.5°, and, since early 2011, 0.2°). The GEMS final report (GEMS, 2010) specifically recommends the target resolution of approximately 10km over Europe as an important objective for further work. Our findings support that recommendation and indicate the potential of higher resolution runs, but they also show that an additional calibration/tuning of the model setup will be necessary in order to fully transfer increased resolution into increased added value for operational forecasting. As a result of the efforts committed to calibrating/tuning the European-scale models over many years, it is not easy to outperform those model configurations by simply increasing the spatial resolution.

- ***Ozone episodes still a challenge for models***

In our study for the years 2008-2010 we find eight episodes with relatively high ozone concentrations. Overall, the MATCH-model has a tendency to underestimate the highest ozone concentrations and appears to have more difficulties with ozone episodes occurring in the eastern parts of Sweden, although our analysis can just be indicative due to the limited amount of available data. The episodes analysed in our study confirm the general pattern of ozone episodes in Sweden, where either ozone and/or its precursors are imported from the continent. As a consequence, it is practically impossible to reproduce ozone episodes with high-resolution models for Sweden if the forcing European-scale model lacks any signal of the ozone episodes. However, the improvement of model resolution clearly helps to provide a more realistic description of the physiography and specific resolution-dependent processes in the model (e.g. deposition) and gives overall slightly better temporal correlation and in particular a more realistic spatial representation than the European-scale model. The latter is desirable for, e.g., longer term environmental assessments, but is does not solve the issue with the underprediction of ozone episodes. In the scientific literature (e.g. Kukkonen et al., 2011 and 2009) and in discussions within current research communities [e.g. COST ES0602 (COST ES0602, 2011), MACC/GEMS] a variety of other potential sources of error are suggested. The latter include incomplete or erroneous emissions, representativeness issues, oversimplifications in the model's physical or chemical processes, the lack of data assimilation and initialization and oversimplified boundary conditions. In the MATCH-HIRLAM operational model analysed in the present study, there is no direct coherence of ozone concentrations in the model and observed concentrations other than through climatological values used as boundaries and within the parameterization of processes. Starting the model integration from a model state which is closer to the observed state can be expected to yield significant improvements. This is one of the

topics investigated in the FP7-project MACC, where significant efforts are dedicated to include (or improve) data assimilation and initialization in European-scale air quality models. Through the core services established in MACC it will be possible to establish a full chain of coupled atmospheric concentration and air quality modelling, ranging from global models via European-scale models to high-resolution models for the specific area of interest, in our case Sweden. In addition to the continuous improvements of the individual models during the coming years, it is thus necessary to improve the coupling of the existing systems. For Sweden this implies work on the establishment of operational high-resolution MATCH-HIRLAM simulations, nested into MATCH-ECMWF, which participates in the MACC regional cluster of air quality models and uses boundary values from the global MACC-products.

- ***Statistical postprocessing a promising technique***

In addition to the improvement of models, their nesting at different scales and their direct integration with observations, the method of statistical post-processing can be used to further improve model output. For the experiments performed in our study we chose model output statistics, i.e. regression as method. While this is a well-approved technique in the domain of meteorology it comes with the disadvantage that it requires a thorough calibration against a consistent long-term archive of data. As the amount of data available for our study is limited to 2 ½ years of data, our results are only indicative but they clearly show the potential of the technique. While it is relatively easy to improve the correlation of model and measurements with this method through the choice of predictors with a high correlation with the measurements, this does not necessarily result in the improvement of other relevant characteristics of the forecast. We thus propose to further explore this technique in possible follow-up projects, using a longer time series of consistent model data and observations for the calibration and validation. Both from a scientific and from an operational forecasting perspective it should be very interesting to perform a high-resolution reanalysis of a longer time period, using e.g. results from European-scale MACC-reanalyses as boundary values, once a longer time slice from MACC is available. The high-resolution reanalysis could then be used for the calibration and validation of statistical post-processing methods. Another idea for a post-processing technique that could not be explored in the current project is to use orography or relative orography for the downscaling of MATCH-output, e.g. through the application of the technique used by Klingberg et al. (2011).

- ***Swedish ozone forecast and information capabilities advancing***

In summary it can be concluded that the existing forecast and monitoring capabilities for ground-level ozone in Sweden provide a valuable basis for operational information and warning services. The current density of ozone monitoring stations, together with the existing model systems, give a good description of ozone concentrations for the operational information and warning services, although selected complementary sites might give further improvements (Engardt et al., 2010a, Sjöberg et al., 2010). Through the GMES-initiative operational global and European-scale atmospheric composition and air quality services are implemented and will be available for use at the national level. The latter is an opportunity to build a nested chain of air quality models from the global scale via the European scale down to the Swedish national and potentially sub-national scale. Within such a configuration, the national and sub-national air quality systems could be operated at very high resolution (even higher than in the present study) in order to resolve more details in physiography and thus provide more realistic forecasts at the local scale. GMES operational core services can be expected to be advanced continuously, both through scientific and technological improvements of the models (e.g., assimilation, initialization and model physics and chemistry) and their indata (e.g., the improvement of emission data bases, enhanced use of remote sensing products). The latter will ensure a continuous improvement of the boundary conditions for the national and sub-national systems and thus also lead to continuous advances of the national and sub-national high-resolution forecast and information services (see e.g. Engardt et al., 2010a and 2010b for further examples on high-resolution modelling of air quality in Sweden, in addition to Section 4.4 in this report).

6 Acknowledgements

This project was financed by the Swedish Environmental Protection Agency under contract 211 1033.

The Swedish Environmental Protection Agency financed the national O_3 monitoring network run by IVL (7 monitoring stations) and partly the measurements at Östad, the latter together with the county administration of Västra Götaland. The O_3 measurements at Asa are financed by the regional air quality protection associations in Kronoberg and Jönköping County. Ozone measurements at Norr Malma are funded by Stockholm and Uppsala County air quality management association. Measurements of ozone concentrations at Prestebakke are financed by Statens Forurensningstilsyn (SFT) in Norway and data are used with permission from Tor Johannesen. Data have been obtained from NILU.

The use of air mass trajectories retrieved from the EMEP-webpage is acknowledged. The trajectories are calculated using the Flextra model developed by Andreas Stohl (NILU) in cooperation with Gerhard Wotawa and Petra Seibert (Institute of Meteorology and Geophysics, Vienna) and using meteorological data provided from ECMWF (European Centre for Medium Range Weather Forecast).

The idea for this project evolved through the cooperation of SMHI and IVL in the international research framework COST ES0602. In particular, the exchange with many international experts from other member states on experiences and scientific and technological know-how in building, operating and evaluating air quality forecast and information systems was very fruitful for this project.

The authors of the present report thank Joakim Langner (SMHI) for valuable comments.

7 References

Agnew, P, Mittermaier, M, Honore, C., Coll, I, Vautard, R., Elbern, H., and Peuch, V.H., 2007. Evaluation of GEMS Regional Air Quality Forecasts. Available from http://gems.ecmwf.int/documents/index.jsp, last access 2011-05-11.

Andersson, C., Langner, J., and Bergstrom, R., 2007. Interannual variation and trends in air pollution over Europe due to climate variability during 1958–2001 simulated with a regional CTM coupled to the ERA40 reanalysis. *Tellus*, **59B**, 77-98.

Berge, E., 1993. Coupling of wet scavenging of sulphur to clouds in a numerical weather prediction model, *Tellus*, **45B**, 1-22.

Bott, A., 1989. A positive definite advection scheme obtained by non-linear renormalization of advective fluxes, *Month. Weath. Rev.*, **117**, 1006-1015.

Carter, W. P. L., 1996. Condensed atmospheric photo oxidation mechanisms for isoprene, *Atm. Env.*, **30,** 4275-4290.

COST ES0602, 2011. COST Action ES0602: Towards a European Network on Chemical Weather Forecasting and Information Systems (ENCWF). http://www.chemicalweather.eu, last access 2011-05-11.

Denby, B., Georgieva, E., Larssen, S., Guerreiro, C., Li, L., Douros, J., Moussiopoulos, N., Fragkou, L., Gauss, M., Olesen, H., Miranda, A.I., Dilara, P., Thunis, P., Lappi S., Rouil, L., Lükewille, A., Querol, X., Martin, F., Schaap, M., van den Hout, D., Kobe, A., Silibello, C., Vincent, K., Stedman, J., Gonçalves, M., Pirovano, G., Volta, L., van Pul, A., Ortiz, A.G., Roberts, P., Oettl, D., and Jericevic, A., 2010. Guidance on the use of models for the European Air Quality Directive. A working document of the Forum of Air Quality Modelling in Europe (FAIRMODE). ETC/ACC report, No. 6.2, 11/10/2010.

EC, 2002. Directive 2002/3/EC of the European Parliament and of the Council of 12 February 2002 relating to ozone in ambient air. Available from http://eur-lex.europa.eu/LexUriServ/LexUriServ.do?uri=OJ:L:2002:067:0014:0030:EN:PDF, last access 2011-08-24.

EC, 2008. Directive 2008/50/EC of the European Parliament and of the Council of 21 May 2008 on ambient air quality and cleaner air for Europe. Available from http://eur-lex.europa.eu/LexUriServ/LexUriServ.do?uri=CELEX:32008L0050:EN:NOT, last access 2011-08-24.

EEA, 2007. Air pollution in Europe 1990-2004. EEA Report No 2/2007. EEA, Copenhagen, Denmark.

Engardt, M., Siniarovina, U., Khairul, N.I. and Leong, C.P., 2005. Country to country transport of anthropogenic sulphur in Southeast Asia. *Atm. Env.*, **39**, 5137-5148.

Engardt, M. Jonsson, Å., Sjöberg, K., and Klein, T., 2009. The MATCH Air Quality Forecast and Information System (MAQS). Report to the Swedish Environmental Protection Agency, 2009.

Engardt, M., Andersson, C. and Bergström, R., 2010a. Modellering av marknära ozon. Regionala och högupplösta tillämpningar av MATCH. Swedish Meteorological and Hydrological Institute, SMHI Meteorologi Nr 145, 27 pp. (In Swedish, English summary).

Engardt, M., Andersson, S., Gidhagen, L., Johansson, C., and Örtegren, L., 2010b. GASLINK - linking the GMES Pilot Atmospheric core Service (GAS) with the Stockholm Air Quality Service. Report to the Swedish National Space Board, 30 November 2010.

FLEXPART, 2011. Homepage of the FLEXPART and FLEXTRA models at the Norwegian Institute for Air Research (NILU). http://transport.nilu.no/flexpart, last access 2011-05-10.

GEMS, 2010. A Monitoring and Forecasting System for Atmospheric Composition. Final report of the project GEMS: Global and regional Earth-system Monitoring. Available from http://gems.ecmwf.int/do/get/PublicDocuments/1529/1434?showfile=true, last access 2011-05-10.

Gidhagen, L., Johansson, C., Langner J. and Foltescu, V.L. 2005. Urban scale modeling of particle number concentration in Stockholm. *Atm. Env.*, **39**, 1711-1725.

GMES, 2011. Global Monitoring for Environment and Security. www.gmes.info, last access 2011-05-09.

Hass, H., van Loon, M., Kessler, C., Stern, R., Matthijsen, J., Sauter, F., Zlatev, Z., Langner, J., Foltescu, V., and Schaap, M., 2003. Aerosol Modelling: Results and Intercomparison from European Regional-scale Modelling Systems EUROTRAC ISS, Munich, EUROTRAC-2 Special Report, 77 pp.

HYSPLIT, 2011. Hybrid Single Particle Lagrangian Integrated Trajectory Model. http://ready.arl.noaa.gov/HYSPLIT.php, last access 2011-05-10.

Kalney, E., 2003. Atmospheric modeling, data assimilation and predictability. Cambridge University Press, Cambridge. 341 pp.

Karlsson, P.E., Pleijel, H., Danielsson, H., Pihl Karlsson, G., Piikki, K., and Uddling, J., 2009. Evidences for impacts of near-ambient ozone concentrations on vegetation in southern Sweden. *Ambio*, **8**, 425-431.

Klingberg, J. Karlsson, P.E., Pihl Karlsson, G., Hu, Y., Chen, D., and Pleijel, H., 2011. Variation in ozone exposure in the landscape of southern Sweden with consideration of topography and coastal climate. Submitted to *Atm. Env.*

Kukkonen, J., T. Klein, K. Karatzas, K. Torseth, A. Fahre Vik, R. San Jose, T. Balk, and M. Sofiev, 2009. COST ES0602: Towards a European network on chemical weather forecasting and information systems, *Adv. Sci. Res.*, **3**, 27-33.

Kukkonen, J., T. Balk, D. M. Schultz, A. Baklanov, T. Klein, A. I. Miranda, A. Monteiro, M. Hirtl, V. Tarvainen, M. Boy, V.-H. Peuch, A. Poupkou, I. Kioutsioukis, S. Finardi, M. Sofiev, R. Sokhi, K. Lehtinen, K. Karatzas, R. San José, M. Astitha, G. Kallos, M. Schaap, E. Reimer, H. Jakobs, and K. Eben, 2011. Operational, regional-scale, chemical weather forecasting models in Europe, *ACPD*, **11**, 5985–6162.

Langner, J., Robertson, L., Persson, C., and Ullerstig, A. 1998a. Validation of the operational emergency response model at the Swedish meteorological and hydrological institute using data from ETEX and the Chernobyl accident. *Atm. Env.*, **32**, 4325-4333.

Langner, J., Bergström R., and Pleijel, K., 1998b. European scale modeling of sulphur, oxidized nitrogen and photochemical oxidants. Model development and evaluation for the 1994 growing season. SMHI-report RMK No. 82, SMHI, Norrköping, Sweden.

Langner, J., Bergström R., and Foltescu V.L., 2005. Impact of climate change on surface ozone and deposition of sulphur and nitrogen in Europe. *Atm. Env.* **39**, 1129-1141.

MACC, 2011. Monitoring Atmospheric Composition and Climate. www.gmes-atmosphere.eu, last access 2011-05-09.

MAQS, 2011. MATCH Air Quality Forecast and Information System, www.airviro.smhi.se/MAQS, last access 2011-05-09.

Persson, C., and Kahnert, M. 2006. Återanalys av föroreningsdepositionen till Sverige 2002-2004. SMHI Rapport 2006 Nr. 8, 8 pp. (In Swedish).

Robertson, L., Langner, J., and Engardt, M., 1999. An Eulerian limited-area atmospheric transport model. *J. Appl. Meteor.*, **38**, 190-210.

Simpson, D., Andersson-Sköld, Y. and Jenkin, M.E., 1993. Updating the chemical scheme for the EMEP MSC-W oxidant model: current status, EMEP MSC-W Note 2/93.

Simpson, D., Guenther, A., Hewitt, C.N., and Steinbrecher, R., 1995. Biogenic emissions in Europe. 1. Estimates and uncertainties. *J. Geophys. Res.*, **100**, 22875-22890.

Sjöberg, K., Karlsson, P.E and Haeger-Eugensson, M., 2010. Förslag till nationellt övervakningsprogram för marknära ozon. Rapport U2325. (In Swedish).

Stohl, A., Haimberger, L., Scheele, M.P., and Wernli, H., 1999. An intercomparison of results from three trajectory models. *Meteor. Appl.*, **8**, 127-135.

Tang, L., Chen, D., Karlsson, P.E., Gu, Y., and Ou, T. 2009a. Synoptic circulation and its influence on spring and summersurface ozone concentrations in southern Sweden. *Boreal Env. Res.*, **14**, 889-902.

Tang, L., Karlsson, P.E., Gu, Y., Chen, D., Grennfelt, P. 2009b. Synoptic weather types and long-range transport patterns for ozone precursors during high-ozone events in southern Sweden. *Ambio*, **8**, 459-464.

Tilmes, S., Brandt, J., Flatøy, F., Bergström, R., Flemming, J., Langner, J., Christensen, J.H., Frohn, L.M., Hov, Ø., Jacobsen, I., Reimer, E., Stern, R., and Zimmermann, J., 2002. Comparison of Five Eulerian Air Pollution Forecasting Systems for the Summer of 1999 Using the German Ozone Monitoring Data. *J. Atm. Chem.*, **42**, 91-121.

Tuovinen J-P., 2000. Assessing vegetation exposure to ozone: properties of the AOT40 index and modifications by deposition modelling. *Environmental Pollution*, **109**, 361-372.

US-EPA, 2003. Guidelines for Developing an Air Quality (Ozone and PM2.5) Forecasting Program. EPA-456/R-03-002, June 2003. Available from http://www.epa.gov/airnow/aq_forecasting_guidance-1016.pdf, last access 2011-05-09.

van Loon, M., Roemer, M.G.M., Builtjes, P.J.H., Bessagnet, B., Rouil, L., Christensen, J., Brandt, J., Fagerli, H., Tarrasson, L., Rodgers, I., Teasdale, I., Stern, R., Bergström, R., Langner, J., and Foltescu, V., 2004. Model inter-comparison. In the framework of the review of the unified EMEP model, TNO-report, TNO-MEP - R 2004/282, 53 pp.

van Loon, M., Vautard, R., Schaap, M., Bergström, R., Bessagnet, B., Brandt, J., Builtjes, P.J.H., Christensen, J., Cuvelier, K., Jonson, J.E., Krol, M., Langner, J., Roberts, P., Rouil, L., Stern, R., Tarrasón, L., Thunis, P., Vignati, E., White, L., and Wind, P., 2007. Evaluation of long-term ozone simulations from seven regional air quality models and their ensemble. *Atm. Env.*, **41(10)**, 2083-2097.

WHO, 2004. Health aspects of air pollution: Results from the WHO project "Systematic review of health aspects of air pollution in Europe". WHO Regional Office For Europe, Copenhagen, Denmark. Available from http://www.euro.who.int/document/E83080.pdf, last access 2011-05-09.

Wilks, D.S., 2006. Statistical Methods in the Atmospheric Sciences. Second Edition. Volume 91 in the International Geophysics series, 627pp. ISBN: 978-0-12-751966-1.

8 Appendix

8.1 Additional material for the evaluation of MATCH-HIRLAM against Swedish in-situ ozone measurements

Figure 8.1a-8.1ab: *Comparison between measured and modelled concentrations of ozone. Results are presented as time series and scatterplots, where the latter are shown both for 1-h mean concentrations as well as 8-h running mean values. In the time series, modelled concentrations are shown, respectively, for analysis, forecast of 1st day and forecast of 2nd day. The sub-panels of the figure are sorted by station and year (2008, 2009 and 2010).*

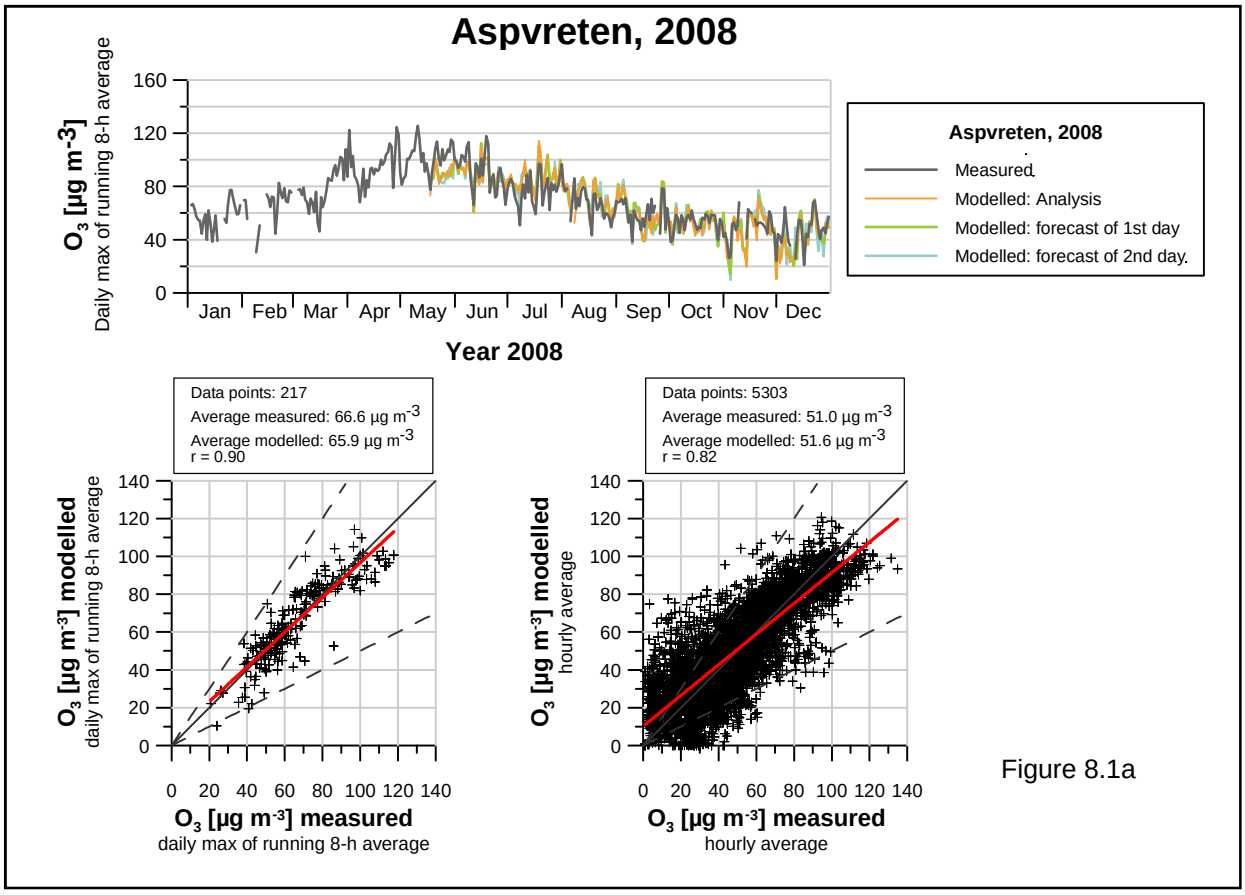

Figure 8.1a

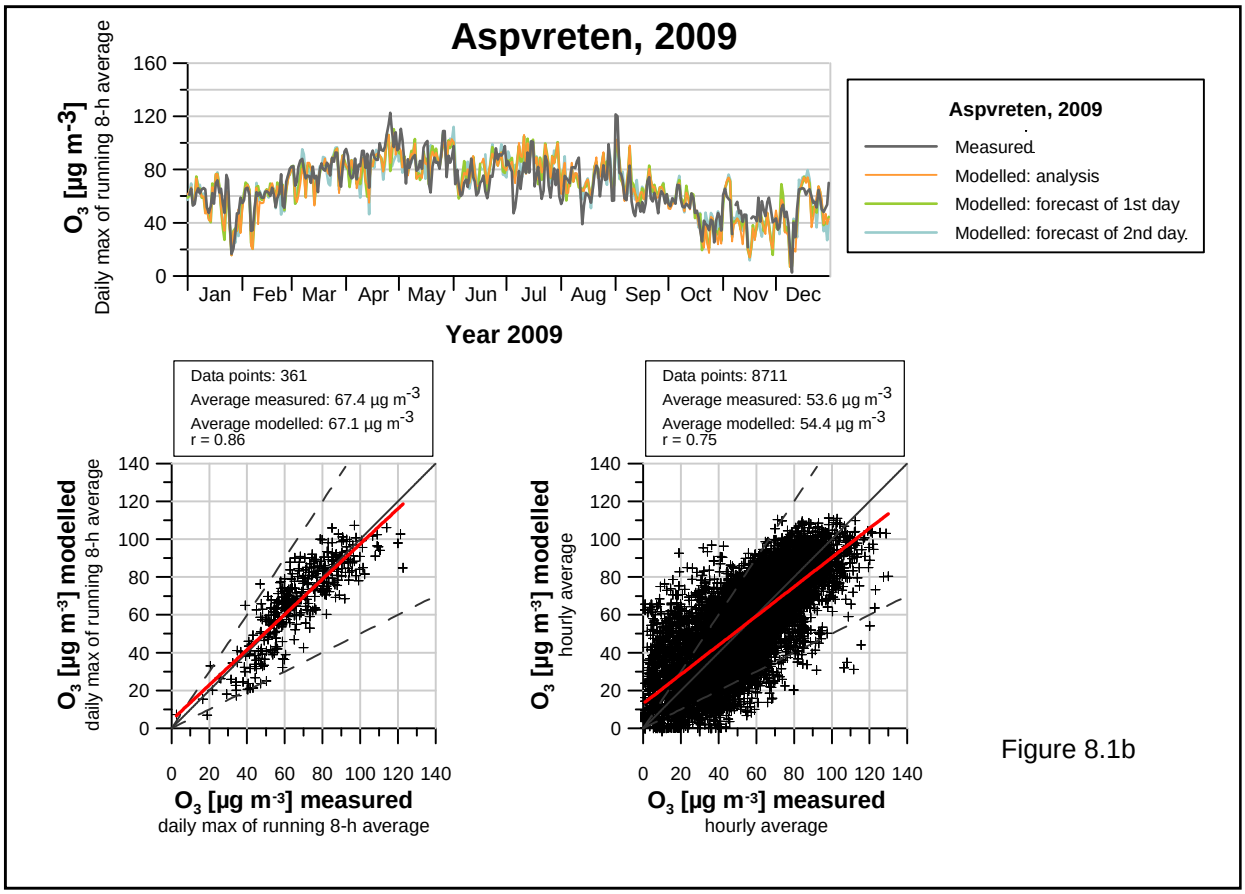

Figure 8.1b

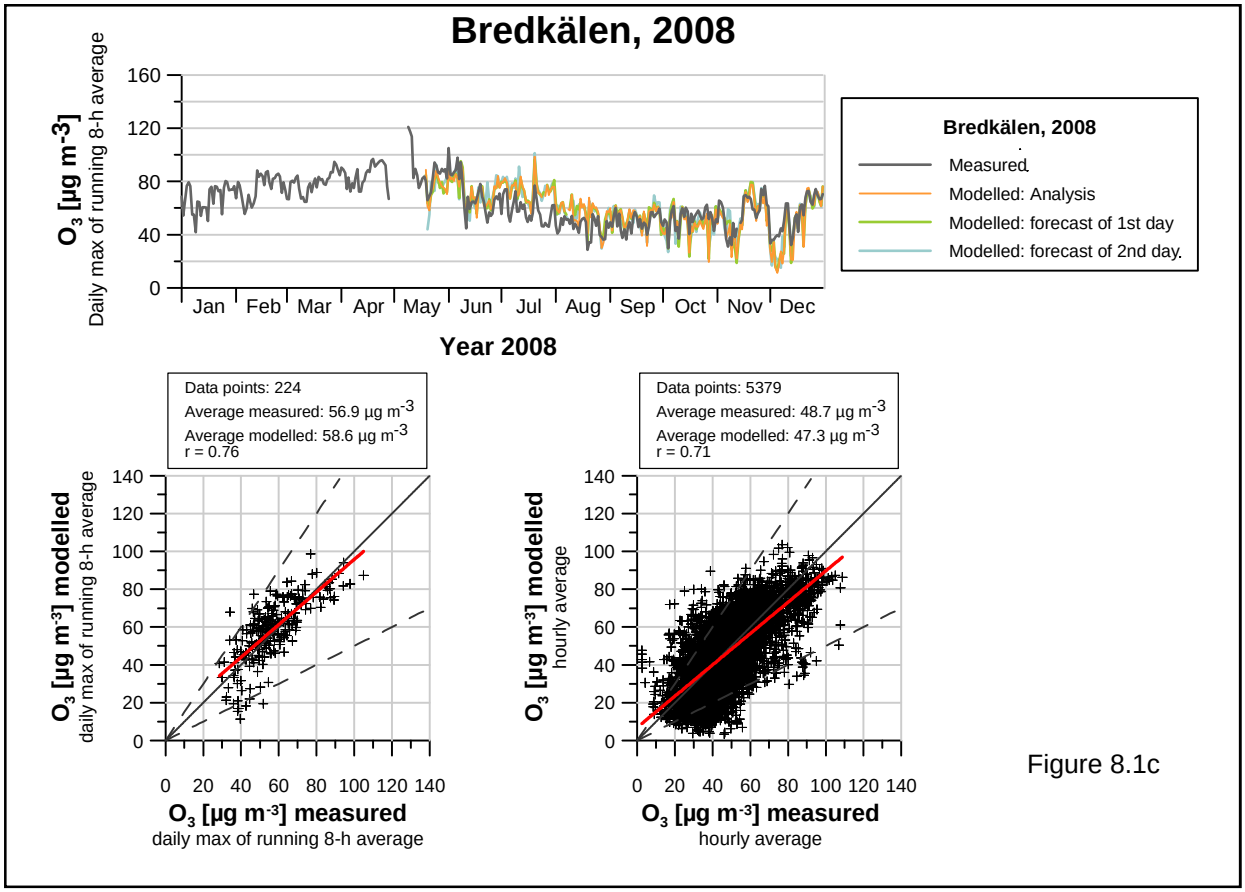

Figure 8.1c

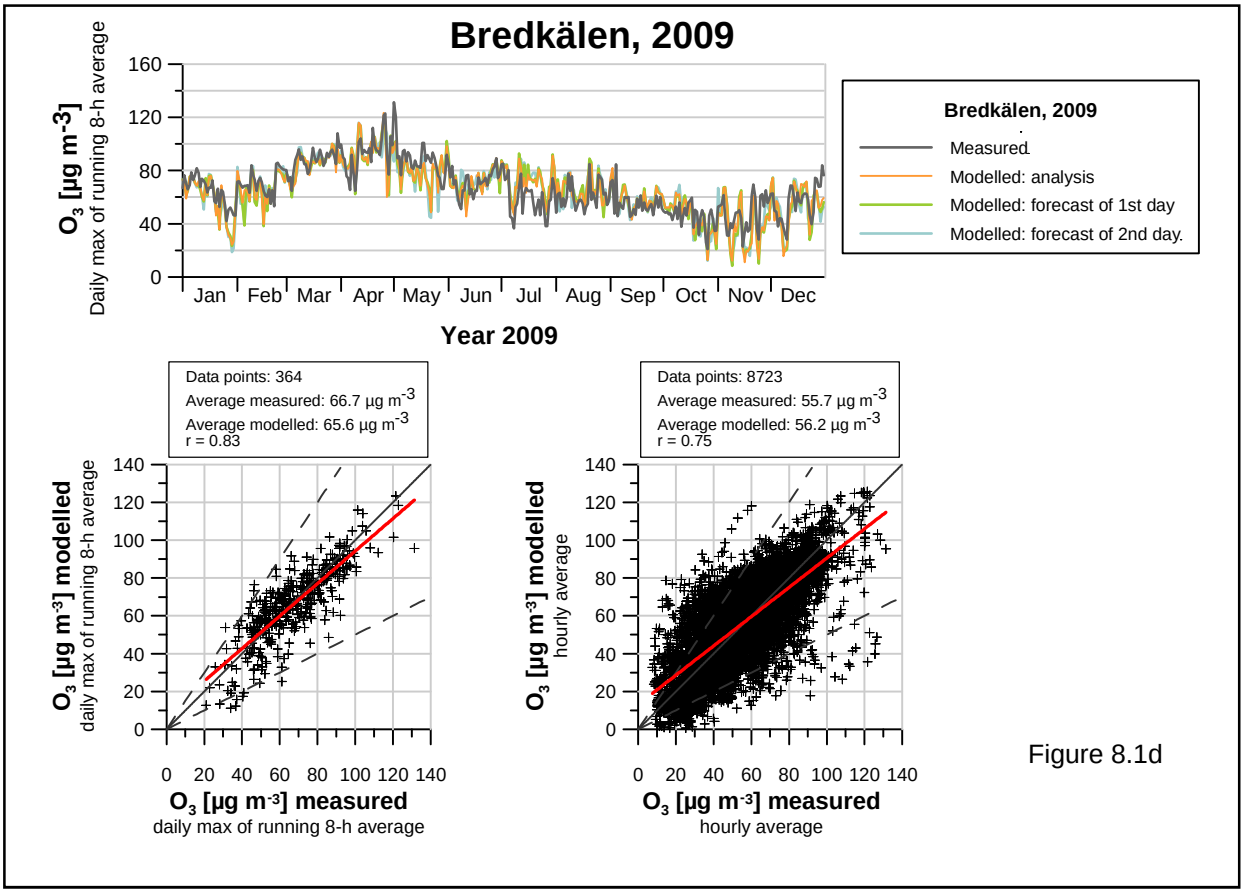

Figure 8.1d

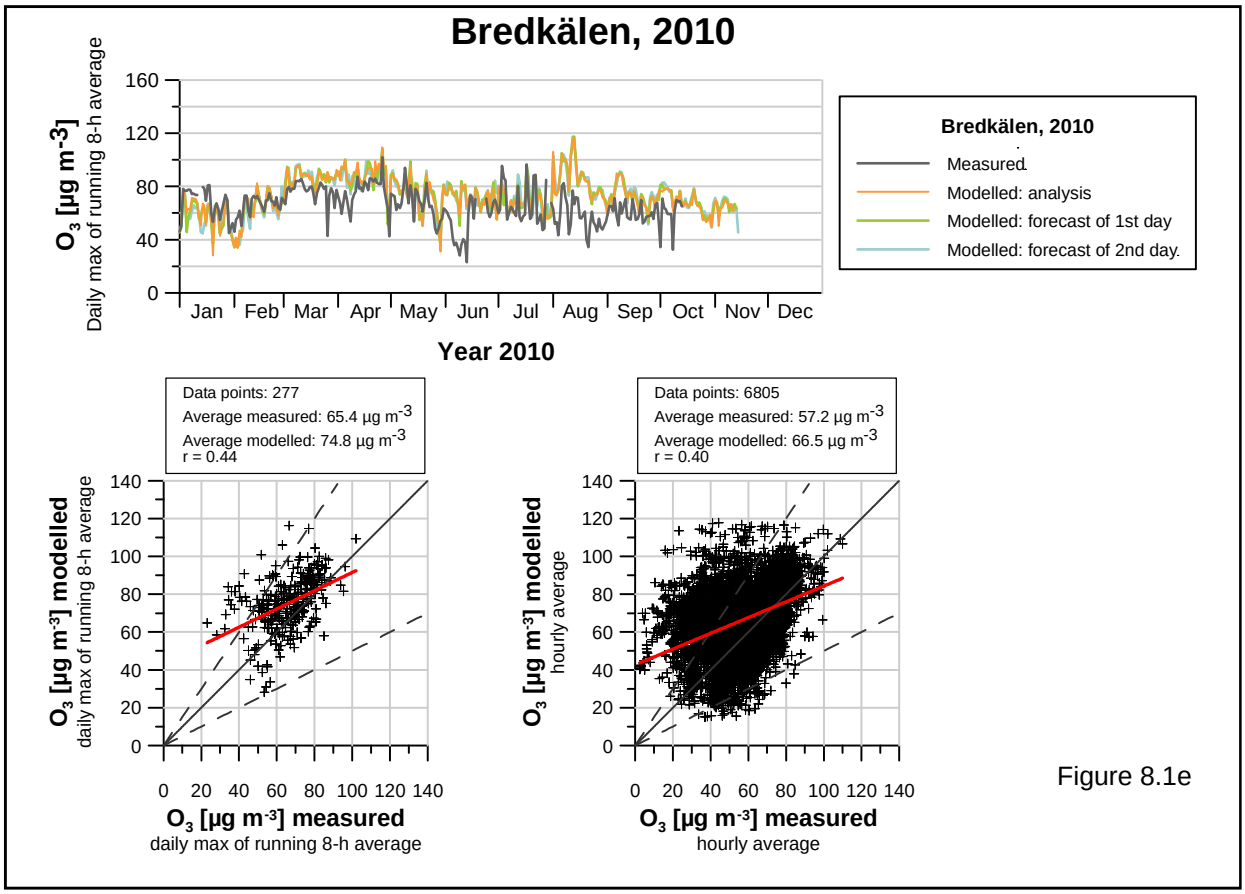

Figure 8.1e

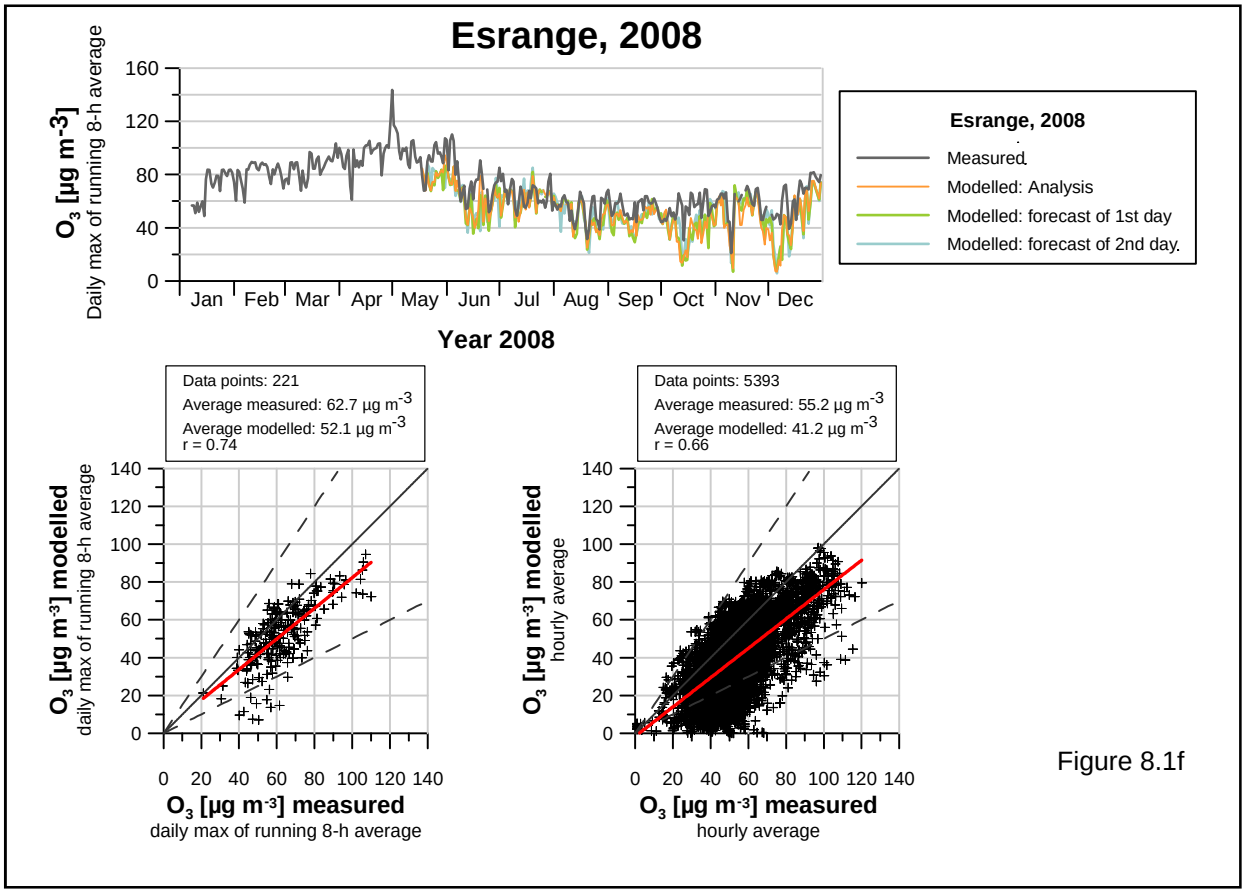

Figure 8.1f

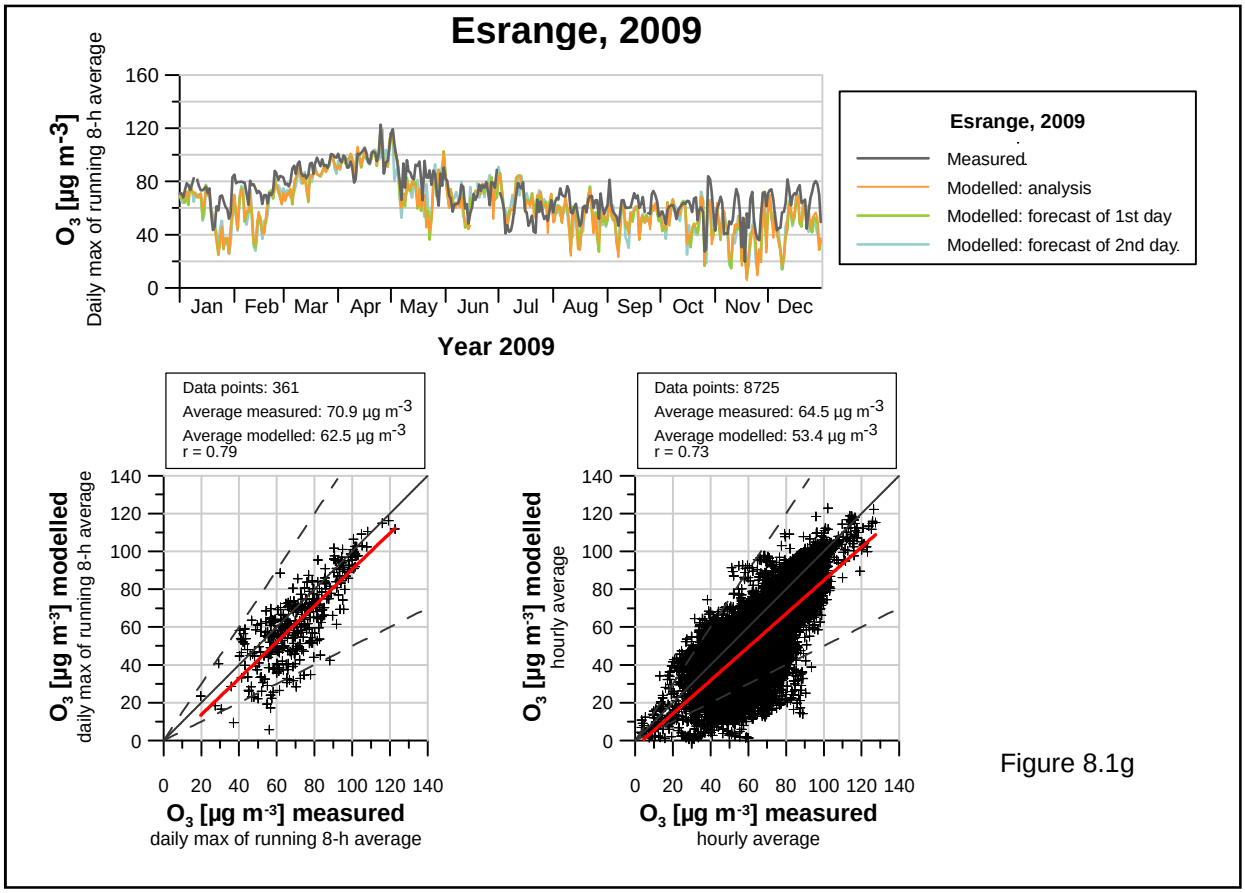

Figure 8.1g

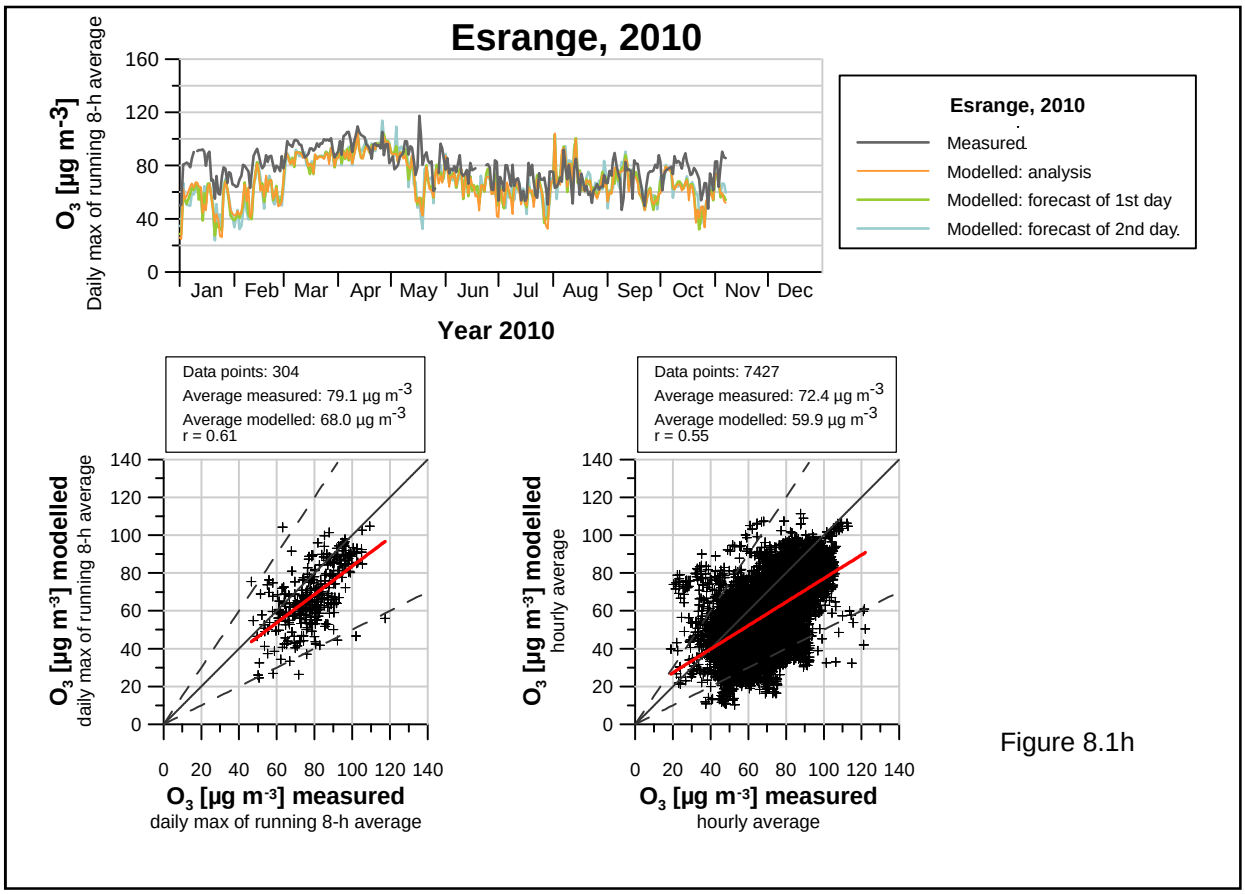

Figure 8.1h

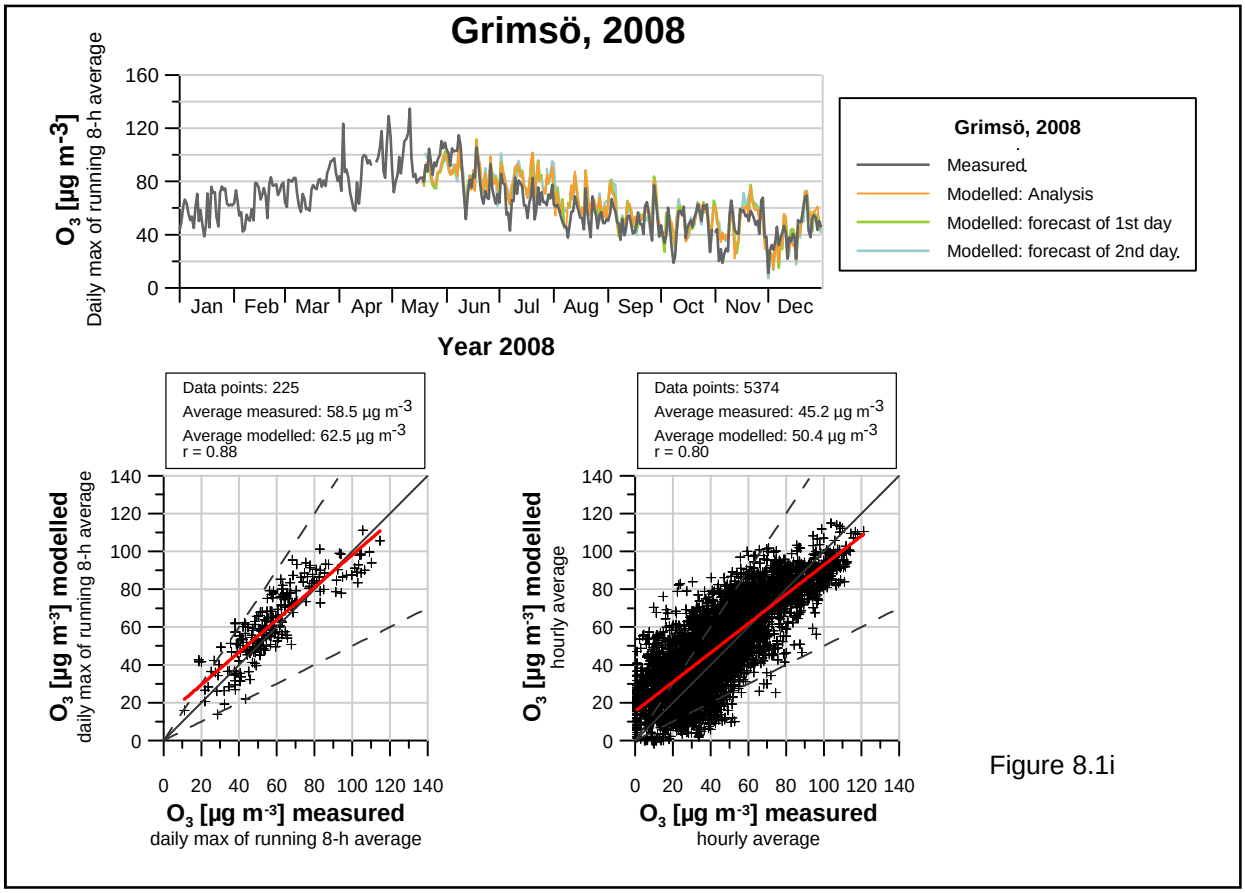

Figure 8.1i

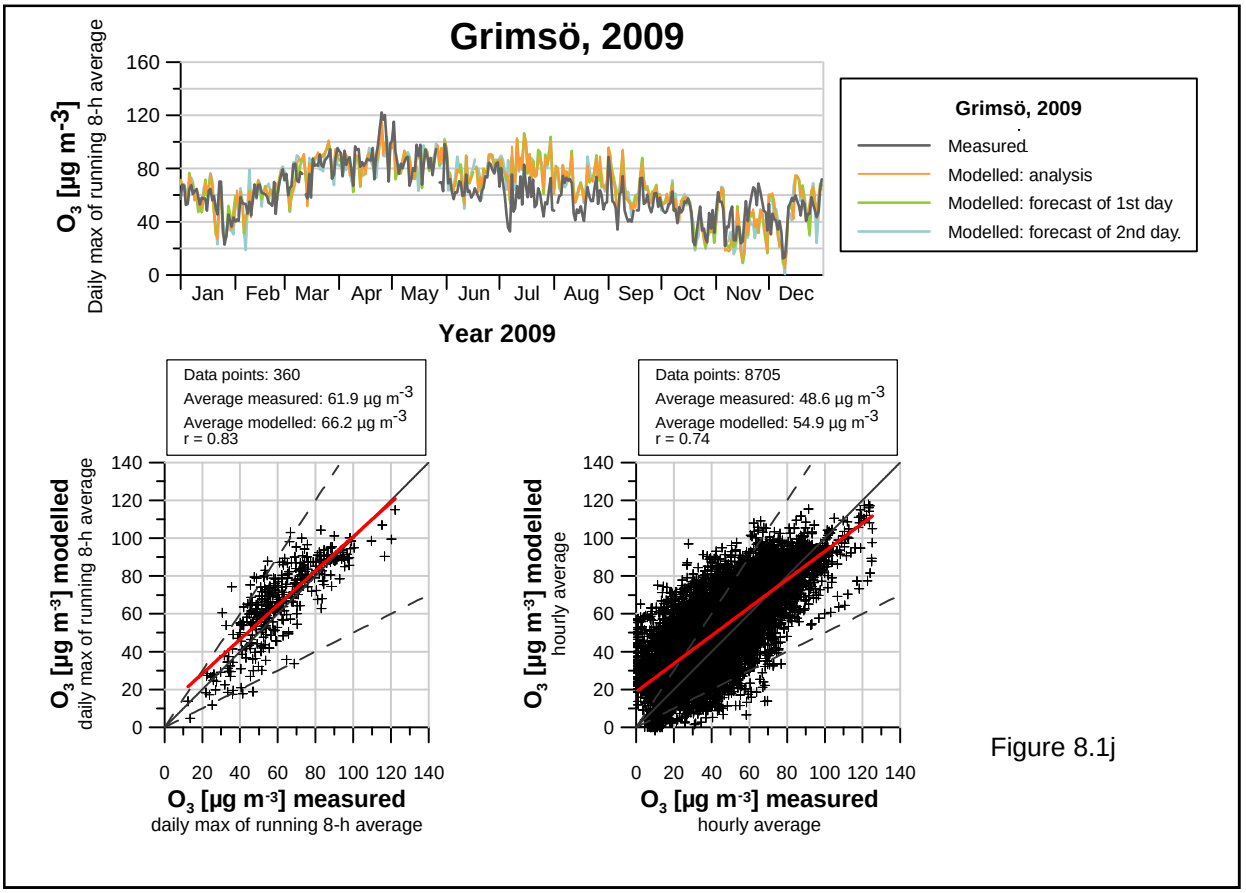

Figure 8.1j

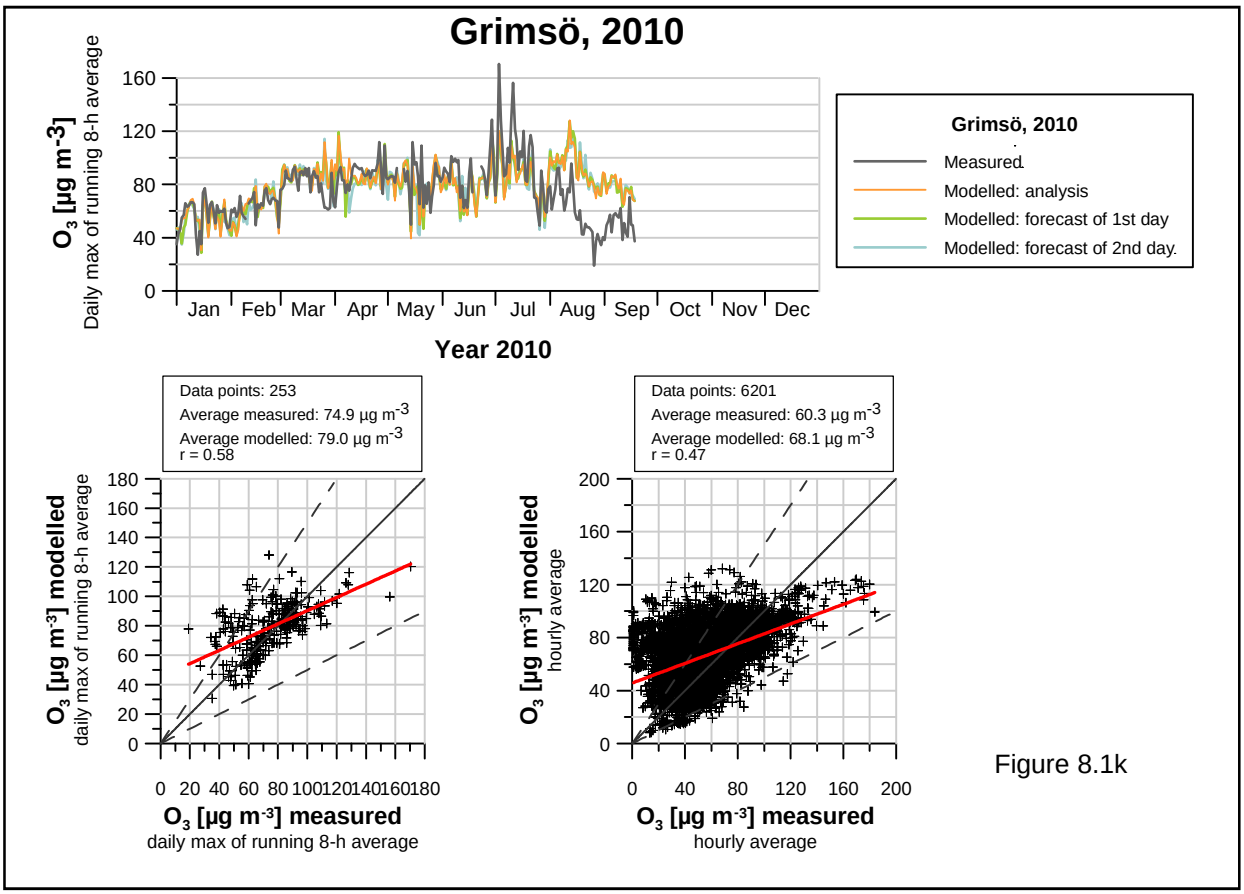

Figure 8.1k

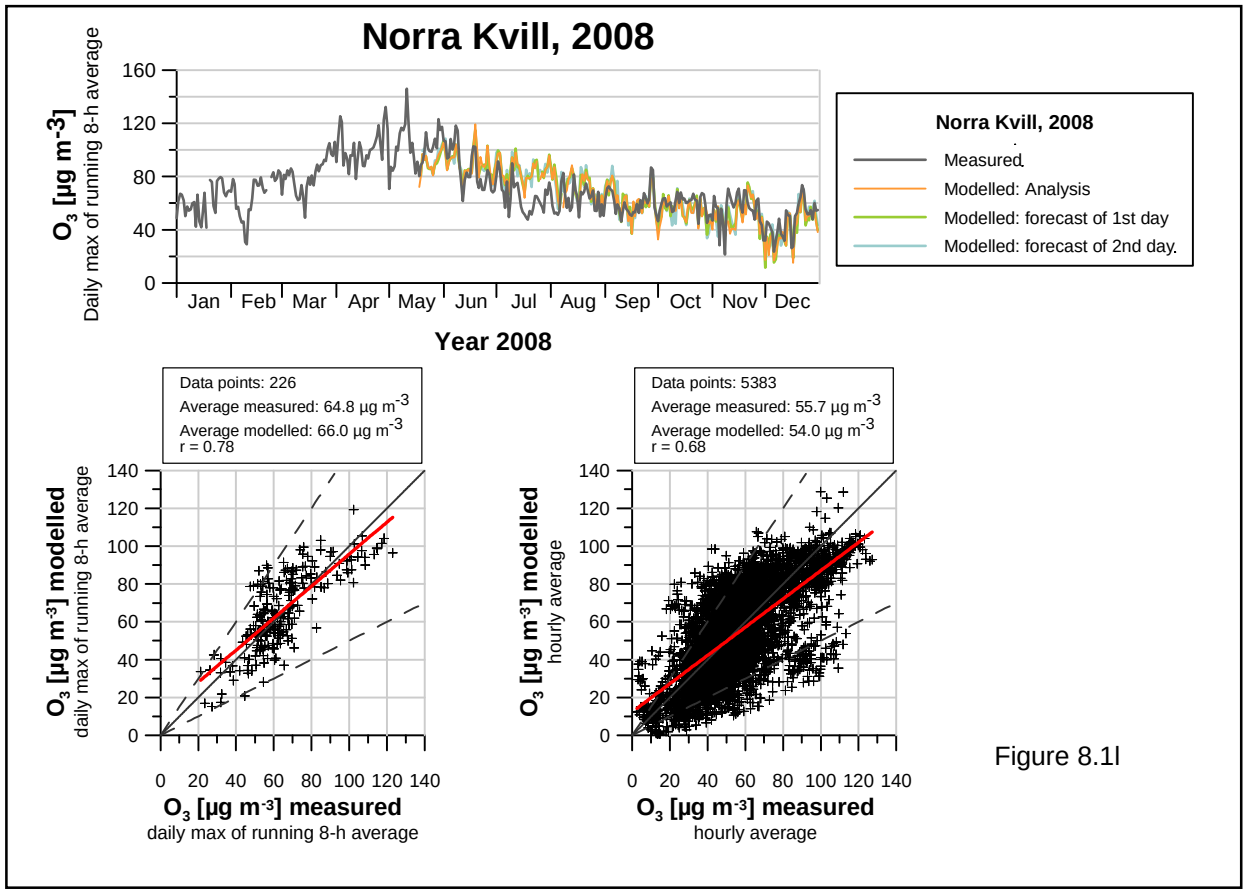

Figure 8.1l

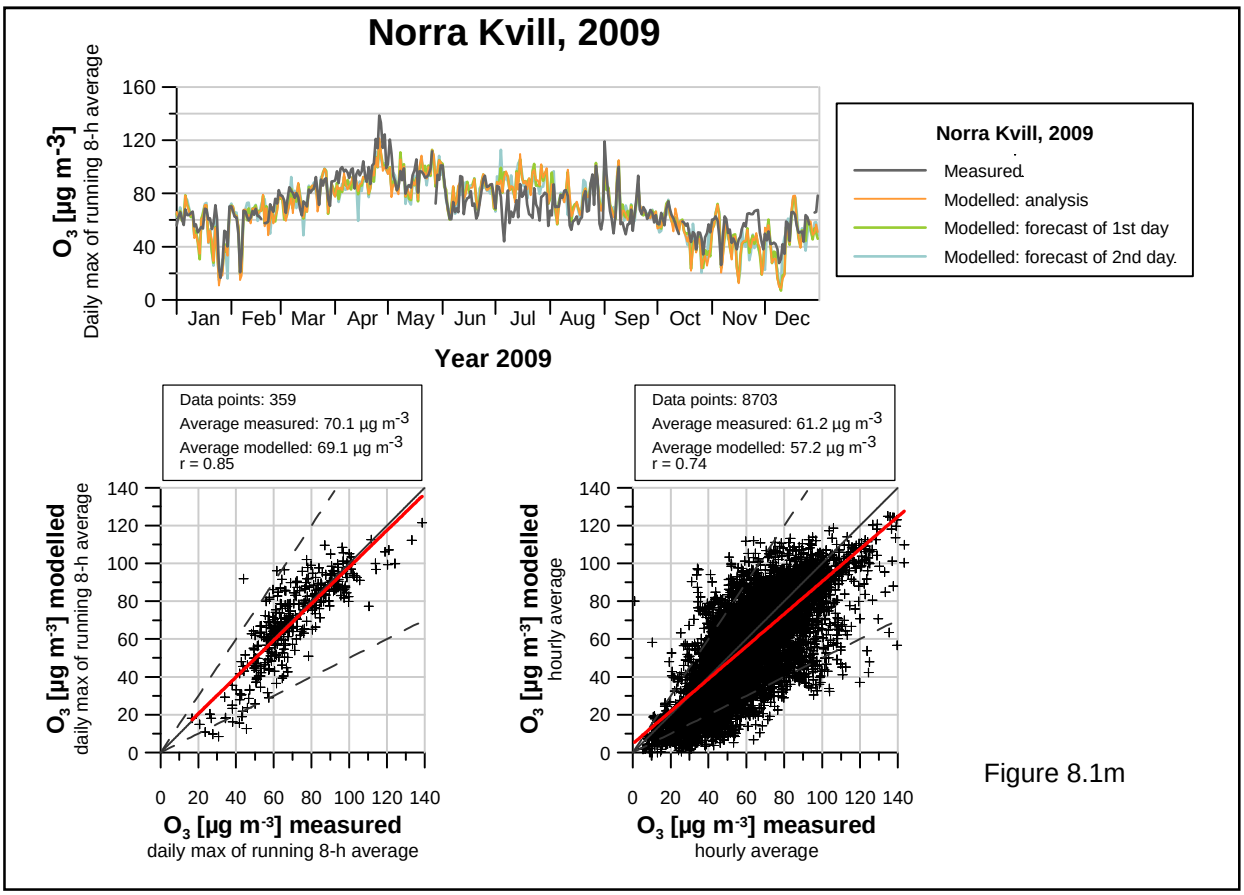

Figure 8.1m

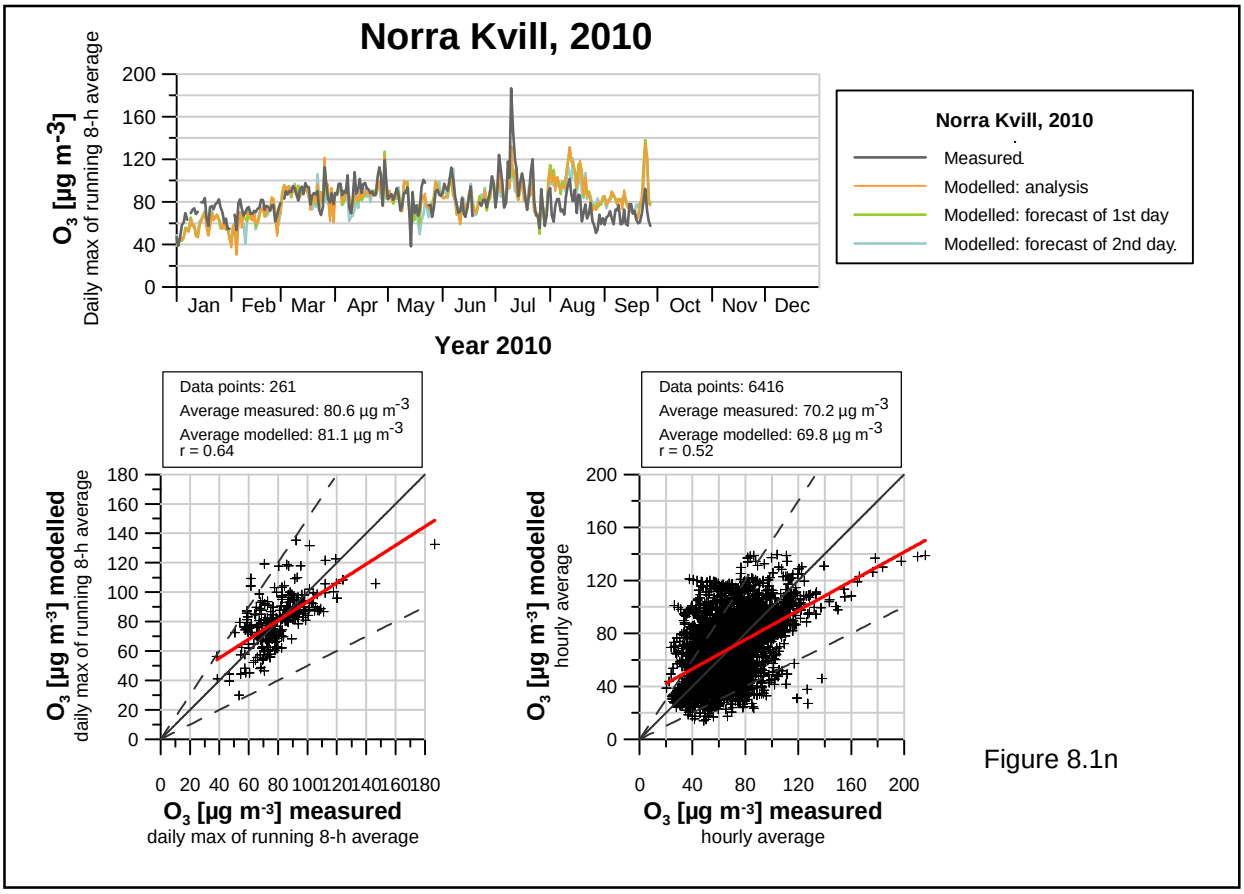

Figure 8.1n

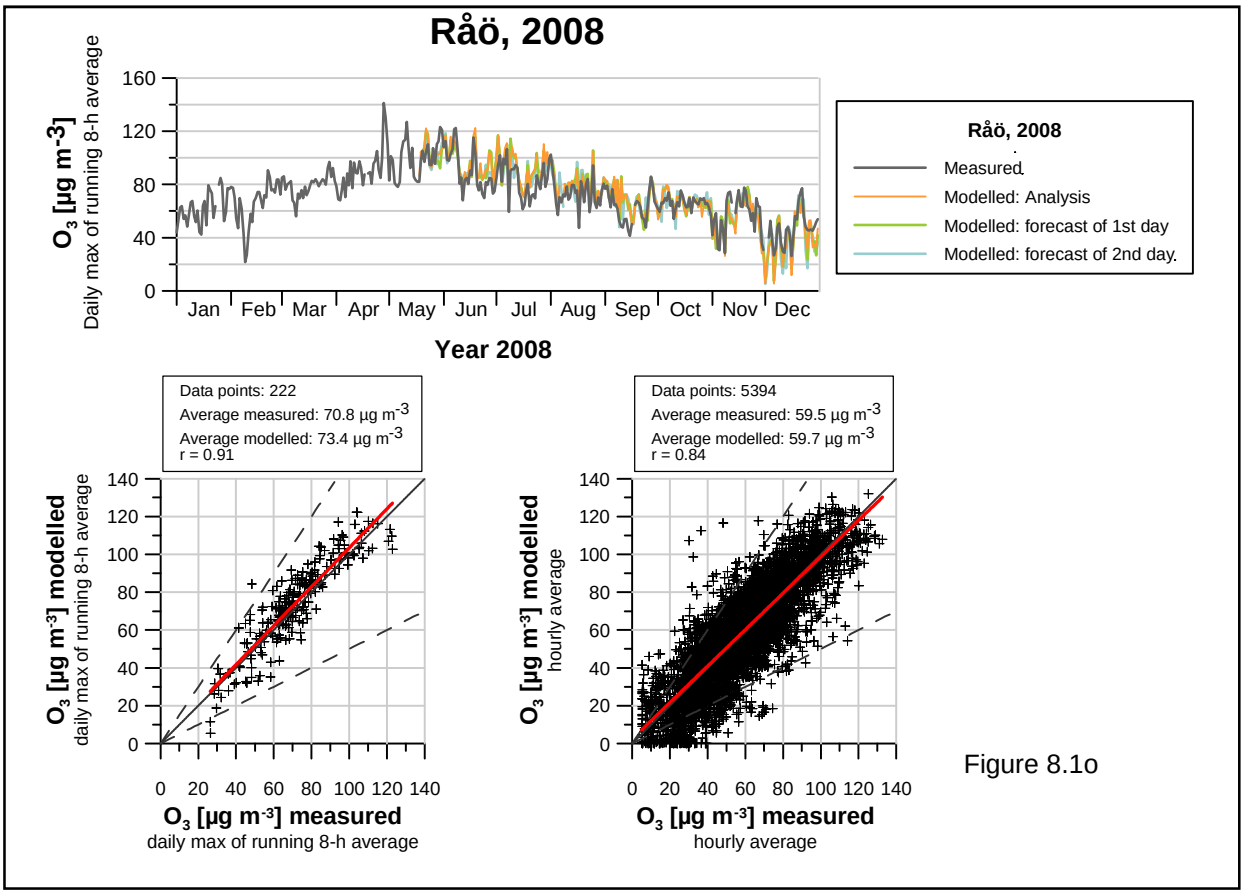

Figure 8.1o

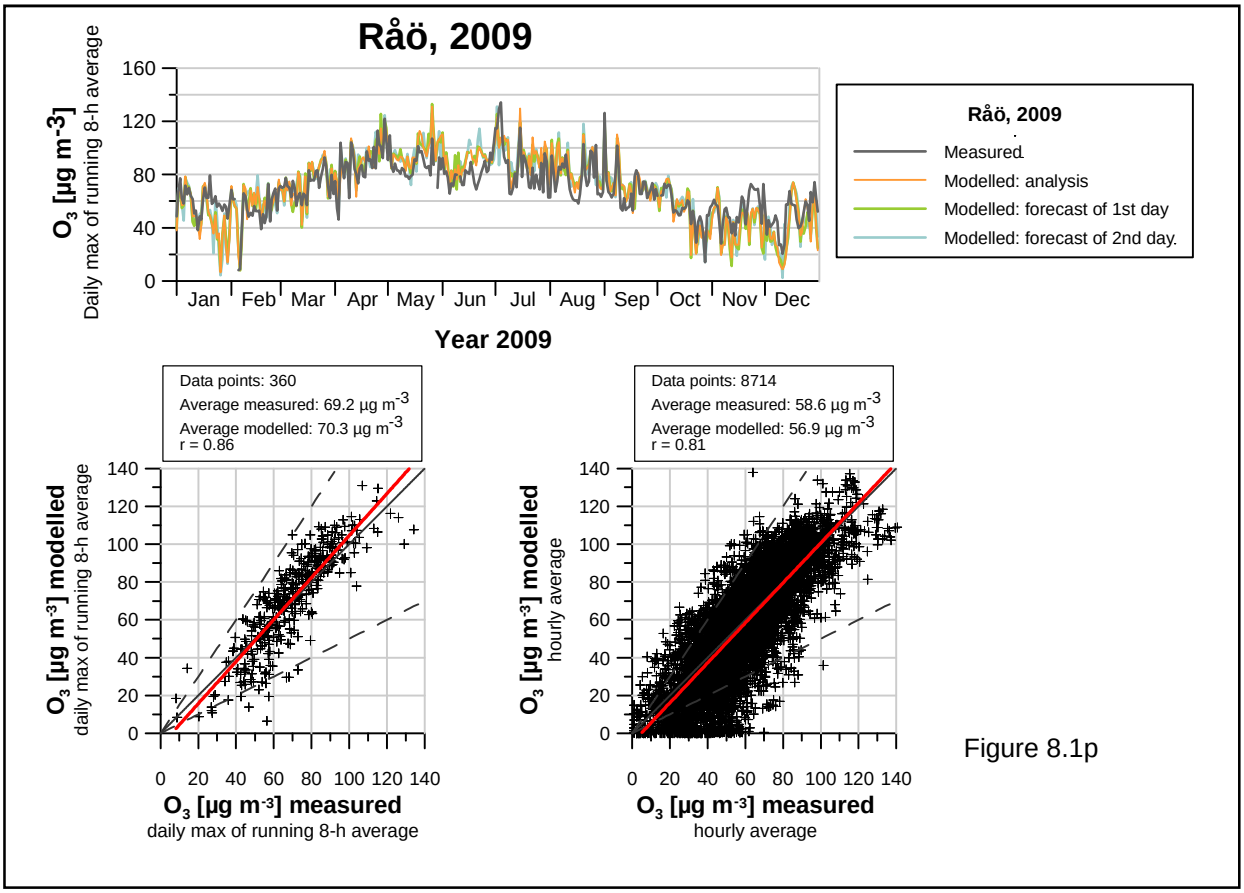

Figure 8.1p

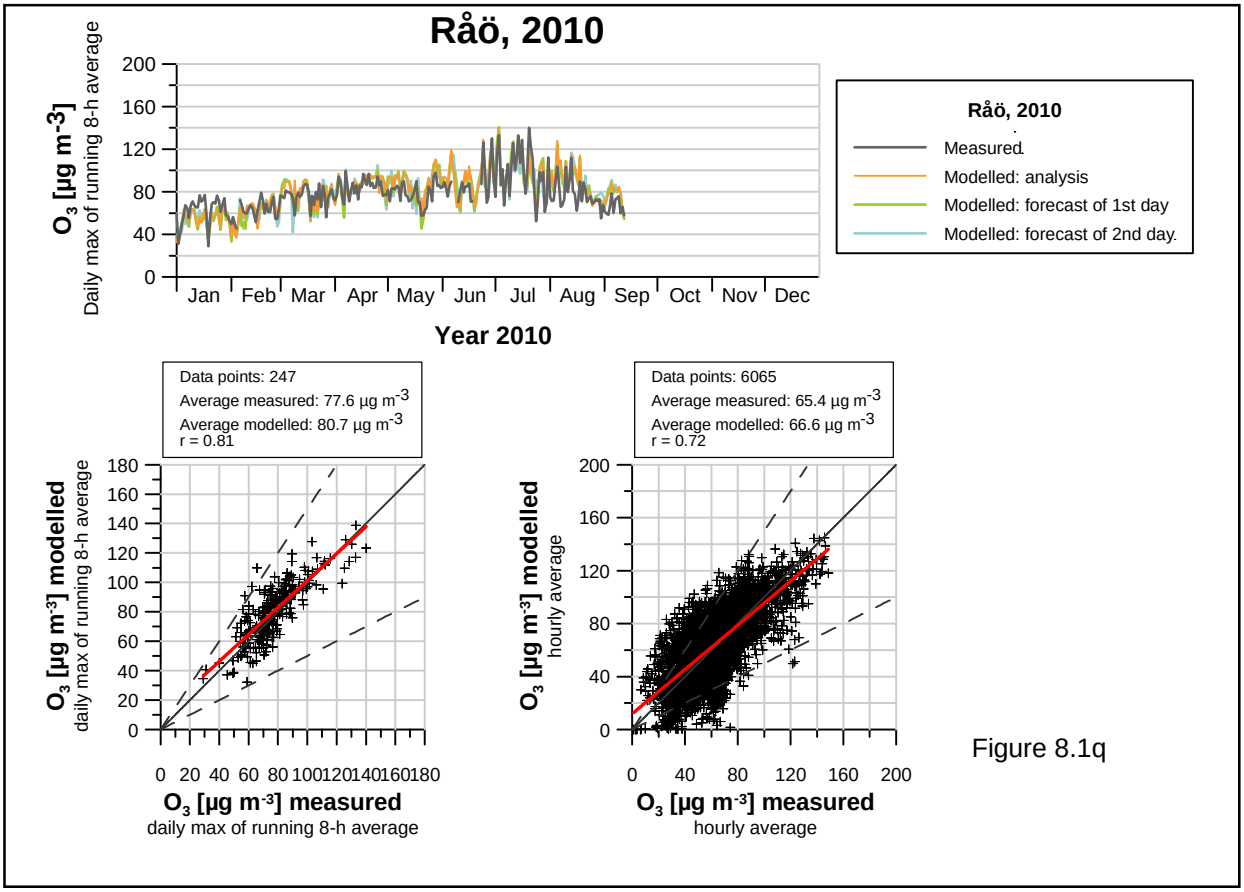

Figure 8.1q

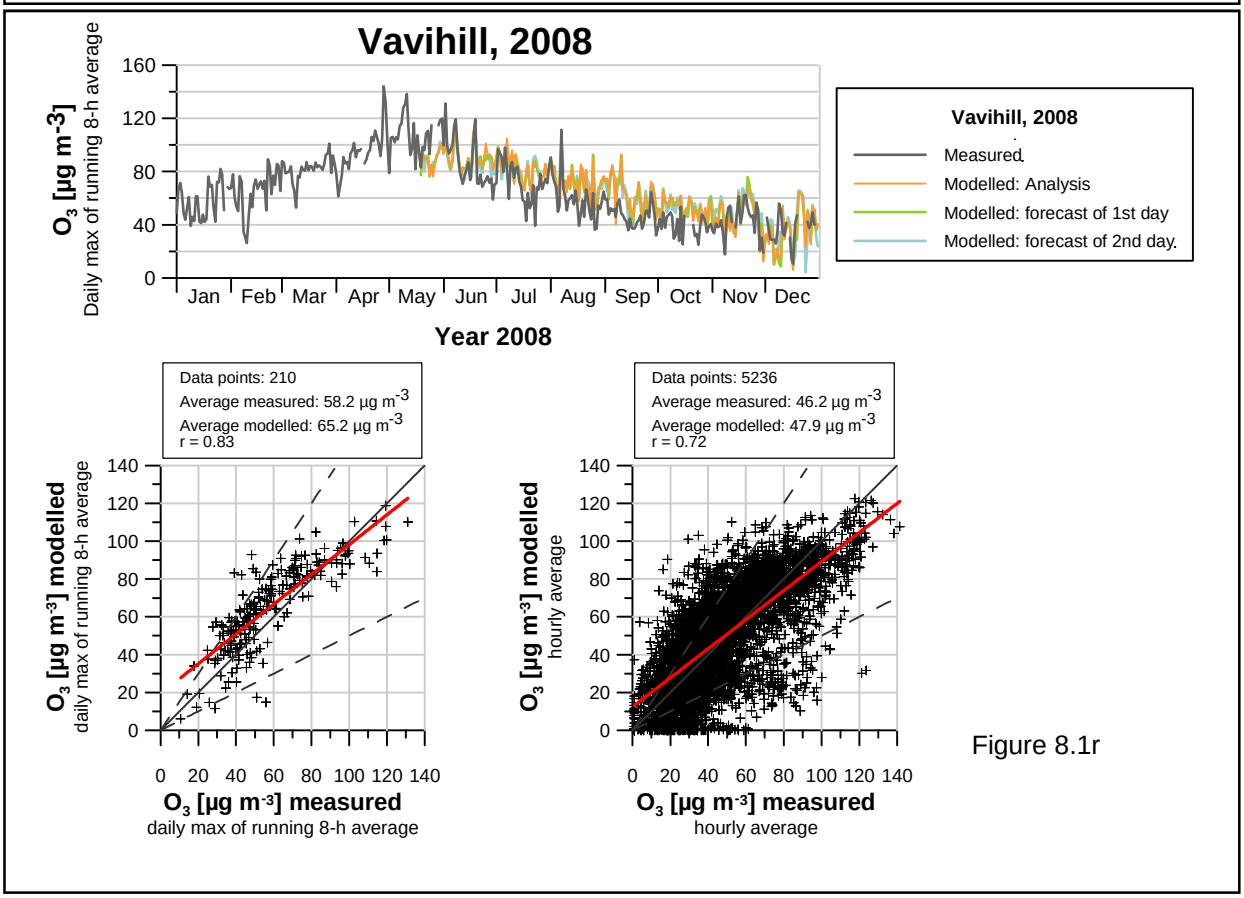

Figure 8.1r

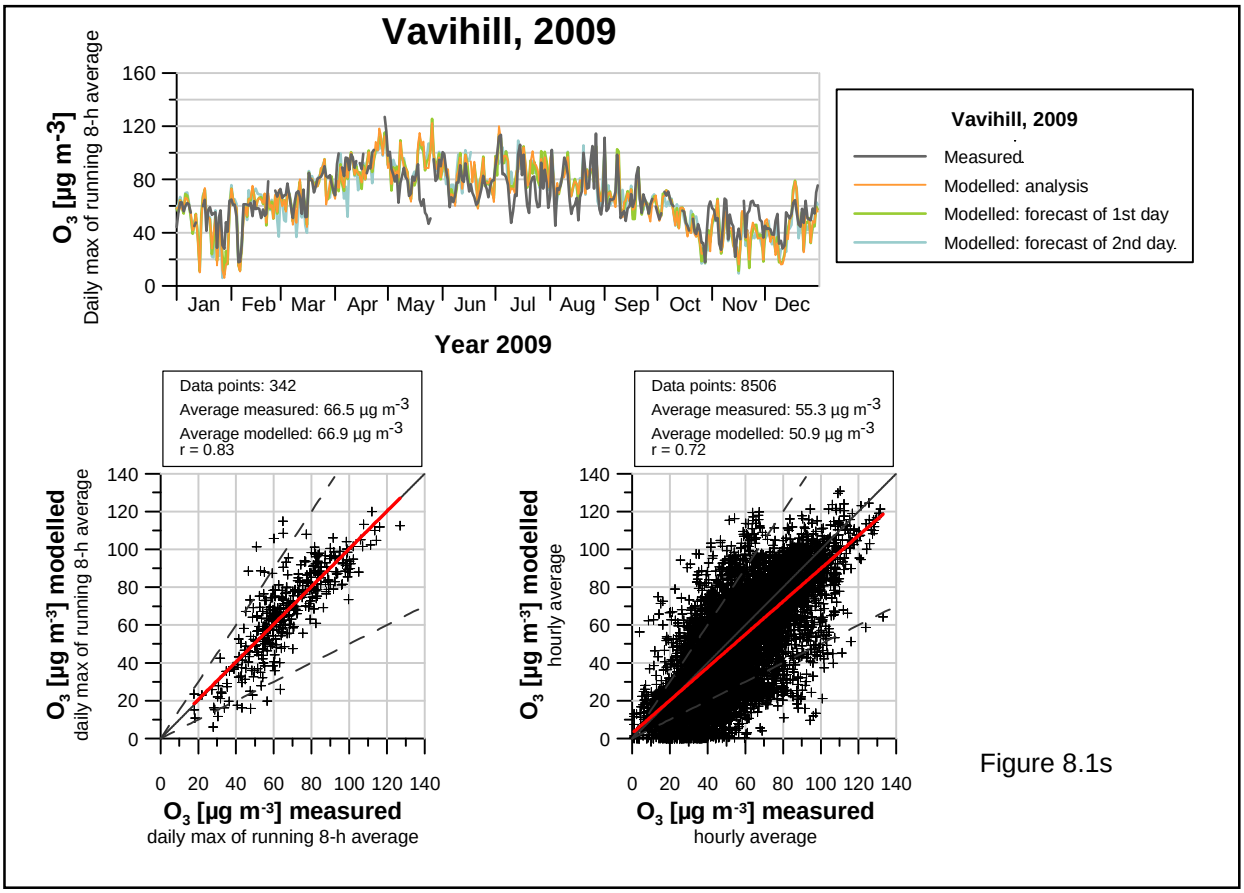

Figure 8.1s

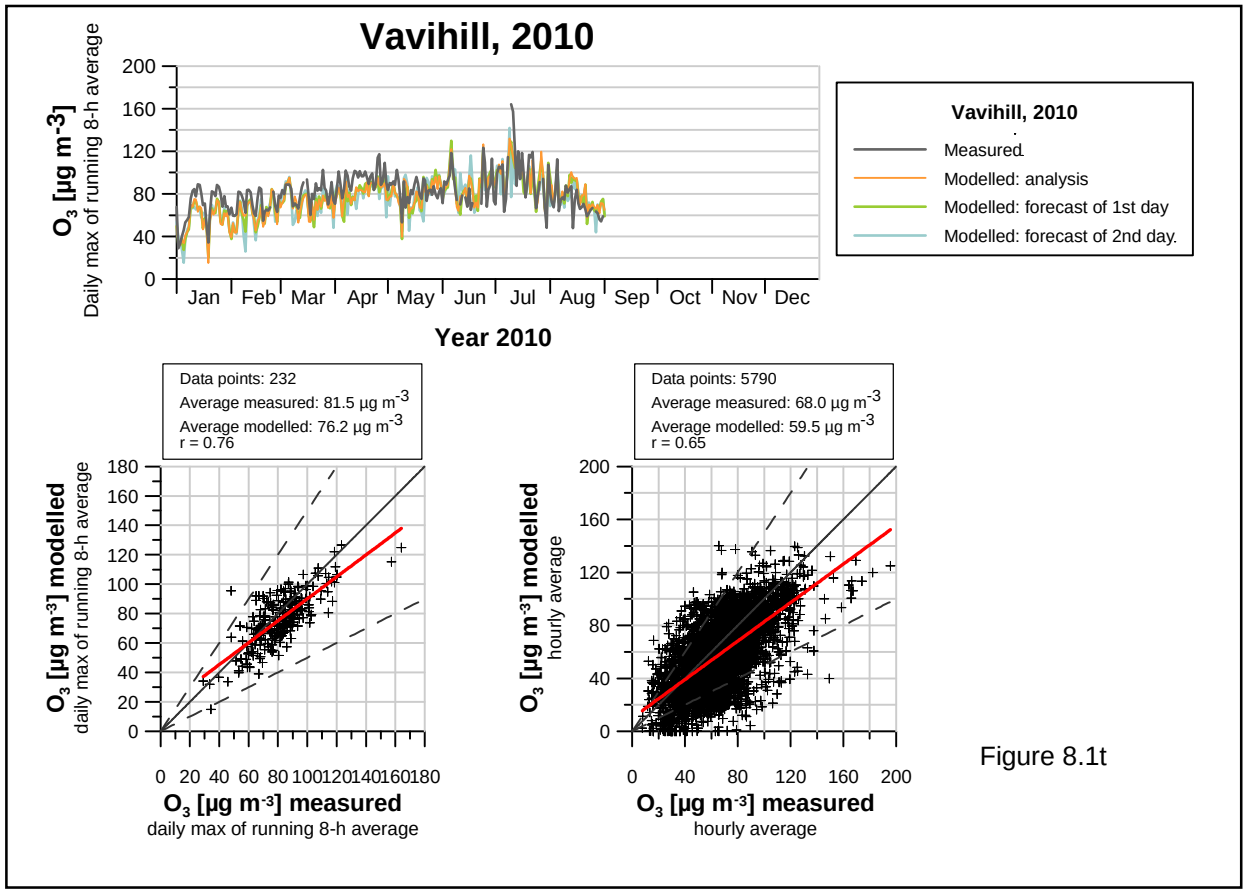

Figure 8.1t

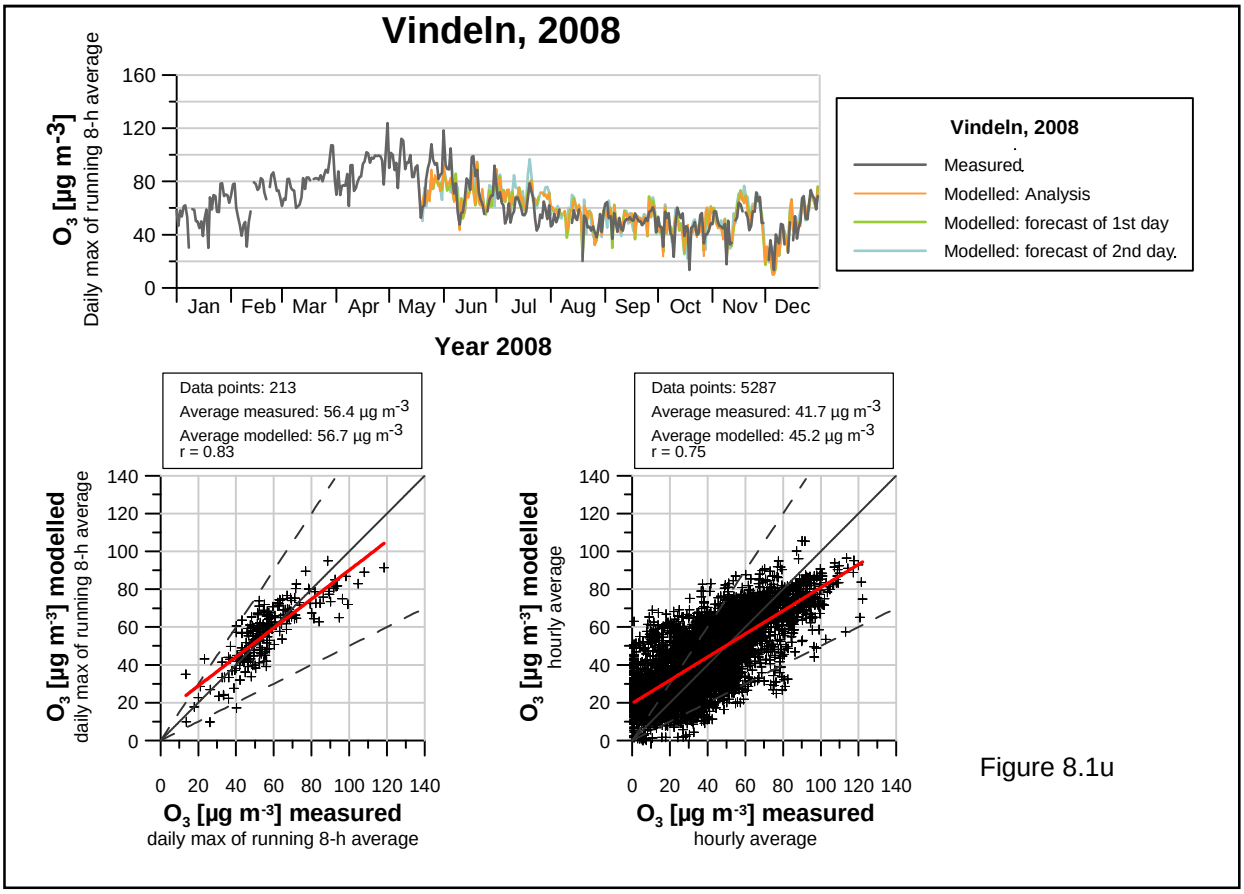

Figure 8.1u

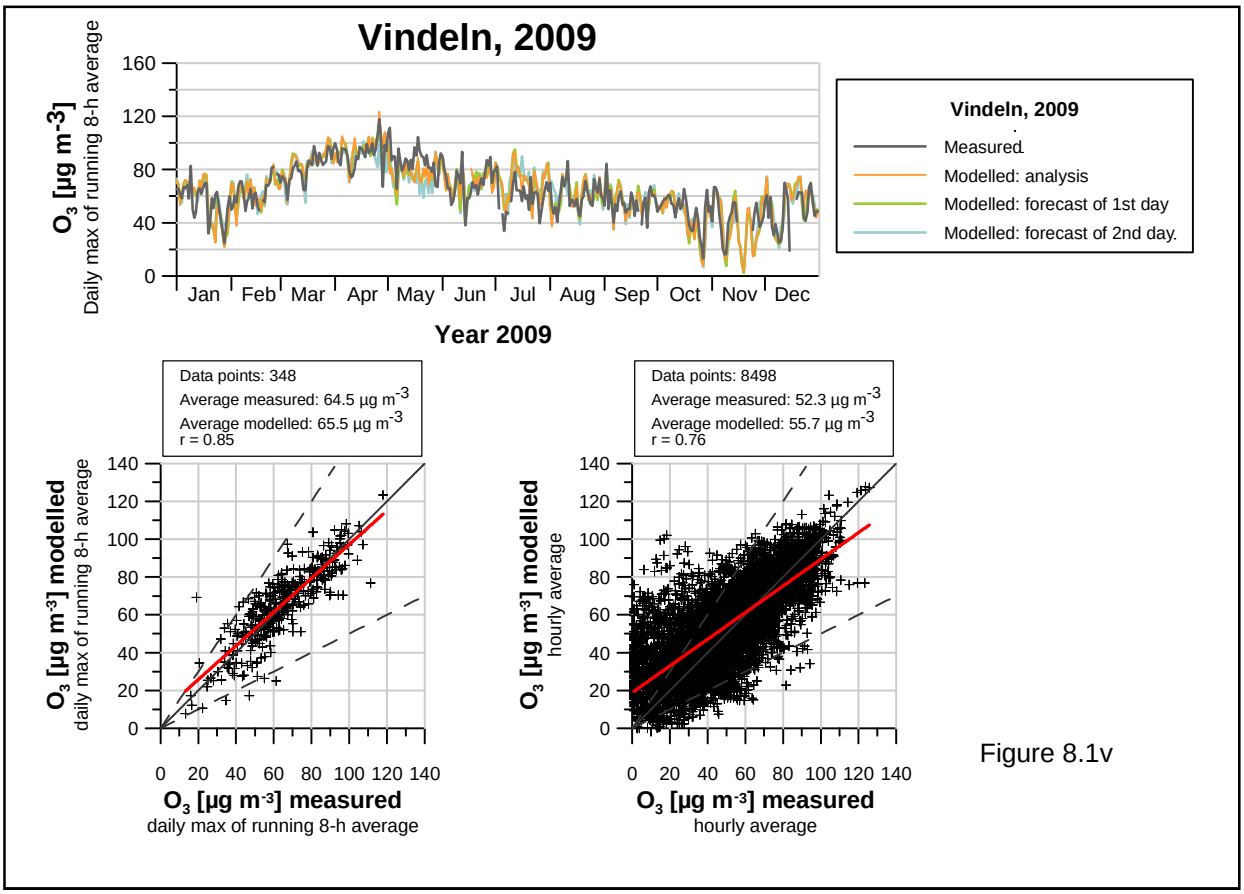

Figure 8.1v

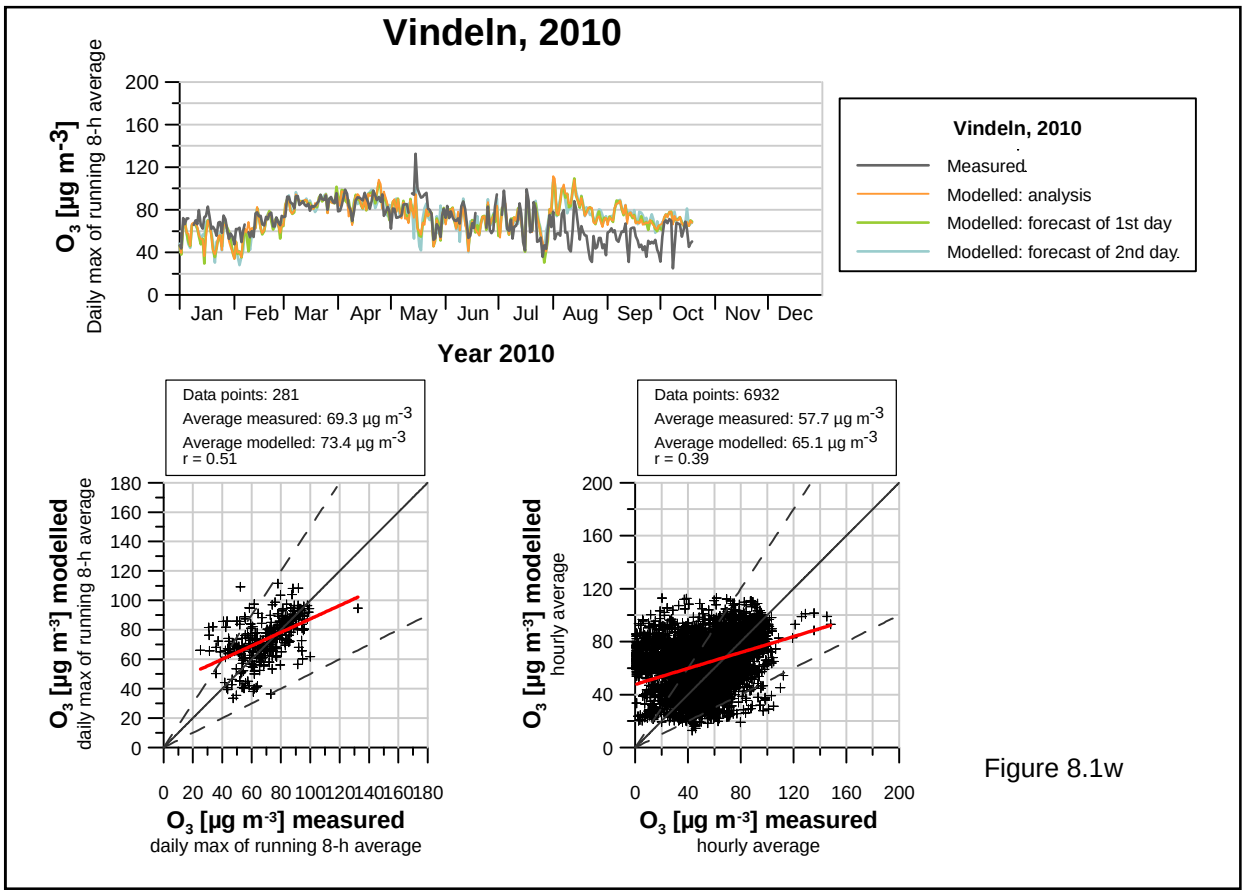

Figure 8.1w

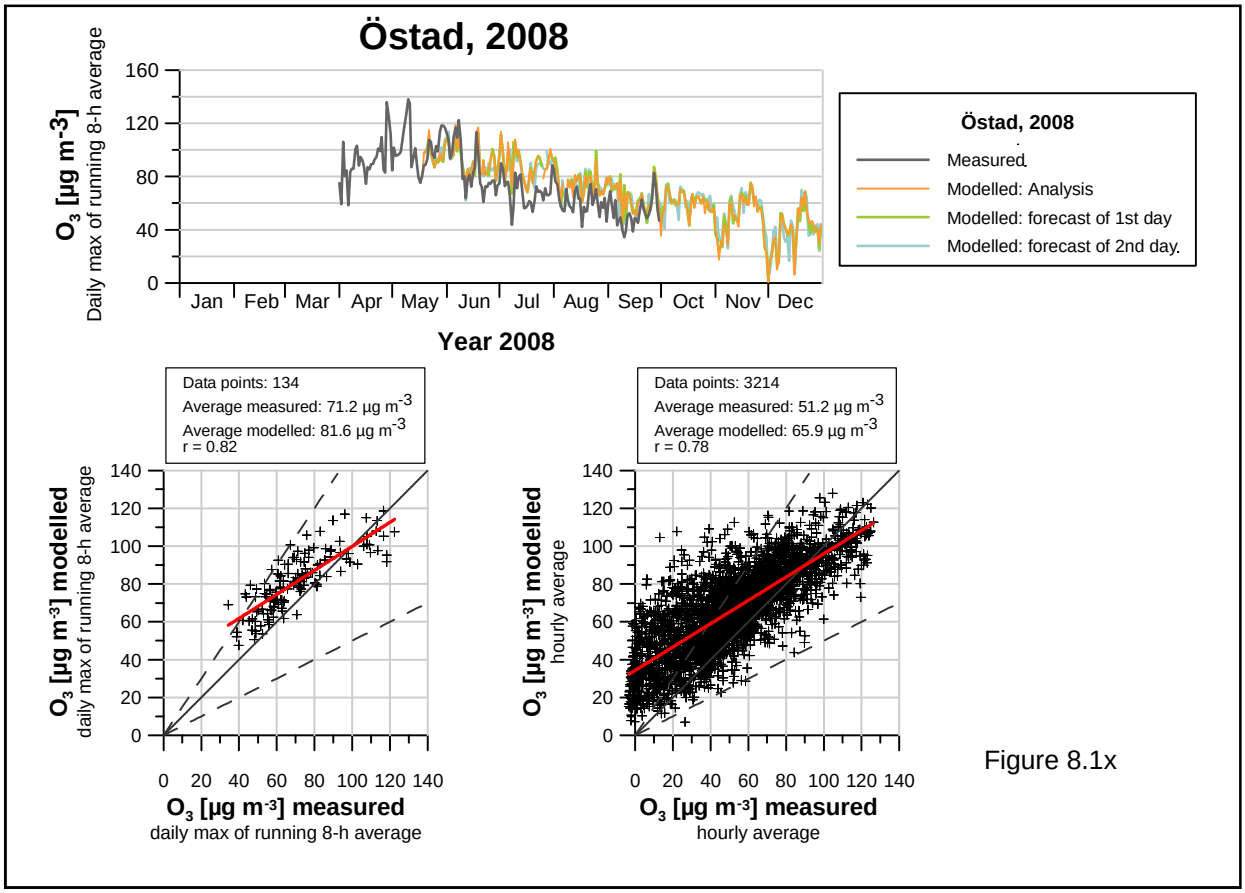

Figure 8.1x

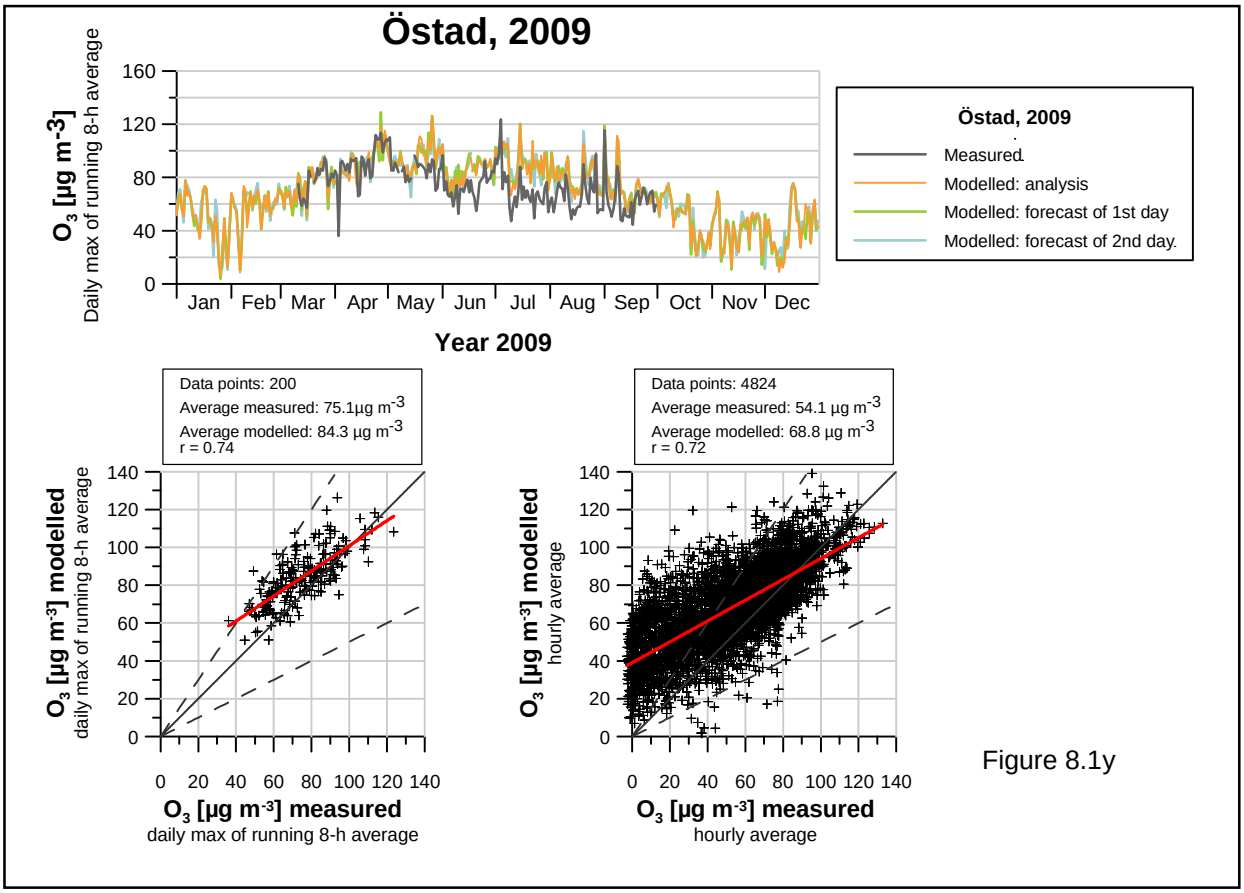

Figure 8.1y

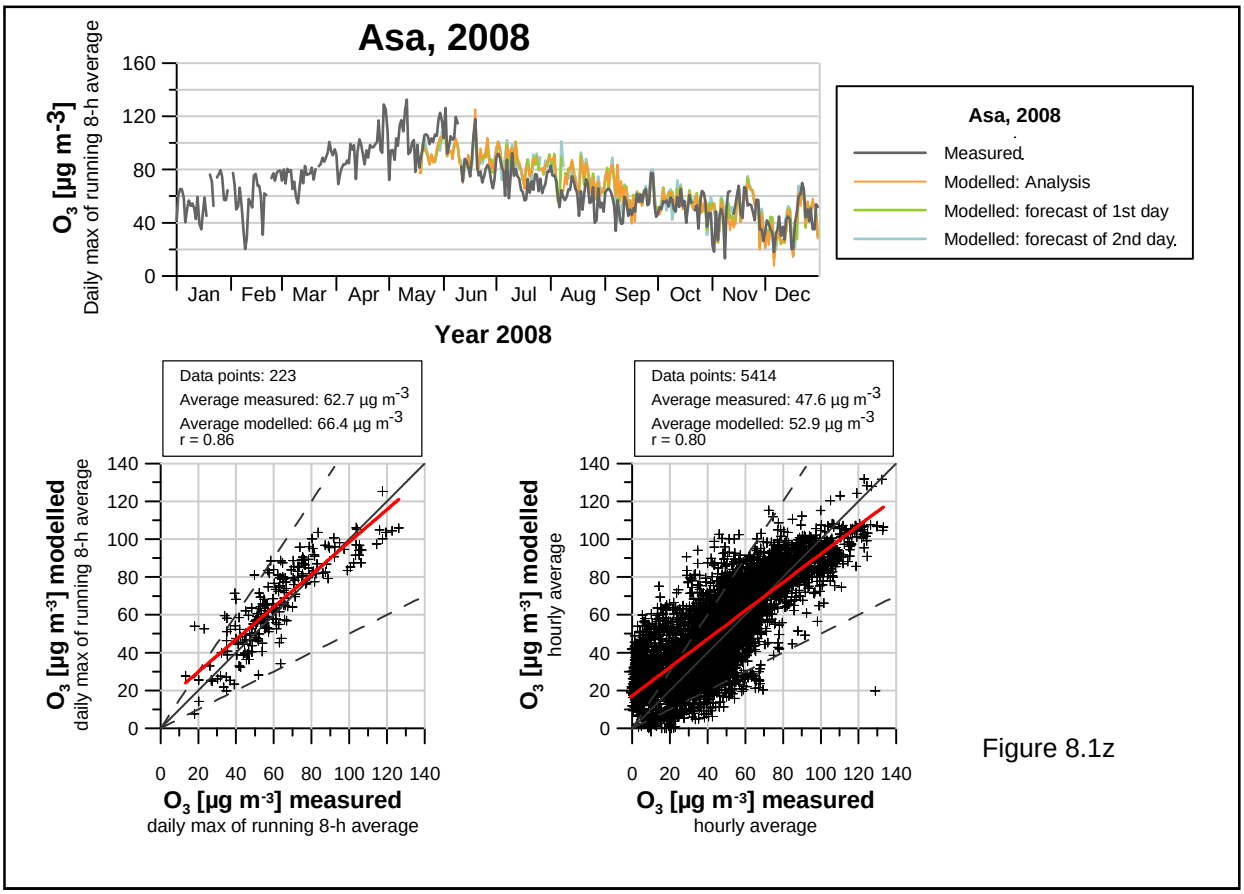

Figure 8.1z

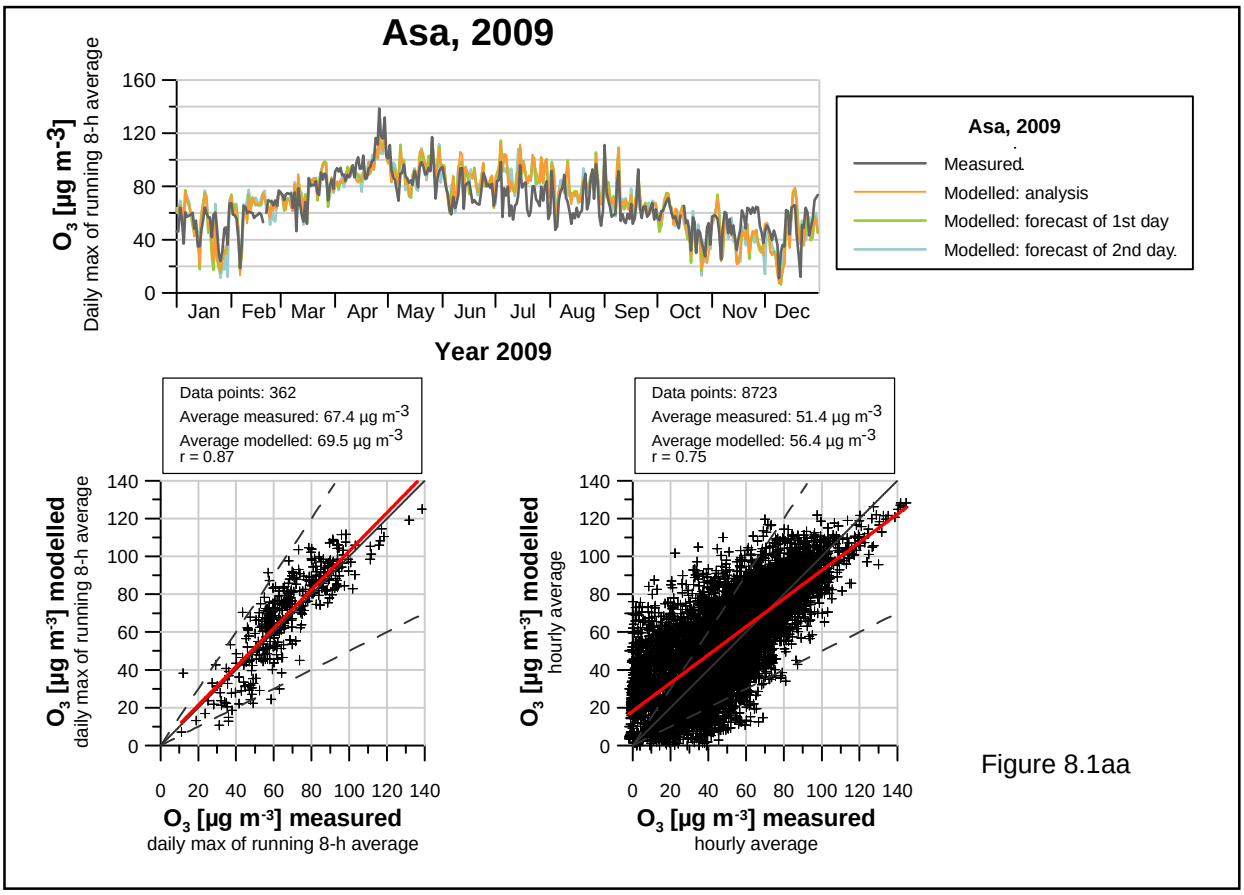

Figure 8.1aa

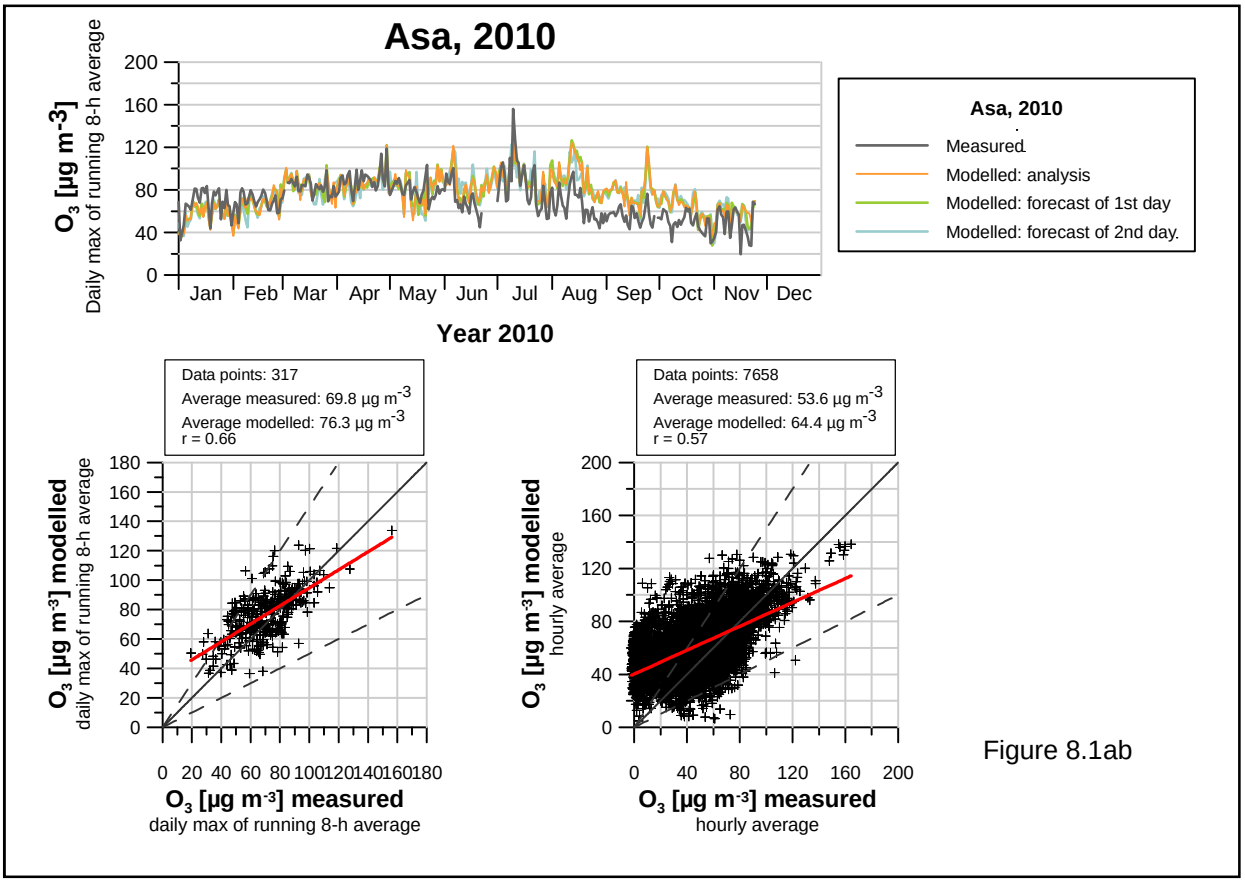

Figure 8.1ab

Table 8.1: *Comparison between measured and modelled concentrations of zone in terms of maximum of hourly average, 98-percentile of hourly average and 95.13-percentie of hourly average. Modelled concentrations are shown both for analysis (An), forecast of 1st day and forecast of 2nd day.*

	O_3 [µg m^{-3}] max hourly average				**O_3 [µg m^{-3}] 98-percentile hourly average**				**O_3 [µg m^{-3}] 93.15-percentile hourly average**			
	Obs	An	d1	d2	Obs	An	d1	d2	Obs	An	d1	d2
Asa, 2008	133.2	131.8	125.0	118.6	105.8	98.6	98.2	98.0	87.9	89.1	88.7	88.8
Asa, 2009	144.7	128.3	122.0	123.3	99.1	102.6	102.1	100.1	87.5	91.0	91.6	90.3
Asa, 2010	164.3	138.3	135.3	137.4	98.4	105.2	105.5	102.5	86.1	92.2	92.5	92.0
Aspvreten, 2008	134.9	120.7	117.4	119.1	102.5	98.0	96.8	95.2	90.2	87.7	87.6	87.3
Aspvreten, 2009	129.9	111.1	114.5	117.8	98.4	96.6	96.8	96.2	87.1	87.8	88.0	88.0
Bredkälen, 2008	108.8	103.5	101.4	103.0	87.6	82.0	81.6	84.2	73.6	75.2	74.8	75.8
Bredkälen, 2009	131.4	125.7	125.1	118.7	96.0	95.8	95.8	95.5	86.8	86.1	86.1	86.3
Bredkälen, 2010	110.0	117.8	118.9	113.7	84.3	99.0	98.2	97.1	79.0	89.6	89.6	89.6
Esrange, 2008	120.2	98.0	89.2	95.3	94.9	78.4	76.7	78.8	81.5	68.0	68.1	69.1
Esrange, 2009	127.4	122.8	124.8	120.9	100.2	98.7	97.7	97.2	93.4	89.2	88.7	88.6
Esrange, 2010	122.0	111.3	111.8	118.7	101.1	93.6	94.3	95.4	95.7	87.7	87.6	88.9
Grimsö, 2008	121.2	114.9	116.5	113.5	99.9	93.9	93.2	94.8	82.1	85.0	84.4	84.8
Grimsö, 2009	125.2	117.6	117.8	117.0	94.0	93.9	94.4	93.2	82.5	87.3	86.8	86.1
Grimsö, 2010	183.8	132.0	128.2	125.0	110.3	104.1	104.0	104.1	93.1	94.4	93.5	94.0
N. Kvill, 2008	127.2	128.8	124.3	119.0	105.4	97.1	96.2	97.8	92.1	88.4	87.8	88.3
N. Kvill, 2009	143.4	125.0	121.4	119.4	104.4	99.6	100.2	98.4	92.5	90.1	90.0	89.9
N. Kvill, 2010	216.1	139.5	144.4	135.8	109.0	111.3	112.8	107.3	95.0	96.2	97.0	95.1
Råö, 2008	132.7	132.0	128.6	125.2	109.0	109.2	107.9	105.3	93.7	96.5	96.1	93.3
Råö, 2009	140.6	137.9	137.9	141.3	102.4	106.4	106.0	106.2	87.9	93.7	94.1	93.8
Råö, 2010	148.6	144.9	146.2	135.9	111.4	111.6	112.0	108.9	91.7	97.2	96.5	96.5
Vavihill, 2008	141.4	122.5	116.6	114.2	107.2	98.1	96.9	95.3	89.0	87.2	86.5	85.9
Vavihill, 2009	133.0	130.9	133.9	132.5	101.7	101.1	101.6	100.0	88.6	89.2	89.4	88.5
Vavihill, 2010	195.6	140.1	136.9	148.6	113.8	104.7	104.3	102.6	96.0	91.9	92.2	91.4
Vindeln, 2008	122.2	105.5	99.5	99.0	92.5	81.2	80.4	81.9	75.6	72.0	71.6	73.3
Vindeln, 2009	125.8	127.7	125.0	114.0	95.4	97.0	96.6	93.2	87.1	87.3	86.7	86.0
Vindeln, 2010	148.1	112.9	112.4	111.8	94.5	96.2	96.2	94.9	87.9	89.1	88.7	88.7
Östad, 2008	126.4	127.9	126.1	117.1	112.2	107.1	105.9	105.3	94.5	97.2	96.8	95.6
Östad, 2009	132.8	139.1	136.3	135.6	100.8	108.0	106.0	106.3	90.3	97.1	97.3	96.5

Table 8.2: *Comparison between measured and modelled concentrations of zone in terms of maximum,, 98-percentile and 95.13-percentie of running 8h-average. Modelled concentrations are shown both for analysis (An), forecast of 1st day and forecast of 2nd day.*

	O_3 [µg m^{-3}] max 8h-average				**O_3 [µg m^{-3}] 98-percentile 8h-average**				**O_3 [µg m^{-3}] 93.15-percentile 8h-average**			
	Obs	An	d1	d2	Obs	An	d1	d2	Obs	An	d1	d2
Asa, 2008	126.2	125.3	115.6	113.8	117.2	104.7	102.9	102.3	103.7	96.8	96.2	97.2
Asa, 2009	138.6	125.0	118.3	121.1	111.1	108.2	109.4	105.5	94.5	100.2	100.2	97.9
Asa, 2010	156.2	133.8	130.8	122.6	105.5	114.3	116.0	113.3	95.4	100.2	103.1	98.2
Aspvreten, 2008	117.7	114.2	112.4	110.0	112.9	102.5	101.5	98.4	101.2	96.4	95.5	95.1
Aspvreten, 2009	122.6	107.3	110.5	112.0	108.8	101.1	102.4	100.6	95.2	93.9	95.6	95.0
Bredkälen, 2008	105.0	98.7	96.4	101.3	90.9	86.6	85.8	90.5	82.3	79.6	80.0	82.6
Bredkälen, 2009	131.4	123.4	116.6	115.9	104.0	101.7	102.2	101.2	94.3	92.1	92.8	92.8
Bredkälen, 2010	102.0	116.3	117.3	110.9	87.9	100.4	100.5	102.4	83.1	94.9	94.6	92.8
Esrange, 2008	110.0	94.6	86.6	87.9	105.1	81.5	82.4	84.3	89.7	75.2	72.7	75.5
Esrange, 2009	122.6	116.3	121.2	119.0	102.9	102.6	102.6	101.5	97.2	95.4	95.3	94.6
Esrange, 2010	117.4	104.7	104.5	113.8	102.9	96.4	97.0	98.9	98.4	91.2	92.5	93.9
Grimsö, 2008	114.8	111.1	111.7	107.7	105.3	98.9	98.1	99.0	95.1	92.8	90.6	93.2
Grimsö, 2009	122.1	115.0	115.0	112.9	98.5	99.3	99.8	99.2	90.9	92.0	92.9	90.4
Grimsö, 2010	170.5	128.2	127.3	120.0	121.7	111.7	115.1	113.1	106.1	101.5	102.0	100.1
N. Kvill, 2008	123.0	119.3	114.7	111.3	114.0	101.3	102.5	101.0	101.2	95.8	95.1	96.2
N. Kvill, 2009	138.6	121.5	118.9	117.2	113.6	105.5	105.0	104.5	98.5	97.7	98.3	95.9
N. Kvill, 2010	186.7	135.3	138.0	131.7	119.0	119.1	118.5	113.2	103.8	104.3	104.0	101.4
Råö, 2008	123.0	122.3	120.3	118.6	114.4	116.3	115.5	111.2	104.6	107.1	105.5	103.6
Råö, 2009	134.2	131.0	132.8	131.0	112.5	112.5	111.8	114.2	97.5	104.8	104.5	103.4
Råö, 2010	140.1	138.8	140.7	131.1	126.4	119.7	120.2	118.5	103.3	109.1	108.6	105.0
Vavihill, 2008	131.1	118.7	111.3	108.9	118.3	107.6	105.8	102.4	98.3	93.8	93.3	92.6
Vavihill, 2009	126.9	119.9	115.3	115.2	107.3	108.0	105.5	104.3	98.1	98.2	100.0	96.1
Vavihill, 2010	164.1	126.5	129.7	125.1	119.5	111.3	108.2	109.0	109.2	100.6	102.6	99.7
Vindeln, 2008	118.4	95.0	93.4	96.8	98.0	86.5	85.6	85.1	88.1	78.9	76.5	77.4
Vindeln, 2009	117.9	123.4	115.2	105.9	99.4	103.7	102.7	98.2	94.1	93.4	93.5	91.2
Vindeln, 2010	132.5	111.5	109.3	108.4	96.8	100.7	100.3	99.2	92.8	94.5	94.0	93.0
Östad, 2008	122.5	118.7	116.7	113.9	117.4	114.2	111.9	109.0	109.3	105.4	106.2	102.8
Östad, 2009	123.5	126.3	128.8	123.5	110.2	115.4	114.1	111.9	97.0	107.2	104.0	104.6

Table 8.3: *Comparison between measured and modelled concentrations of zone in terms of coefficient of variation CoV, i.e. normalized standard deviation (standard deviation divided by mean value).*

	CoV hourly average				**CoV running 8h-average**			
	Obs	An	d1	d2	Obs	An	d1	d2
Asa, 2008	0.52	0.44	0.45	0.43	0.35	0.33	0.32	0.31
Asa, 2009	0.47	0.43	0.44	0.43	0.29	0.33	0.33	0.31
Asa, 2010	0.46	0.30	0.32	0.32	0.26	0.22	0.22	0.22
Aspvreten, 2008	0.47	0.47	0.46	0.45	0.31	0.32	0.32	0.30
Aspvreten, 2009	0.42	0.43	0.44	0.43	0.29	0.31	0.30	0.30
Bredkälen, 2008	0.34	0.41	0.41	0.40	0.25	0.28	0.27	0.27
Bredkälen, 2009	0.37	0.38	0.39	0.39	0.28	0.30	0.30	0.30
Bredkälen, 2010	0.28	0.26	0.27	0.26	0.20	0.19	0.19	0.19
Esrange, 2008	0.30	0.46	0.46	0.44	0.24	0.31	0.31	0.29
Esrange, 2009	0.29	0.42	0.43	0.42	0.24	0.33	0.33	0.32
Esrange, 2010	0.22	0.30	0.32	0.31	0.17	0.24	0.24	0.24
Grimsö, 2008	0.50	0.44	0.44	0.43	0.35	0.32	0.32	0.32
Grimsö, 2009	0.45	0.40	0.42	0.42	0.30	0.31	0.31	0.32
Grimsö, 2010	0.40	0.28	0.30	0.30	0.29	0.21	0.22	0.22
N. Kvill, 2008	0.36	0.41	0.42	0.40	0.29	0.31	0.31	0.29
N. Kvill, 2009	0.33	0.40	0.41	0.41	0.27	0.32	0.31	0.30
N. Kvill, 2010	0.25	0.27	0.29	0.28	0.21	0.21	0.21	0.19
Råö, 2008	0.38	0.43	0.43	0.42	0.29	0.32	0.31	0.30
Råö, 2009	0.35	0.47	0.48	0.47	0.28	0.36	0.36	0.35
Råö, 2010	0.29	0.34	0.35	0.34	0.22	0.24	0.24	0.23
Vavihill, 2008	0.52	0.54	0.53	0.51	0.41	0.35	0.34	0.32
Vavihill, 2009	0.38	0.51	0.51	0.51	0.29	0.34	0.34	0.34
Vavihill, 2010	0.30	0.39	0.41	0.41	0.22	0.23	0.24	0.24
Vindeln, 2008	0.55	0.41	0.41	0.41	0.30	0.28	0.27	0.27
Vindeln, 2009	0.44	0.38	0.39	0.38	0.29	0.30	0.30	0.28
Vindeln, 2010	0.39	0.26	0.28	0.28	0.24	0.20	0.21	0.20
Östad, 2008	0.54	0.33	0.34	0.32	0.29	0.19	0.19	0.19
Östad, 2009	0.49	0.29	0.31	0.30	0.21	0.17	0.16	0.16

* Coefficient of variation CoV = standard daviation / average

Table 8.4: *Relative error between measured and modelled concentrations of ozone, regarding maximum of running 8h-average and AOT40 respectively.*

	RE max running 8h-average			**RE AOT40**		
	An	d1	d2	An	d1	d2
Asa, 2008	0.007	0.084	0.099	0.088	0.135	0.146
Asa, 2009	0.098	0.146	0.126	0.978	1.029	0.745
Asa, 2010	0.143	0.163	0.215	0.360	0.424	0.481
Aspvreten, 2008	0.030	0.045	0.066	0.218	0.268	0.330
Aspvreten, 2009	0.125	0.099	0.086	0.414	0.525	0.549
Bredkälen, 2008	0.060	0.082	0.035	0.653	0.692	0.471
Bredkälen, 2009	0.061	0.113	0.118	0.272	0.216	0.259
Bredkälen, 2010	0.140	0.151	0.087	0.405	0.560	0.780
Esrange, 2008	0.140	0.213	0.201	0.876	0.917	0.913
Esrange, 2009	0.051	0.011	0.029	0.382	0.366	0.479
Esrange, 2010	0.108	0.110	0.031	0.676	0.598	0.366
Grimsö, 2008	0.032	0.027	0.061	0.195	0.258	0.211
Grimsö, 2009	0.059	0.059	0.076	0.673	0.833	0.723
Grimsö, 2010	0.248	0.254	0.296	0.534	0.544	0.517
N. Kvill, 2008	0.030	0.068	0.096	0.171	0.198	0.168
N. Kvill, 2009	0.123	0.142	0.154	0.379	0.494	0.356
N. Kvill, 2010	0.276	0.261	0.295	0.329	0.300	0.292
Råö, 2008	0.005	0.022	0.035	0.227	0.176	0.017
Råö, 2009	0.024	0.010	0.024	0.768	0.787	0.738
Råö, 2010	0.009	0.004	0.064	0.382	0.369	0.306
Vavihill, 2008	0.094	0.151	0.169	0.200	0.270	0.313
Vavihill, 2009	0.055	0.092	0.093	0.821	0.756	0.604
Vavihill, 2010	0.229	0.210	0.238	0.126	0.135	0.173
Vindeln, 2008	0.198	0.211	0.183	0.778	0.818	0.744
Vindeln, 2009	0.047	0.023	0.102	0.645	0.611	0.654
Vindeln, 2010	0.159	0.175	0.182	0.672	0.638	0.516
Östad, 2008	0.031	0.047	0.070	0.152	0.124	0.042
Östad, 2009	0.023	0.043	0.000	1.591	1.698	1.591

* RE = (observation – model) / observation

Table 8.5: *Fraction of data points within a factor of 2 in the scatterplots presented above in this section.*

.

	F2 hourly average			**F2 running 8h-average**		
	An	d1	d2	An	d1	d2
Asa, 2008	0.85	0.85	0.85	0.98	0.99	0.99
Asa, 2009	0.85	0.85	0.84	0.98	0.98	0.98
Asa, 2010	0.85	0.85	0.85	0.99	0.99	1.00
Aspvreten, 2008	0.87	0.87	0.86	0.99	1.00	0.99
Aspvreten, 2009	0.87	0.88	0.87	0.99	0.99	0.99
Bredkälen, 2008	0.91	0.91	0.91	0.97	0.98	0.99
Bredkälen, 2009	0.93	0.92	0.93	0.98	0.99	0.99
Bredkälen, 2010	0.90	0.91	0.91	0.96	0.97	0.96
Esrange, 2008	0.80	0.79	0.81	0.95	0.94	0.94
Esrange, 2009	0.87	0.86	0.87	0.95	0.96	0.96
Esrange, 2010	0.92	0.91	0.91	0.97	0.98	0.97
Grimsö, 2008	0.86	0.87	0.85	0.98	0.98	0.98
Grimsö, 2009	0.87	0.87	0.86	0.98	0.98	0.98
Grimsö, 2010	0.87	0.88	0.87	0.98	0.97	0.97
N. Kvill, 2008	0.91	0.91	0.91	1.00	1.00	1.00
N. Kvill, 2009	0.92	0.90	0.90	0.98	0.98	0.97
N. Kvill, 2010	0.97	0.96	0.96	1.00	1.00	1.00
Råö, 2008	0.92	0.92	0.91	0.99	1.00	0.99
Råö, 2009	0.89	0.88	0.87	0.96	0.97	0.96
Råö, 2010	0.95	0.94	0.94	1.00	1.00	1.00
Vavihill, 2008	0.84	0.83	0.82	0.98	0.98	0.98
Vavihill, 2009	0.84	0.83	0.82	0.97	0.98	0.96
Vavihill, 2010	0.90	0.88	0.86	1.00	1.00	0.99
Vindeln, 2008	0.82	0.82	0.81	0.99	0.99	0.99
Vindeln, 2009	0.89	0.89	0.89	0.98	0.99	0.99
Vindeln, 2010	0.87	0.86	0.85	0.97	0.98	0.97
Östad, 2008	0.83	0.83	0.83	0.99	0.99	1.00
Östad, 2009	0.82	0.82	0.81	1.00	1.00	1.00

8.2 Additional material for ozone episodes during June 2008 and November 2010 and results from trajectory modelling

8.2.1 The ozone episode of 2010-07-02 to 2010-07-04

In the beginning of July 2010, there was an ozone episode with highest ozone concentrations at Grimsö, in the middle parts of Sweden but also in the western parts (Figure 8.2).

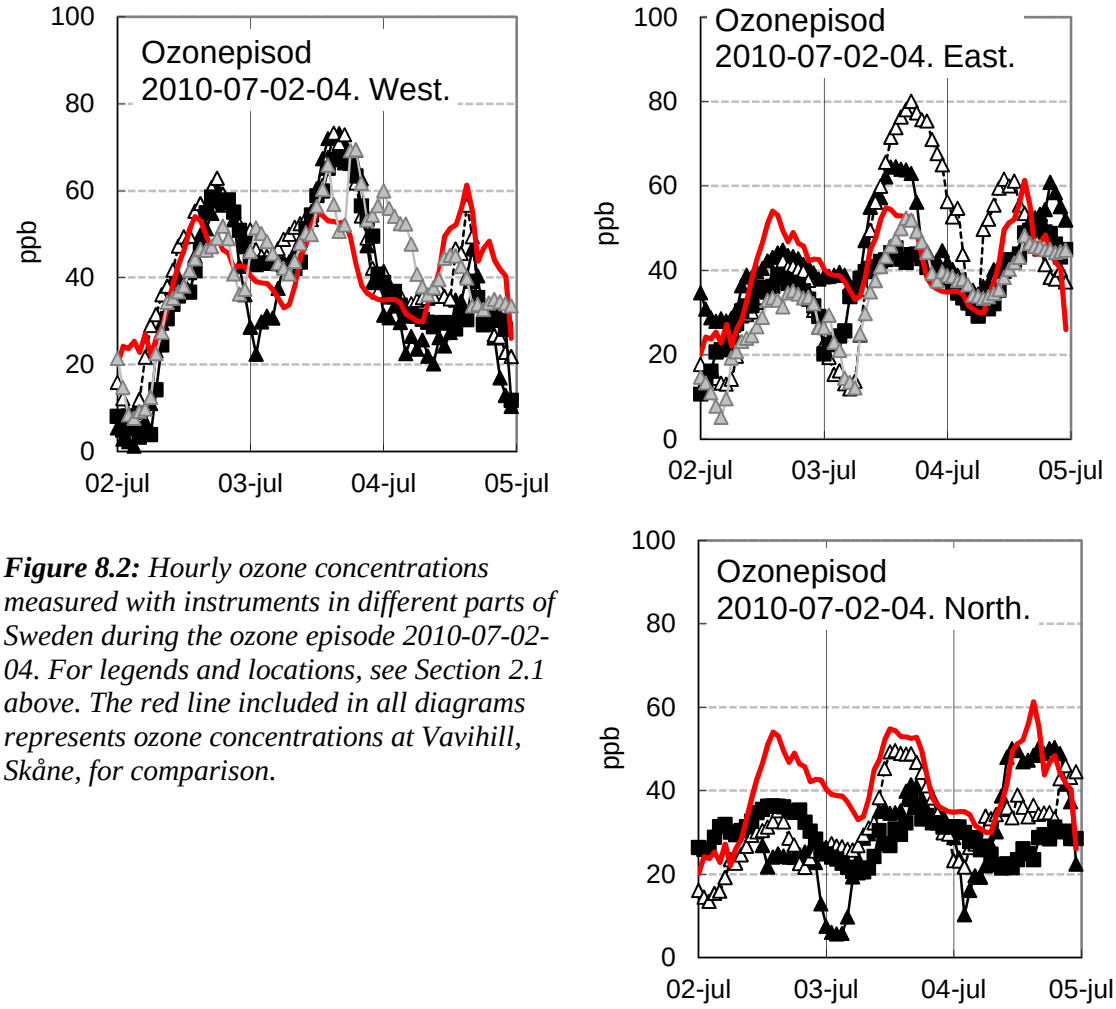

Figure 8.2: *Hourly ozone concentrations measured with instruments in different parts of Sweden during the ozone episode 2010-07-02-04. For legends and locations, see Section 2.1 above. The red line included in all diagrams represents ozone concentrations at Vavihill, Skåne, for comparison.*

Trajectory analysis made by NILU with the FLEXTRA model (Figure 8.3) indicated that the air arriving in the afternoon at Grimsö on 2010-07-03 originated from northern Germany, BeNeLux and to some extent from northern France. On the other hand, the air arriving at Aspvreten closest to the ground in fact originated from Norway and the Atlantic, explaining the low ozone concentrations measured at Aspvreten. The air arriving at the Eastern parts (Råö) also originated from northern Germany, BeNeLux and to some extent northern France and resulted in relatively high ozone concentrations

Vavihill 2010-07-03 18:00

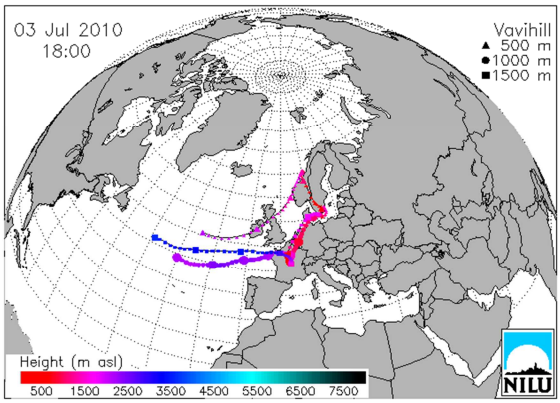

Råö 2010-07-03 18:00

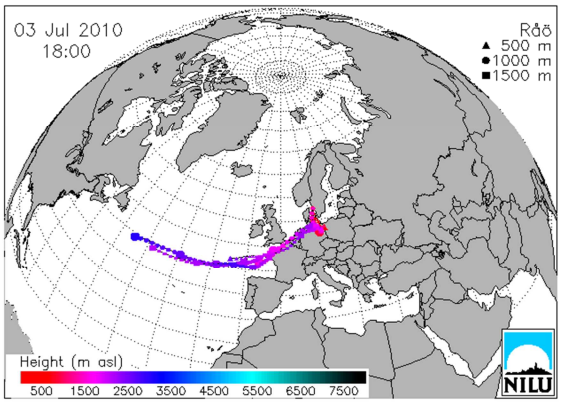

Grimsö 2010-07-03 18:00.

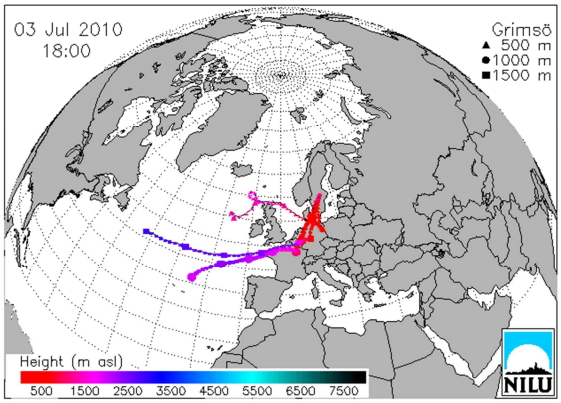

Figure 8.3: *Trajectories for air masses arriving at Vavihill, Råö and Grimsö during an ozone episode 2010-07-02-04, as estimated with the FLEXTRA model available at NILU. The exact time for arrival is indicated in association with each diagram.*

The highest ozone concentration during this episode was measured at Grimsö in the afternoon 2010-07-03, 80 ppb (Table 8.6), while lower concentrations were measured at Råö and Östad in the western parts the same day, 73 ppb. In the north of Sweden, the ozone concentrations reached a maximum of 45 ppb.

Table 8.6: *Highest ozone concentrations observed and modelled during the ozone episode 2010-07-02 to 2010-07-04.*

	West part of southern Sweden	East part of southern Sweden	Northern Sweden
Highest measured one-hour ozone concentration (ppb)	73.2	80.1	50.3
No of days with ozone concentrations >70 ppb	1	1	
Highest modelled one-hour ozone concentration (ppb)	72.4	62.0	44.7
Ratio modelled vs measured	0.99	0.77	0.89

Modelled ozone concentrations agree relatively well with measurements during this episode, except for the eastern sites Norra Kvill and, in particular, Grimsö (Figure 8.4). Note that ozone concentrations at Grimsö are under re-evaluation. It is interesting that also the measured ozone concentrations at Bredkälen are clearly above modelled values.

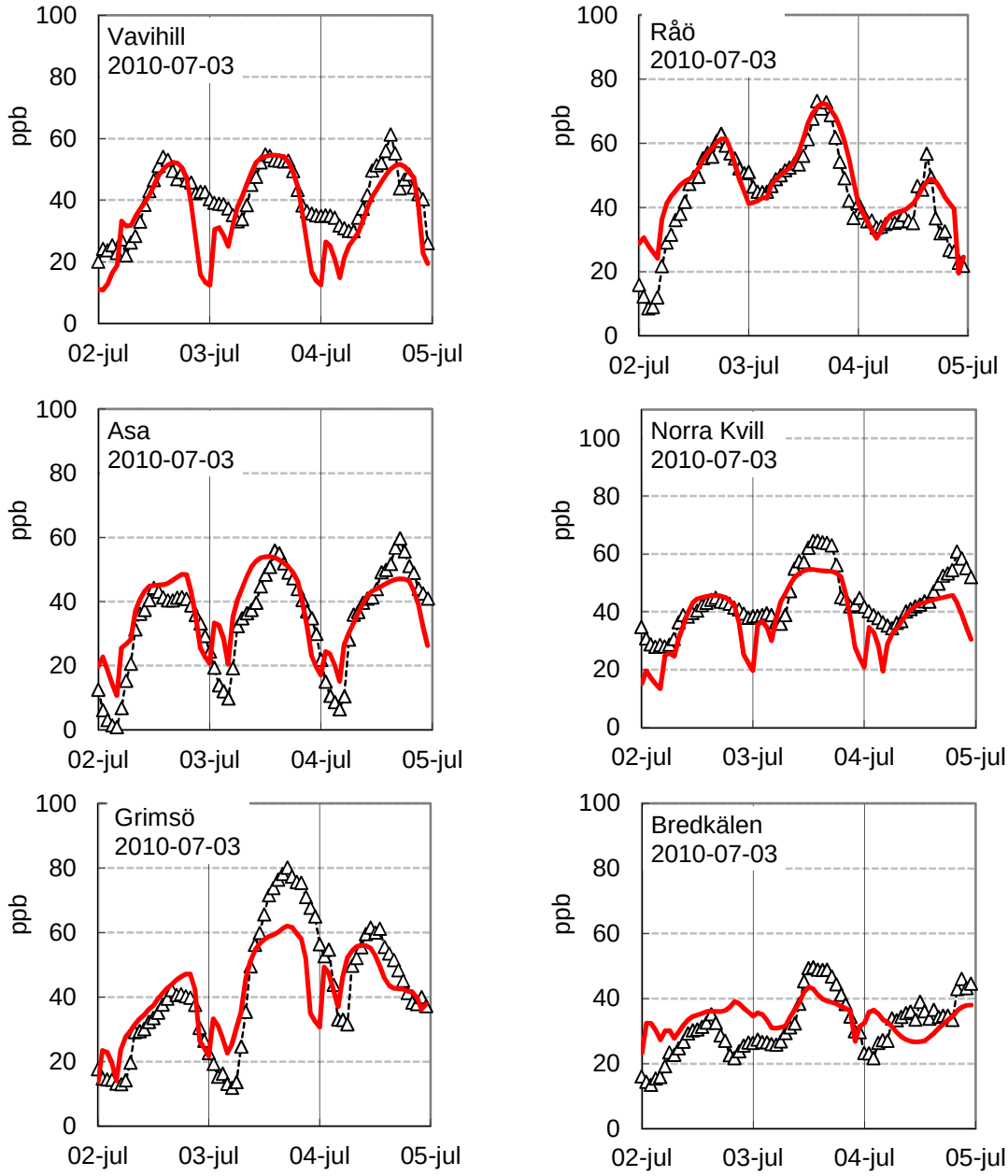

Figure 8.4: *Comparison between modelled and measured hourly ozone concentrations at three sites in different parts of Sweden during an ozone episode 2010-07-02-04. Black open triangles represents measured values, red line modelled values.*
(Note that ozone concentrations at Grimsö are under re-evaluation.)

8.2.2 The ozone episode of 2010-06-28 to 2010-06-30

In the end of June 2010, there was an ozone episode with highest ozone concentrations in the southern and western parts of Sweden but also in mid Sweden (Figure 8.5). Trajectory analysis made by NILU with the FLEXTRA model are given in Figure 8.6. The highest ozone concentration during this episode, 72 ppb, was measured at Prestebakke at lunchtime 2010-06-29 (Table 8.7). Also Råö and Grimsö showed high ozone concentrations, 70 ppb, in the

afternoon the same day. Ozone concentrations in northern Sweden did not exceed 52 ppb. Ozone concentrations were modelled relatively well during this episode (Figure 8.7).

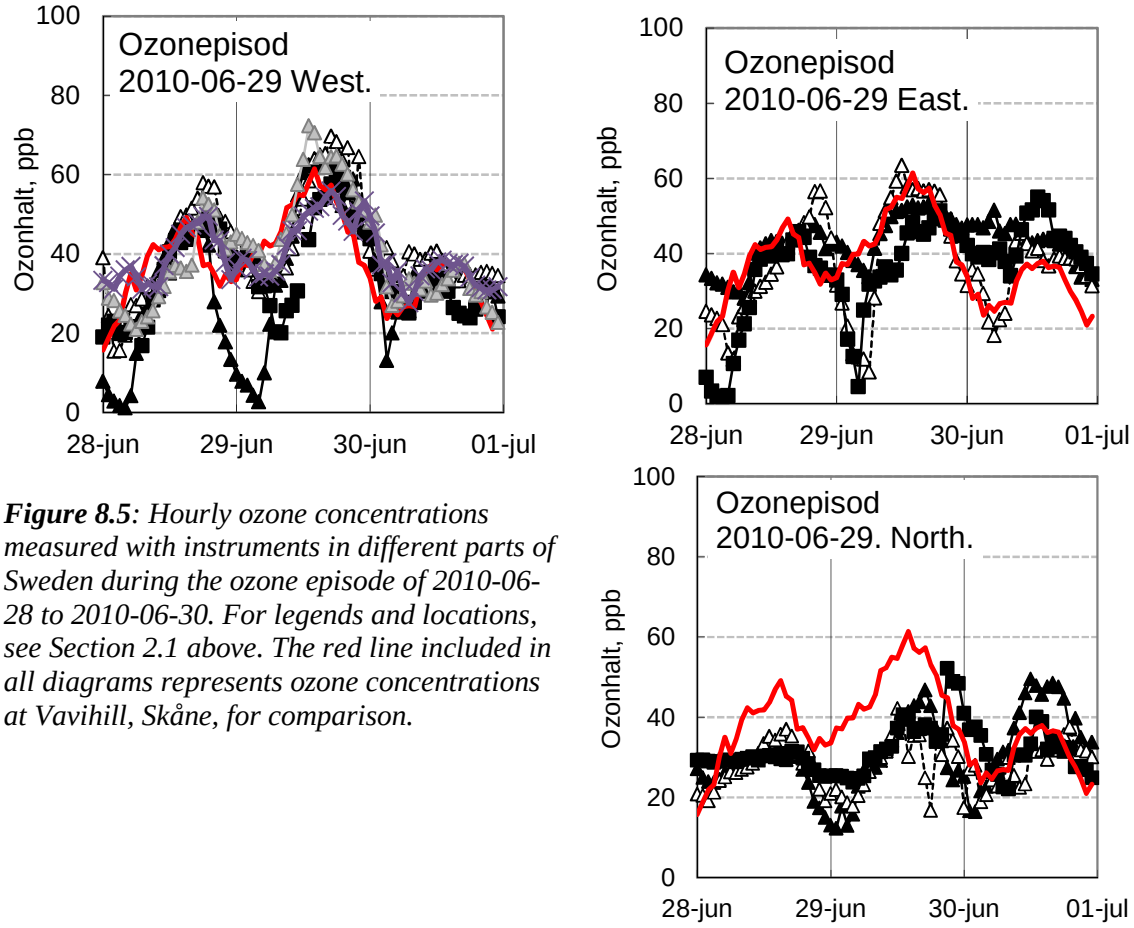

***Figure 8.5**: Hourly ozone concentrations measured with instruments in different parts of Sweden during the ozone episode of 2010-06-28 to 2010-06-30. For legends and locations, see Section 2.1 above. The red line included in all diagrams represents ozone concentrations at Vavihill, Skåne, for comparison.*

Vavihill 2010-06-28 18:00.

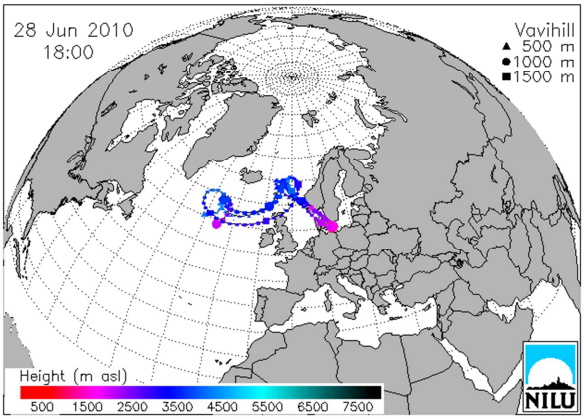

Vavihill 2010-06-29 18:00

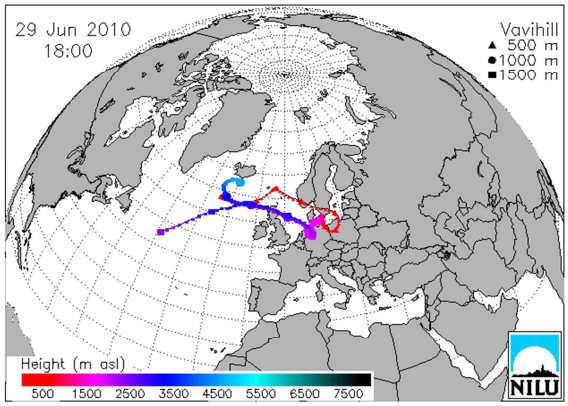

Råö 2010-06-28 18:00

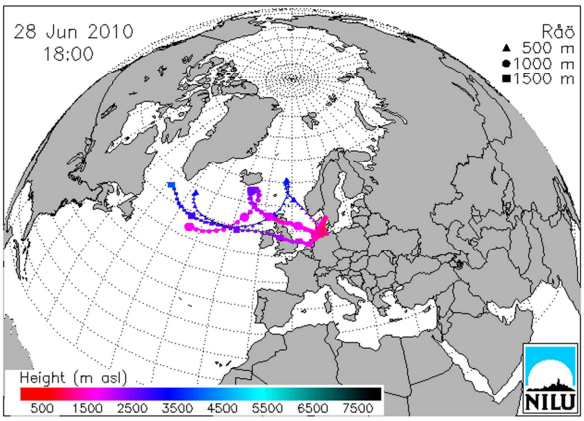

Råö 2010-06-29 18:00

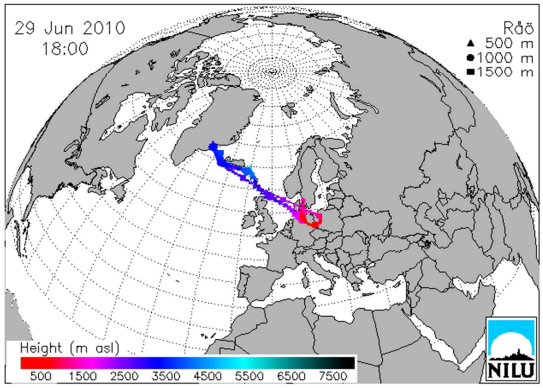

Grimsö 2010-06-28 18:00.

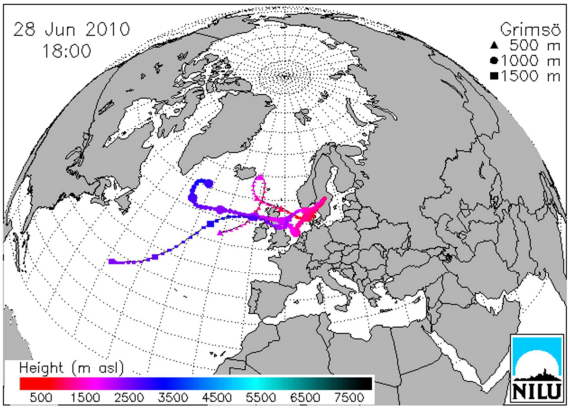

Grimsö 2010-06-29 18:00.

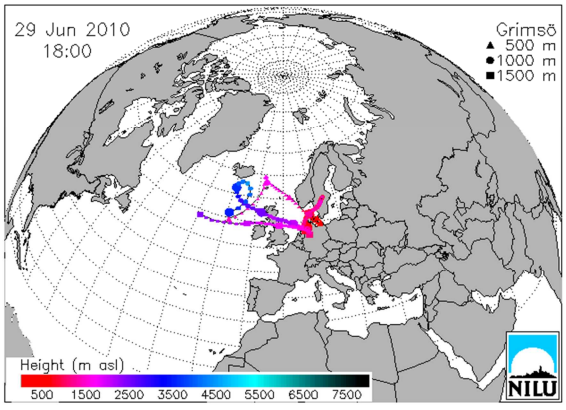

Figure 8.6: *Trajectories for air masses arriving at Vavihill, Råö and Grimsö during an ozone episode of 2010-06-28 to 2010-06-30, as estimated with the FLEXTRA model available at NILU. The exact time for arrival is indicated in association with each diagram.*

Table 8.7: *Highest ozone concentrations observed and modelled during the ozone episode 2010-06-28 to 2010-06-30.*

	West part of southern Sweden	East part of southern Sweden	Northern Sweden
Highest measured one-hour ozone concentration (ppb)	72.3	63.4	52.2
No of days with ozone concentrations >70 ppb	1	1	0
Air pressure dynamics	Decreasing over three days from 1019 to 1012 mbar	Decreasing over three days from 1014 to 1004 mbar	-
Local weather			
Highest modelled one-hour ozone concentration (ppb)	64.8	59.7	45.6
Ratio modelled vs measured	0.90	0.94	0.87

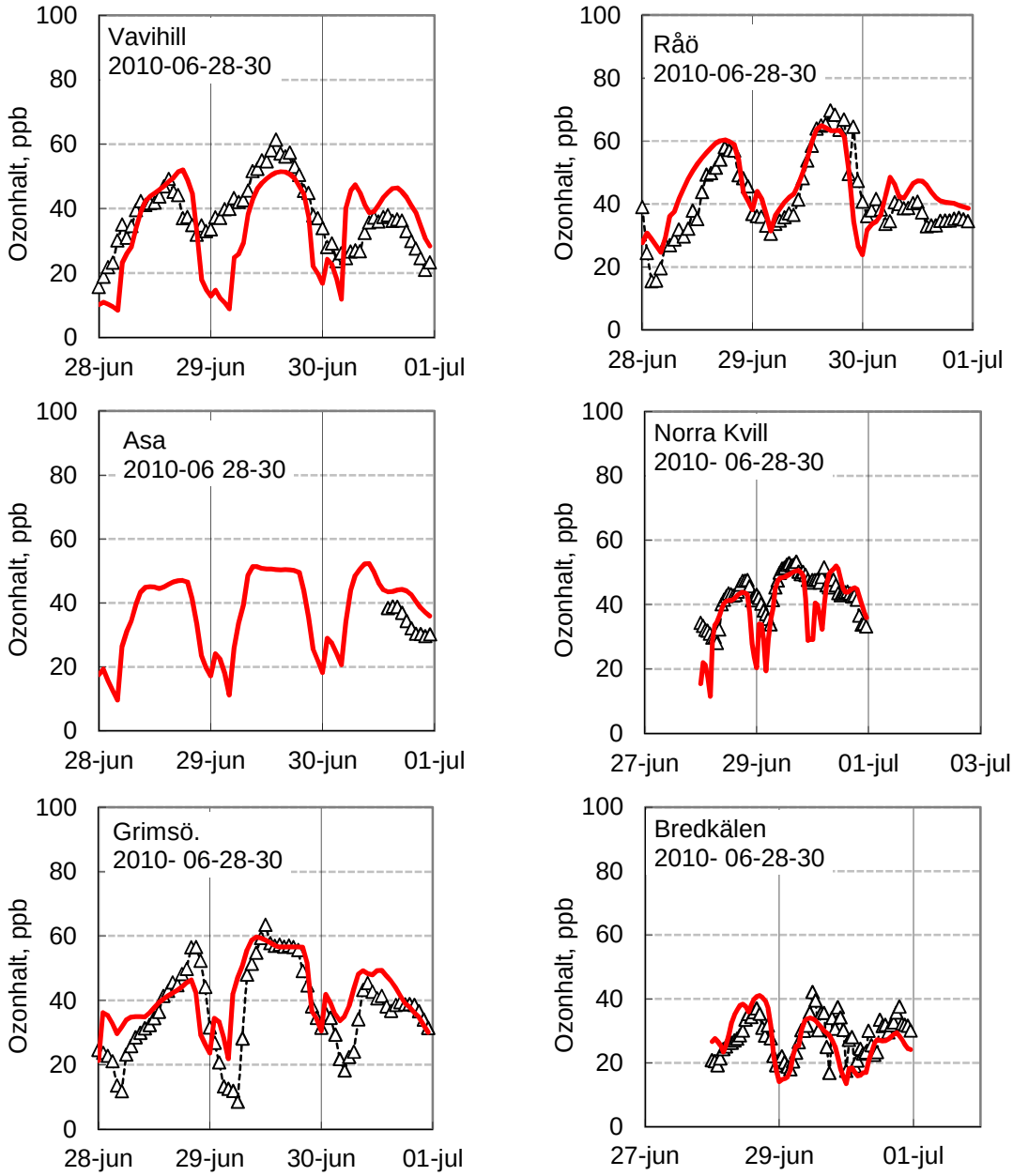

Figure 8.7: *Comparison between modelled and measured hourly ozone concentrations at three sites in different parts of Sweden during an ozone episode 2010-06-28 to 2010-06-30. Black open triangles represents measured values, red line modelled values.*

8.2.3 The ozone episode of 2010-05-14 to 2010-05-16

In mid May 2010, there was an unusual ozone episode with highest ozone concentrations in the north part of Sweden at Vindeln (Figure 8.8).

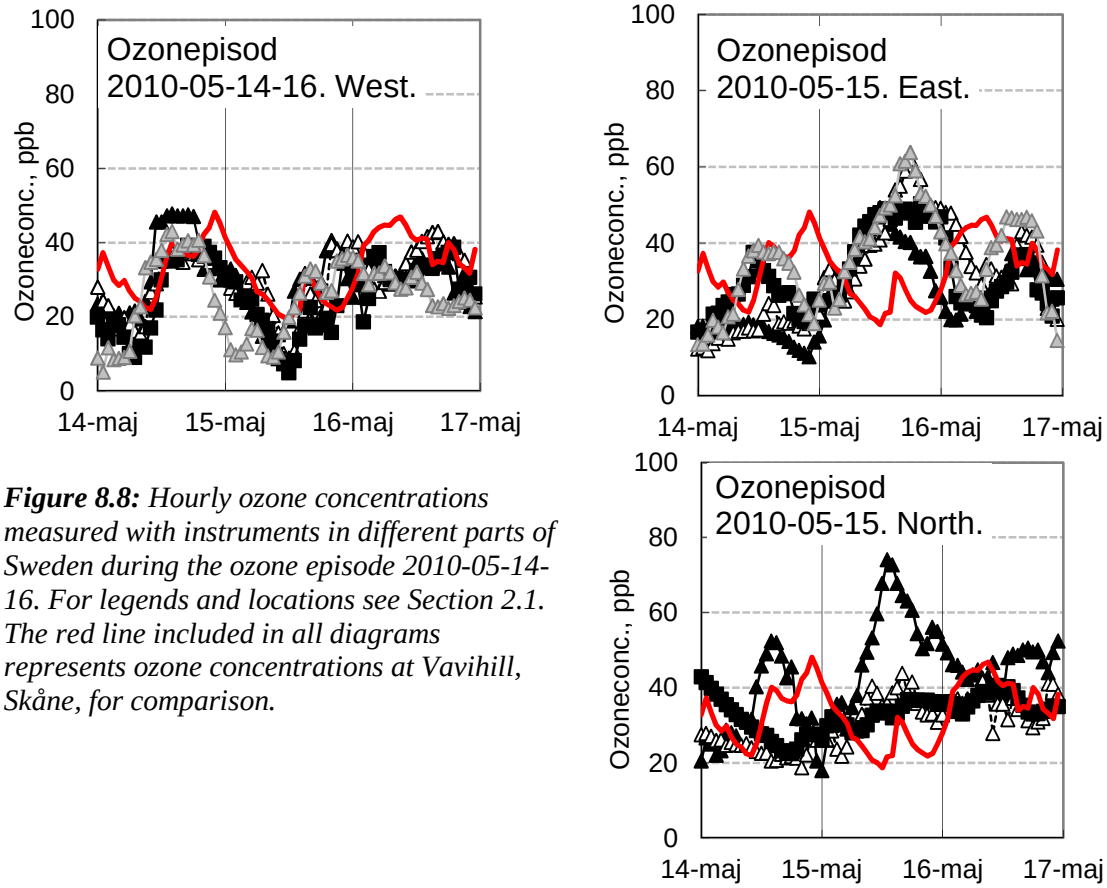

Figure 8.8: *Hourly ozone concentrations measured with instruments in different parts of Sweden during the ozone episode 2010-05-14-16. For legends and locations see Section 2.1. The red line included in all diagrams represents ozone concentrations at Vavihill, Skåne, for comparison.*

Trajectory analysis made by NILU with the FLEXTRA model indicated that the air arriving in Vindeln in the afternoon 2010-05-15 originated from Russia and countries beyond (Figure 8.9). Extensive biomass burning in Russia might be an explanation for the high ozone concentrations at Vindeln. The air arriving at Grimsö followed a slightly more southern path and the ozone concentrations measured at Grimsö were not that high. Air arriving at low elevation at Vavihill originated from Ukraine via Belarus and the Baltic states and did not cause high ozone concentrations.

Vavihill 2010-05-15 18:00

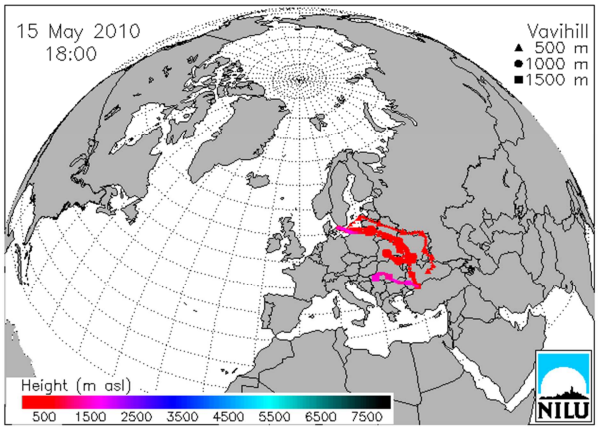

Grimsö 2010-05-15 18:00

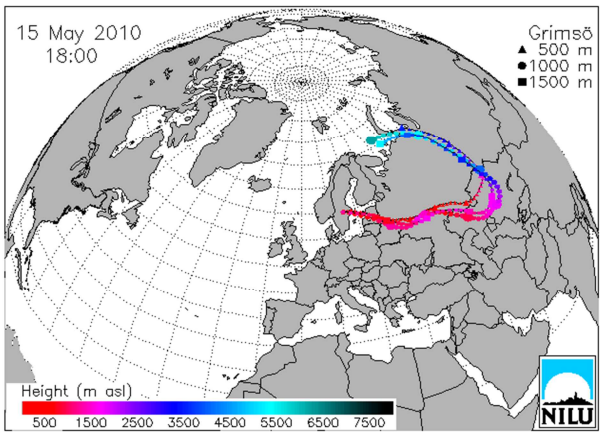

Vindeln 2010-05-15 18:00.

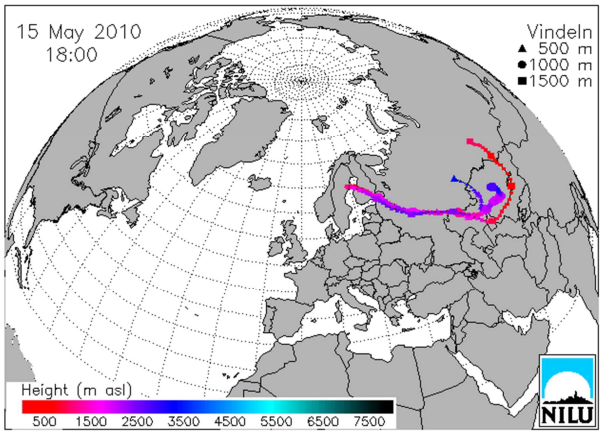

Figure 8.9: *Trajectories for air masses arriving at Vavihill, Grimsö and Vindeln during an ozone episode 2010-05-14 to 2010-05-16, as estimated with the FLEXTRA model available at NILU. The exact time for arrival is indicated in association with each diagram.*

The highest ozone concentration during this episode, 74 ppb, was measured at Vindeln at lunchtime 2010-05-15 (Table 8.8). The highest ozone concentration in the east part of southern

Sweden, 64 ppb, was measured at Norr Malma north of Stockholm, in the afternoon the same day. Ozone concentrations in west Sweden did not exceed 48 ppb.

Table 8.8: *Highest ozone concentrations observed and modelled during the ozone episode of 2010-05-14 to 2010-05-16.*

	West part of southern Sweden	East part of southern Sweden	Northern Sweden
Highest measured one-hour ozone concentration (ppb)	48.2	63.8	74.1
No of days with ozone concentrations >70 ppb	0	0	1
Air pressure dynamics	Variable 997-1007 mbar, first decreasing, then increasing	Variable 999-1004 mbar, first decreasing, then increasing	-
Local weather			
Highest modelled one-hour ozone concentration (ppb)	48.1	49.6	50.8
Ratio modelled vs measured	1.00	0.78	0.69

The highest ozone concentration at Vindeln was not modelled very well during this episode, reaching only 78% of the measured concentration. Most likely the emissions from the Russian biomass burning were not in the emission database of MATCH. Also ozone concentrations at Grimsö and Norra Kvill were not modelled very well, probably due to influence from easterly winds. Ozone concentrations at Råö were on the other hand to some extent overestimated by the model (Figure 8.10).

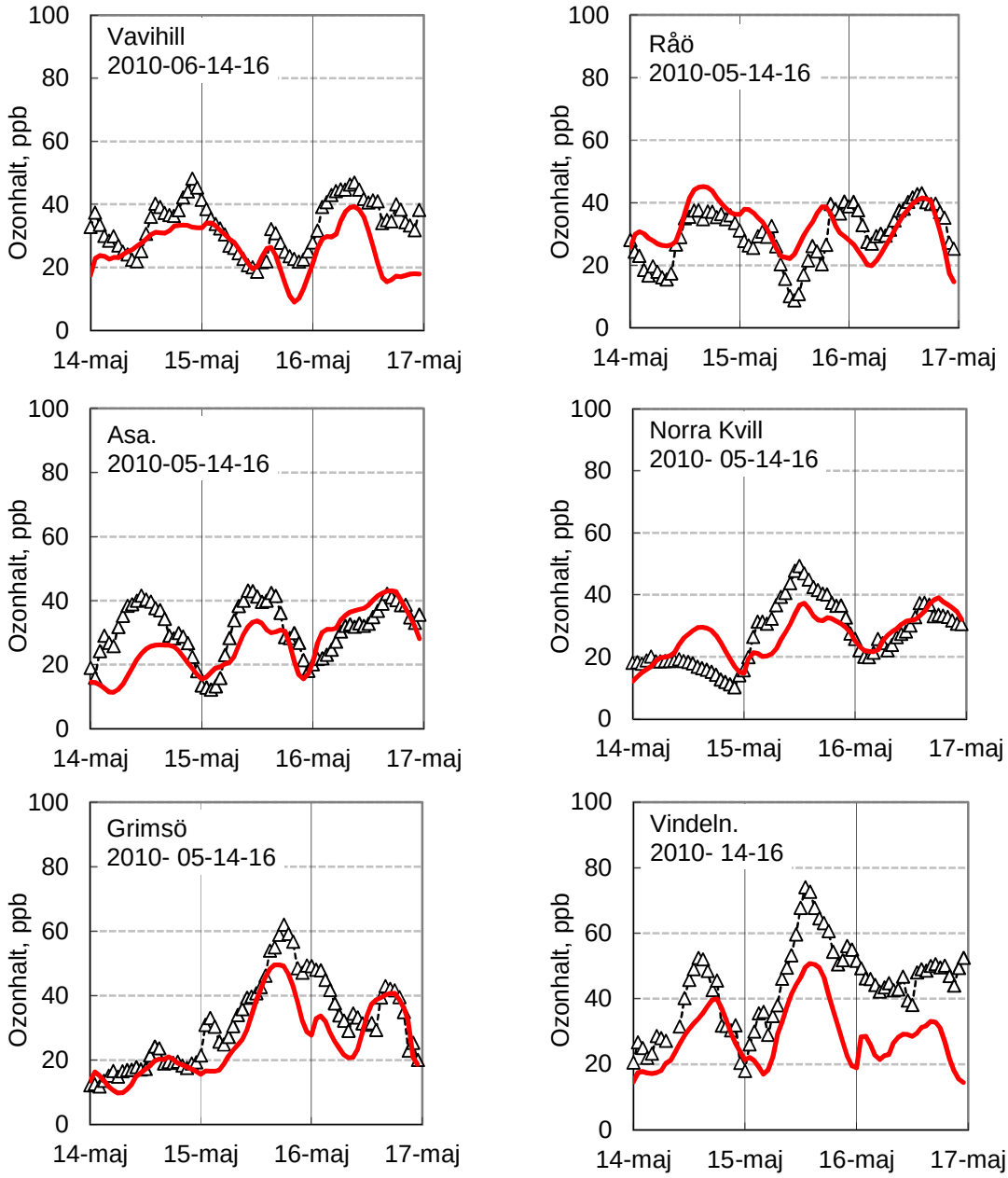

Figure 8.10: *Comparison between modelled and measured hourly ozone concentrations at three sites in different parts of Sweden during an ozone episode 2010-05-14-16. Black open triangles represents measured values, red line modelled values.*

8.2.4 The ozone episode of 2009-07-03 to 2009-07-05

In the beginning of July 2009, there was an ozone episode with highest ozone concentrations in the western part of Sweden (Figure 8.11). Ozone concentrations in the eastern and northern parts were considerably lower.

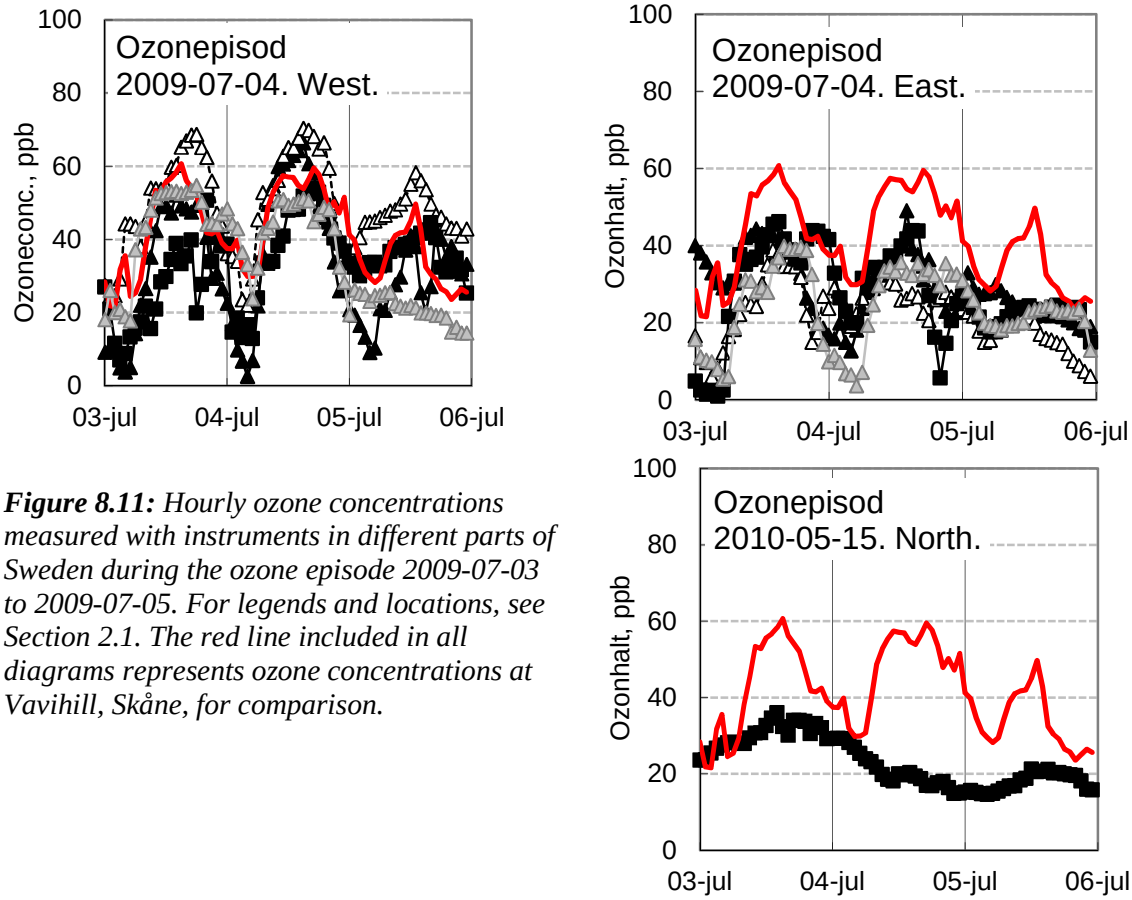

Figure 8.11: *Hourly ozone concentrations measured with instruments in different parts of Sweden during the ozone episode 2009-07-03 to 2009-07-05. For legends and locations, see Section 2.1. The red line included in all diagrams represents ozone concentrations at Vavihill, Skåne, for comparison.*

Trajectory analysis made by NILU with the FLEXTRA model indicated that the air arriving at Råö in the afternoon 2009-07-04 came over parts of the North Sea but originated from Netherlands, northern Germany and Poland, evidently moving relatively slowly (Figure 8.12). The air arriving at Vavihill originated from the Baltic states, Belarus and Russia, passed over northern Germany and resulted in lower ozone concentrations as compared to Råö. Air arriving at the eastern parts of south Sweden, e.g. Aspvreten, had a completely different origin, originating from northern Atlantic and passing over Finland and northern Sweden, resulting in lower concentrations.

The highest ozone concentration during this episode, 70 ppb, was measured at Råö in the afternoon 2009-07-04. The highest ozone concentration in the eastern part of southern Sweden was only 54 ppb, while ozone concentrations in northern Sweden did not exceed 36 ppb.

The MATCH model overestimated ozone concentrations at Vavihill and underestimated for Råö (Table 8.9, Figure 8.13). Even in the eastern part of southern Sweden the MATCH model tended to overestimate the ozone concentrations.

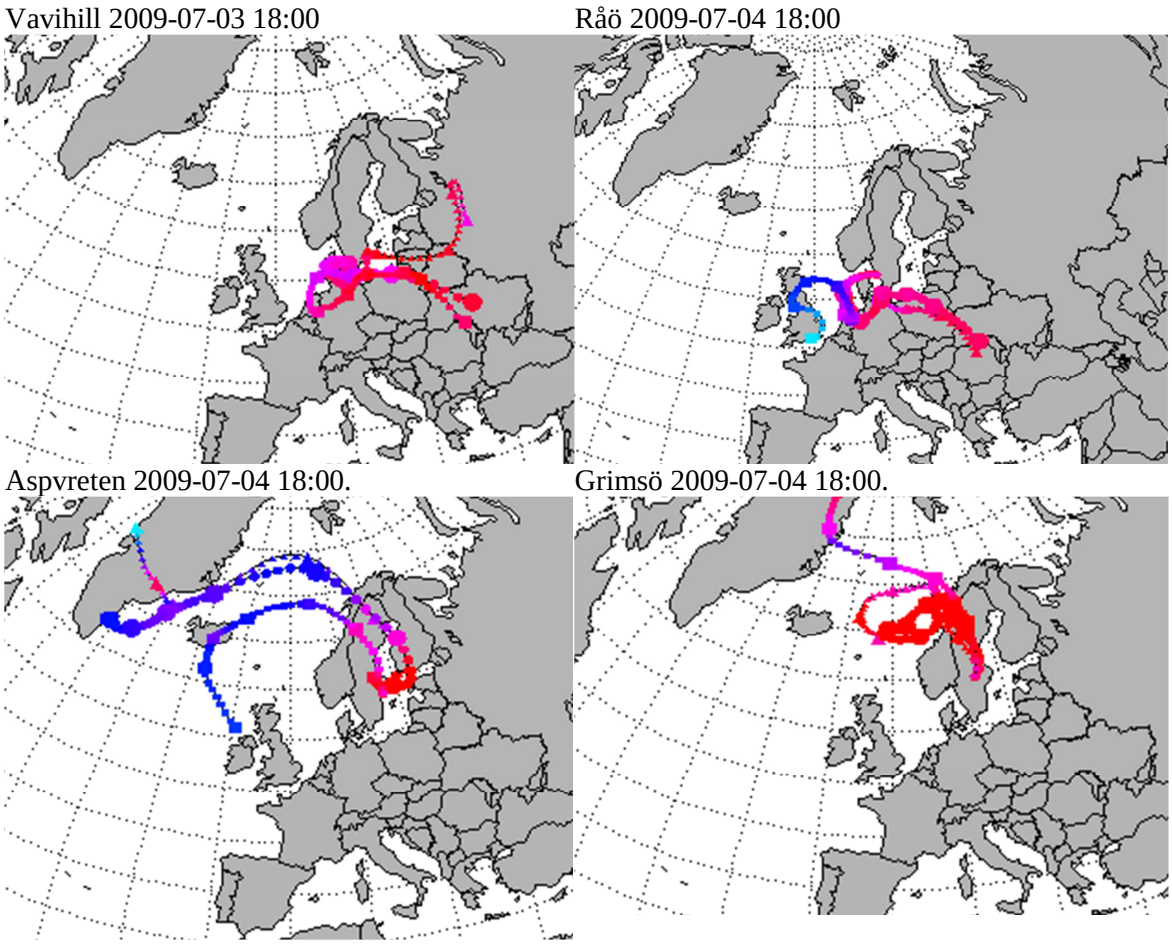

Figure 8.12: *Trajectories for air masses arriving at Vavihill, Råö, Aspvreten and Grimsö during an ozone episode 2009-07-03 to 2009-07-05, as estimated with the FLEXTRA model available at NILU. The exact time for arrival is indicated in association with each diagram.*

Table 8.9: *Highest ozone concentrations observed and modelled during the ozone episode of 2010-07-03 to 2010-07-05.*

	West part of southern Sweden	East part of southern Sweden	Northern Sweden
Highest measured one-hour ozone concentration (ppb)	70.3	54.3	36.1
No of days with ozone concentrations >70 ppb	1	0	0
Air pressure dynamics	Decrease over three days from 1015 to 1002 mbar.	Decrease over three days from 1012 to 1003 mbar.	
Local weather			
Highest modelled one-hour ozone concentration (ppb)	62.0	58.4	42.6
Ratio modelled vs measured	0.88	1.08	1.18

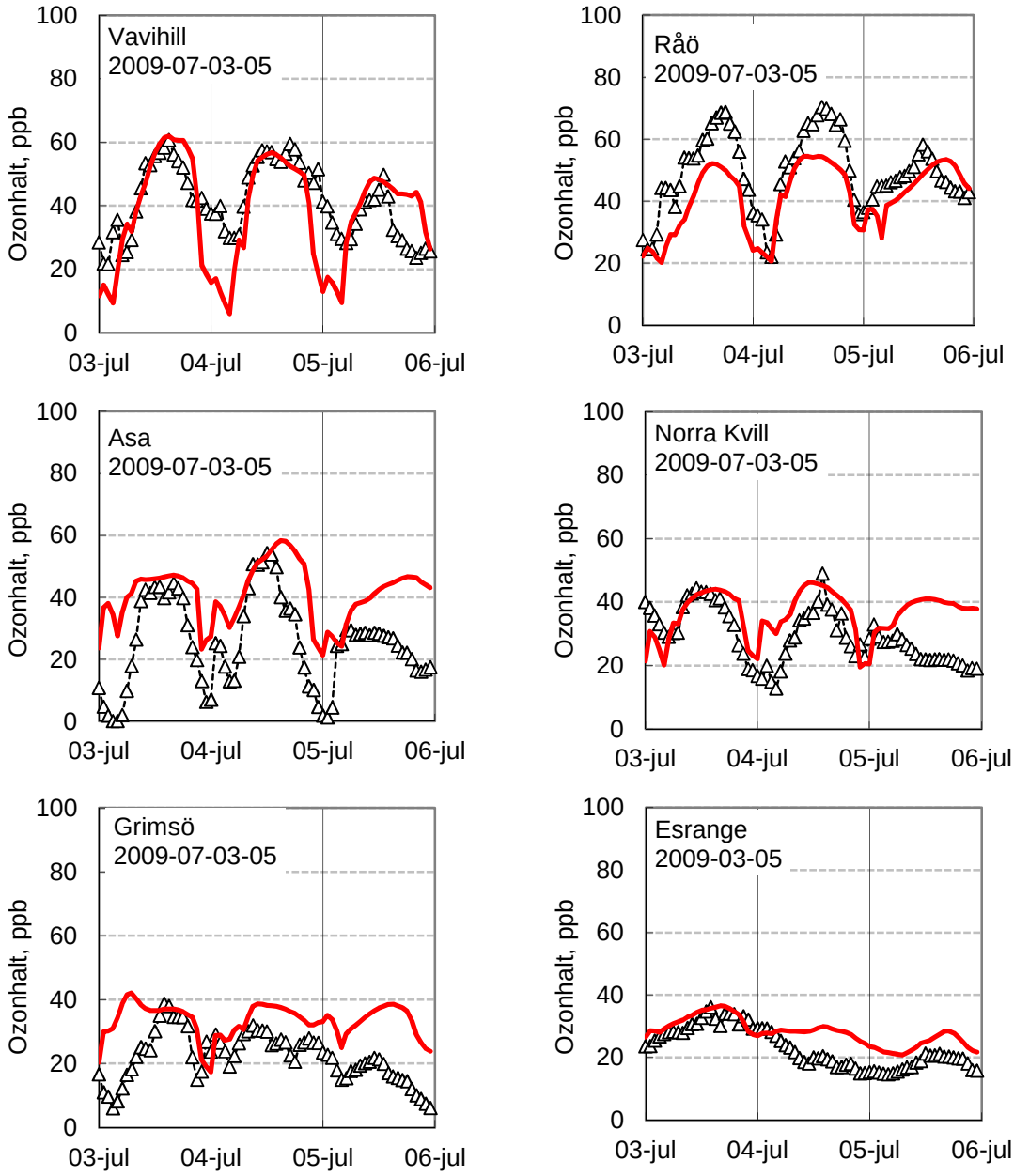

Figure 8.13: *Comparison between modelled and measured hourly ozone concentrations at three sites in different parts of Sweden during an ozone episode 2009-07-03 to 2009-07-05. Black open triangles represents measured values, red line modelled values.*

8.2.5 The ozone episode of 2009-04-25 to 2009-04-27

At the end of April 2009, there was an ozone episode with highest ozone concentrations in the eastern part of south Sweden (Figure 8.14). Ozone concentrations were also relatively high in northern Sweden. Trajectories, highest ozone concentrations and time series of modelled and measured concentrations are given in Figure 8.15, Table 8.10 and Figure 8.16, respectively.

The highest ozone concentration during this episode, 72 ppb, was measured at Asa and Norra Kvill in south eastern Sweden in the afternoon and evening 2009-04-26. The highest ozone concentration in the western part of southern Sweden was 66 ppb. There are some missing data

at Vavihill, however, so the ozone concentrations at this site might have been higher. Ozone concentrations in north Sweden were unusually high, 64 ppb.

The MATCH model simulated ozone concentrations in south western Sweden very well, while the higher concentrations in the eastern part of Sweden were simulated less well. Even the unusually high concentrations in northern Sweden were simulated well by the MATCH model. We assume that the mechanism responsible for the higher concentration is a downward transport of ozone from higher tropospheric levels, i.e. it can be concluded that the MATCH model captures that mechanism relatively well.

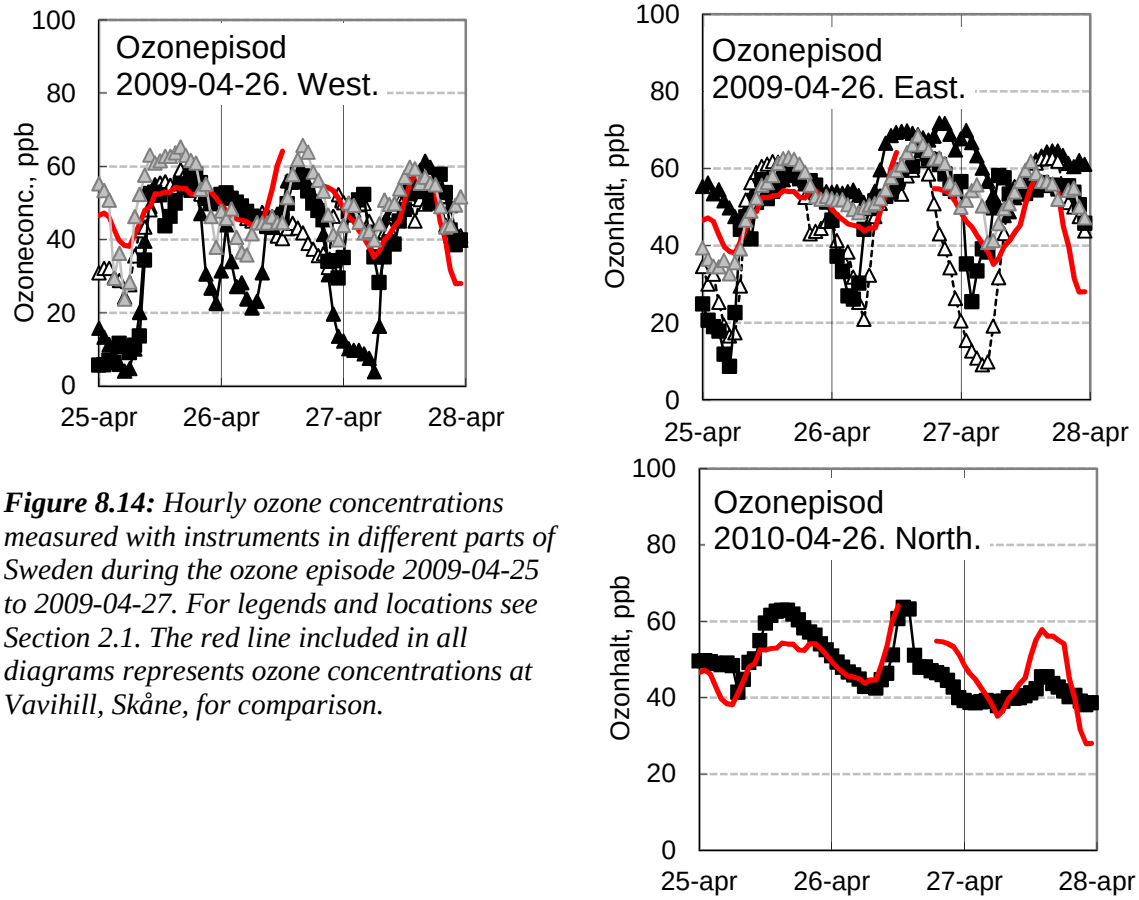

Figure 8.14: *Hourly ozone concentrations measured with instruments in different parts of Sweden during the ozone episode 2009-04-25 to 2009-04-27. For legends and locations see Section 2.1. The red line included in all diagrams represents ozone concentrations at Vavihill, Skåne, for comparison.*

Vavihill 2009-04-26 18:00

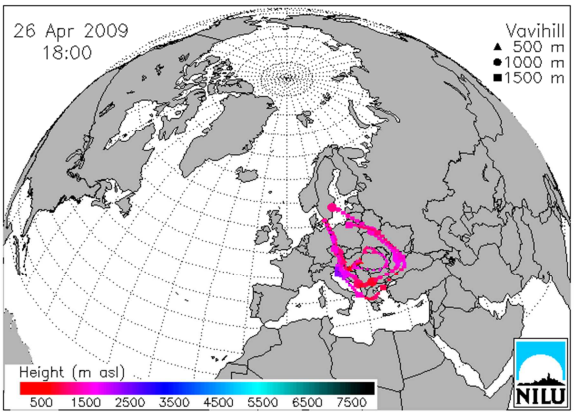

Råö 2009-04-26 18:00

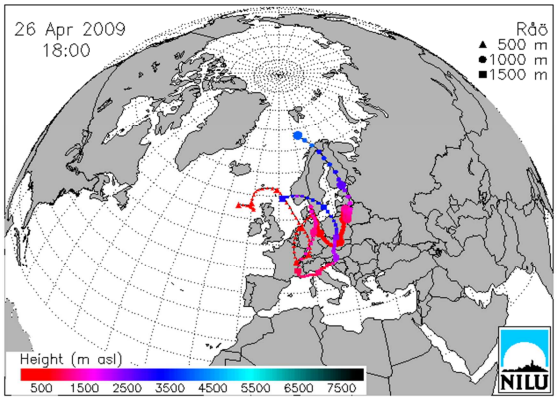

Aspvreten 2009-04-26 18:00.

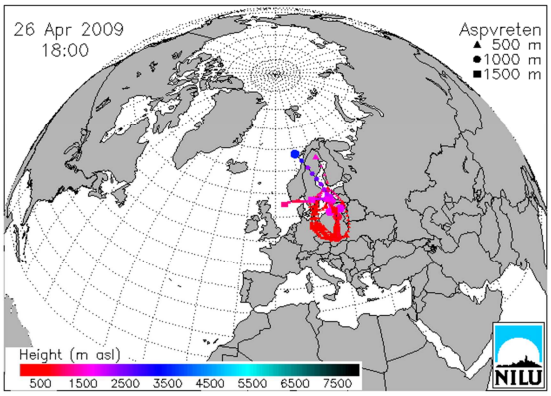

Grimsö 2009-04-26 18:00.

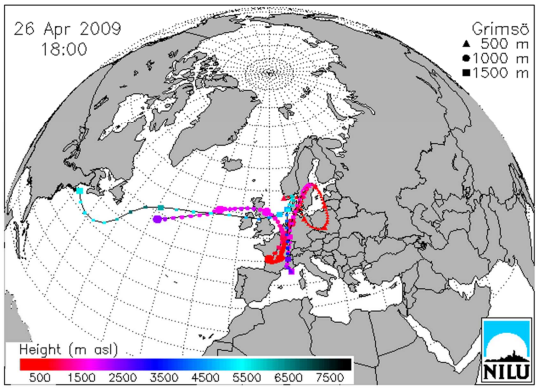

Vindeln 2009-04-26 18:00.

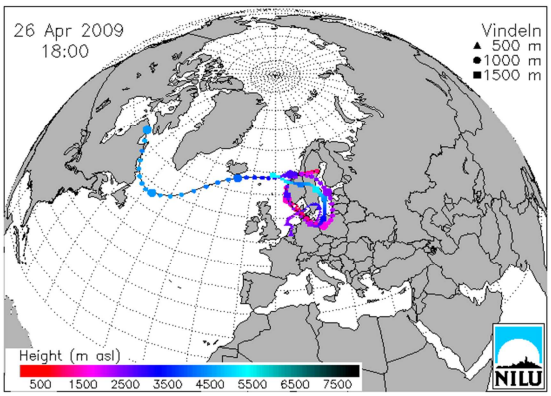

Figure 8.15: *Trajectories for air masses arriving at Vavihill, Råö, Aspvreten, Grimsö and Vindeln during an ozone episode 2009-04-25 to 2009-04-27, as estimated with the FLEXTRA model available at NILU. The exact time for arrival is indicated in association with each diagram.*

Table 8.10: *Highest ozone concentrations observed and modelled during the ozone episode of 2010-04-25 to 2010-04-27.*

	West part of southern Sweden	East part of southern Sweden	Northern Sweden
Highest measured one-hour ozone concentration (ppb)	65.7	72.3	63.7
No of days with ozone concentrations >70 ppb	0	1	0
Air pressure dynamics	Decrease from 1021 to 998 mbar over three days	Decrease from 1017 to 1000 mbar over three days	-
Local weather			
Highest modelled one-hour ozone concentration (ppb)	64.3	64.1	63.9
Ratio modelled vs measured	0.98	0.89	1.00

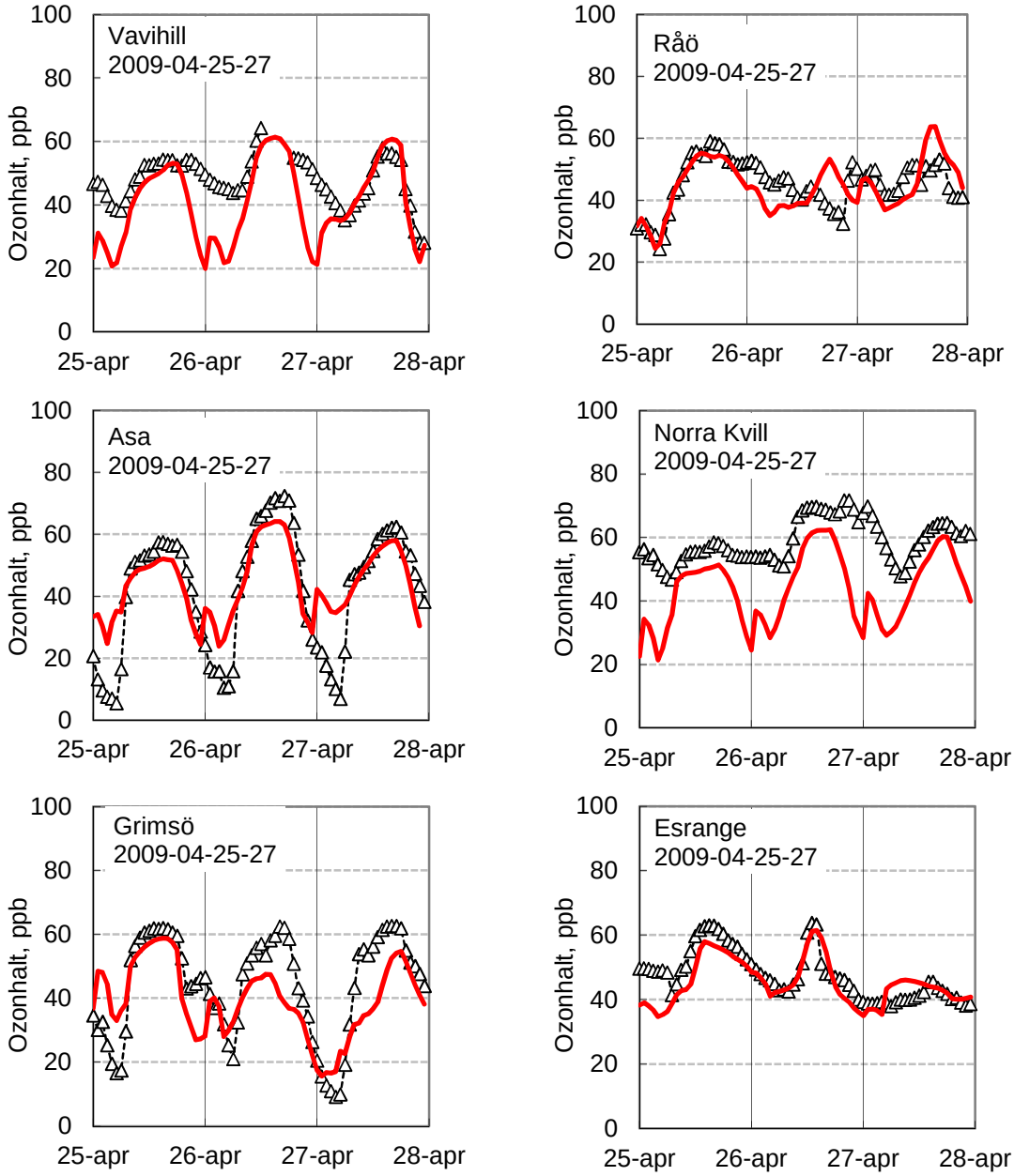

Figure 8.16: *Comparison between modelled and measured hourly ozone concentrations at three sites in different parts of Sweden during an ozone episode 2009-04-25 to 2009-04-27. Black open triangles represents measured values, red line modelled values.*

8.2.6 The ozone episode of 2008-06-01 to 2008-06-03

The complementary material for our analysis of this case is given in Figures 8.17-8.19 and Table 8.11.

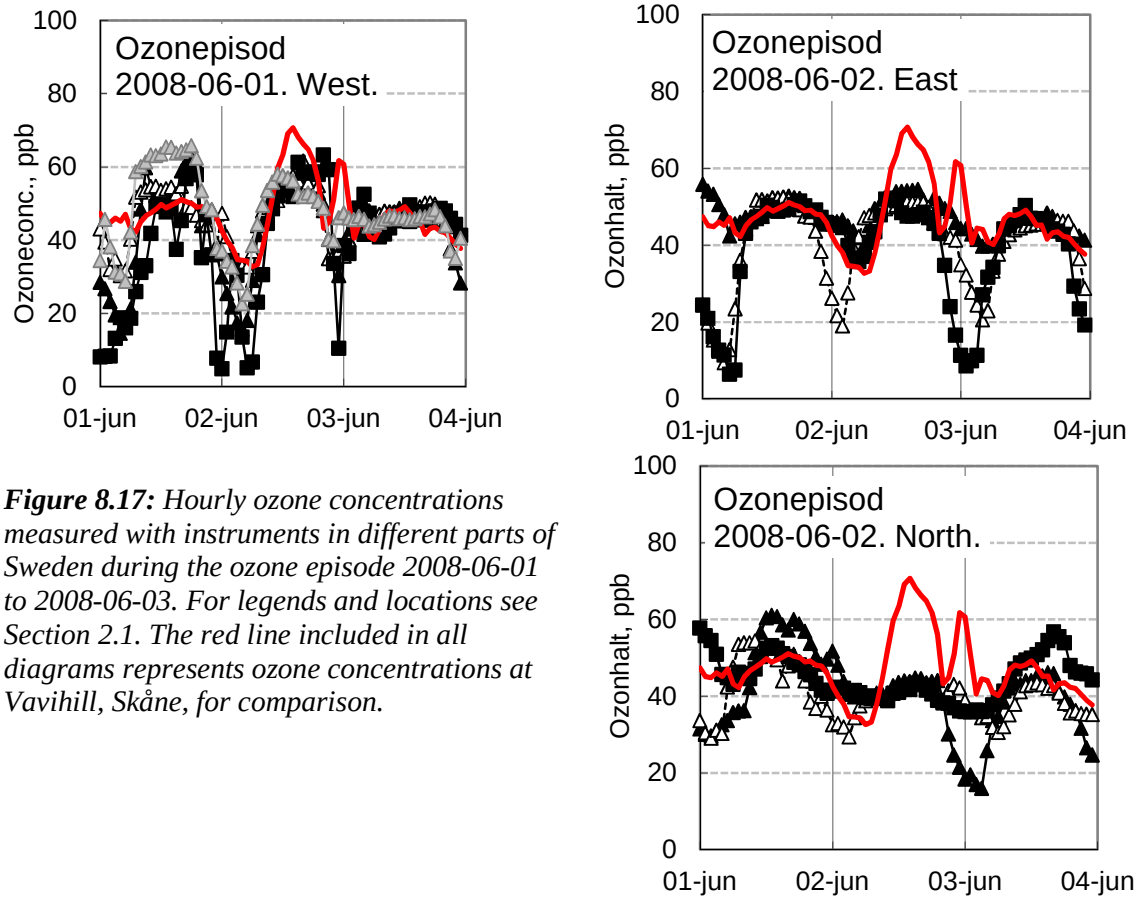

Figure 8.17: *Hourly ozone concentrations measured with instruments in different parts of Sweden during the ozone episode 2008-06-01 to 2008-06-03. For legends and locations see Section 2.1. The red line included in all diagrams represents ozone concentrations at Vavihill, Skåne, for comparison.*

Table 8.11: *Highest ozone concentrations observed and modelled during the ozone episode of 2008-06-01 to 2008-06-03.*

	West part of southern Sweden	East part of southern Sweden	Northern Sweden
Highest measured one-hour ozone concentration (ppb)	70.7	66.6	61.1
No of days with ozone concentrations >70 ppb	1	0	0
Air pressure dynamics	Variable, 1012-1019 mbar	Variable, 1013-1017 mbar	
Local weather			
Highest modelled one-hour ozone concentration (ppb)	61.9	54.0	48.2
Ratio modelled vs measured	0.88	0.81	0.79

Vavihill 2008-06-02 18:00

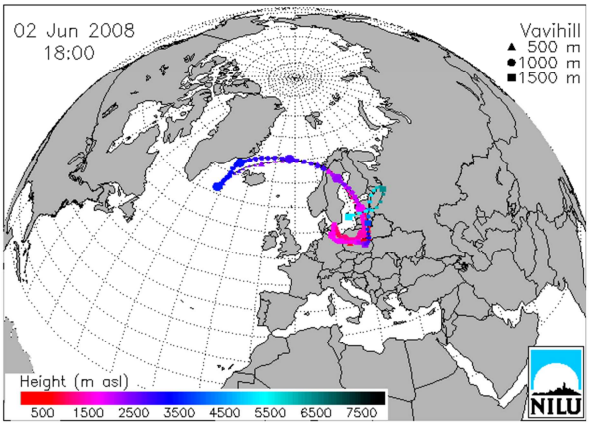

Råö 2008-06-02 18:00

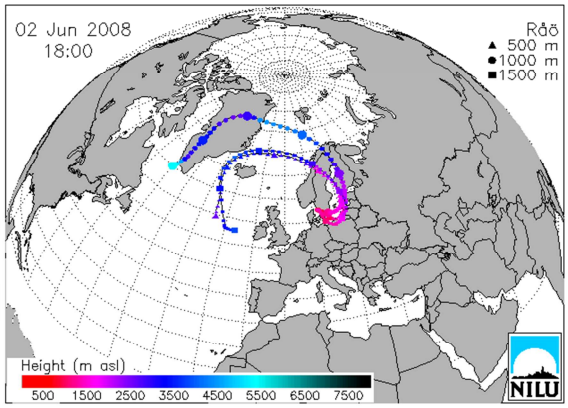

Aspvreten 2008-06-02 18:00.

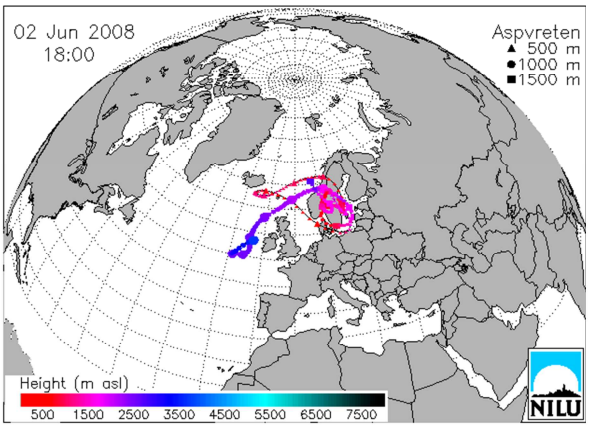

Grimsö 2008-06-02 18:00.

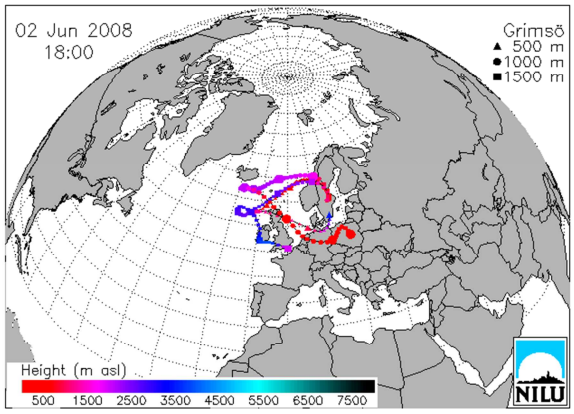

Vindeln 2008-06-02 18:00.

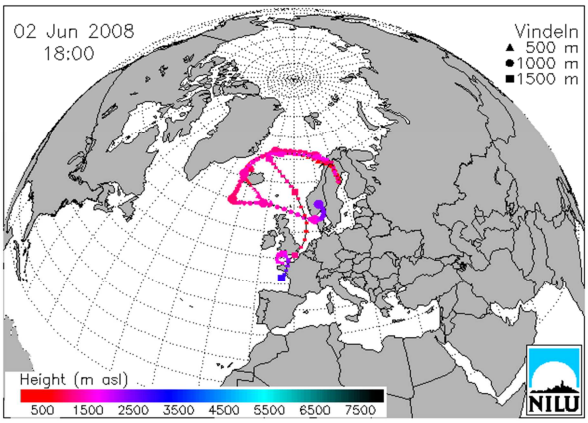

Figure 8.18: *Trajectories for air masses arriving at Vavihill, Råö, Aspvreten, Grimsö and Vindeln during an ozone episode 2008-06-01 to 2008-06-03, as estimated with the FLEXTRA model available at NILU. The exact time for arrival is indicated in association with each diagram.*

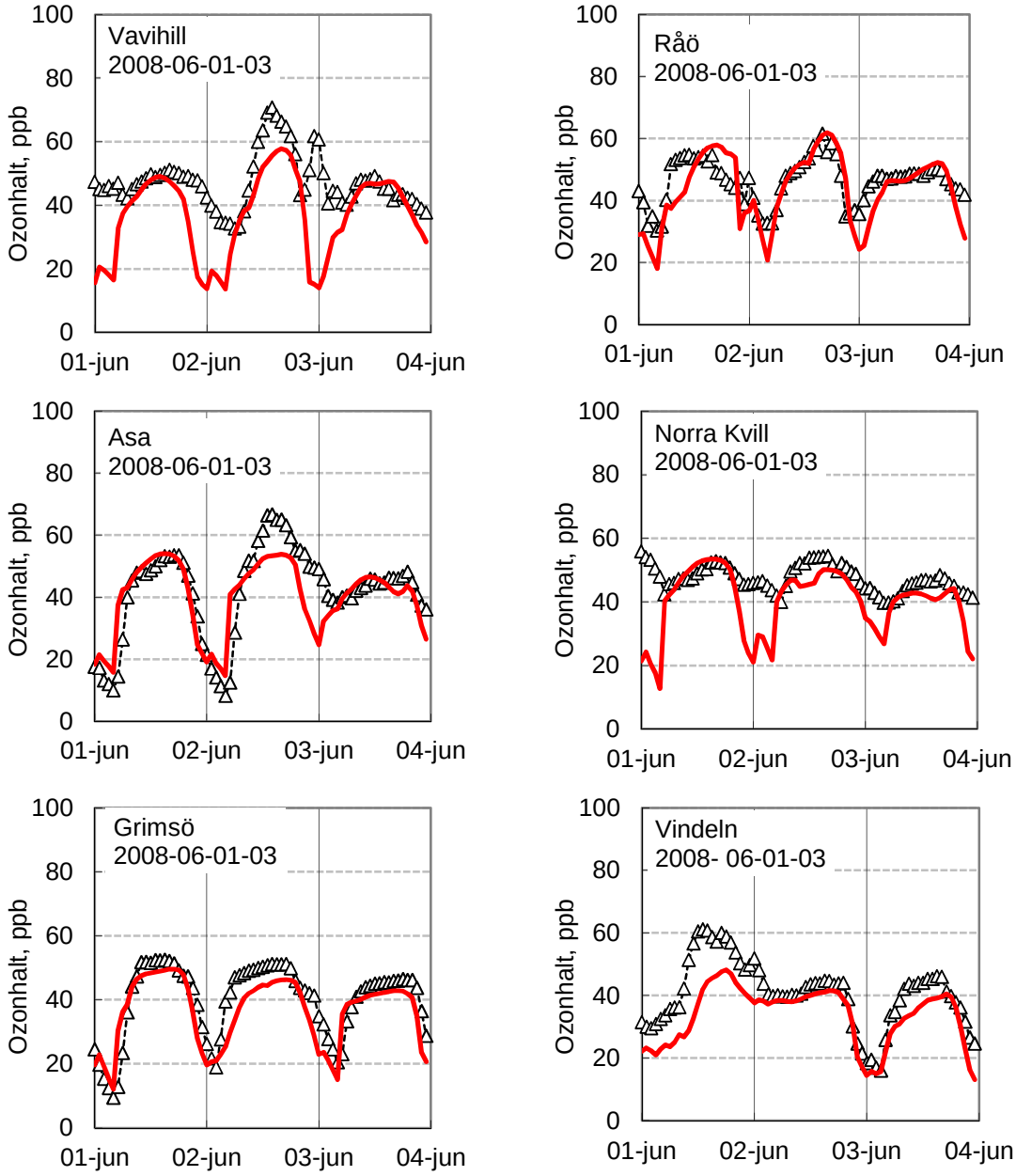

Figure 8.19: *Comparison between modelled and measured hourly ozone concentrations at three sites in different parts of Sweden during an ozone episode 2008-06-01 to 2008-06-03. Black open triangles represents measured values, red line modelled values.*

8.2.7 A case study for northerly winds (2010-05-01 to 2010-05-03)

Ozone concentrations over Sweden can be relatively high during springtime even when the air masses over Sweden have its origin from far northern latitudes. The causes behind these relatively high concentrations remain to a large extent unknown but hypotheses are intrusion from the stratosphere alternatively that high concentrations of ozone precursors are built up over the Arctic during wintertime and then transported to the south during spring. Ozone concentrations over Sweden can under these conditions exceed 50 ppb (Karlsson, IVL, unpublished). It is thus of interest to analyse if the MATCH model has the capability to simulate these relatively high ozone concentrations when there are northerly winds during spring. Such conditions prevailed over Sweden during the days of 2010-05-01 to 2010-05-03. Ozone

concentrations were very similar across the country (Figure 8.20). It should be noted that this case is not an ozone episode according to the definition used in our analysis (exceedance of 70ppb). The case is discussed here because of the interesting meteorological situation and because it provides another useful test for the performance of the MATCH model.

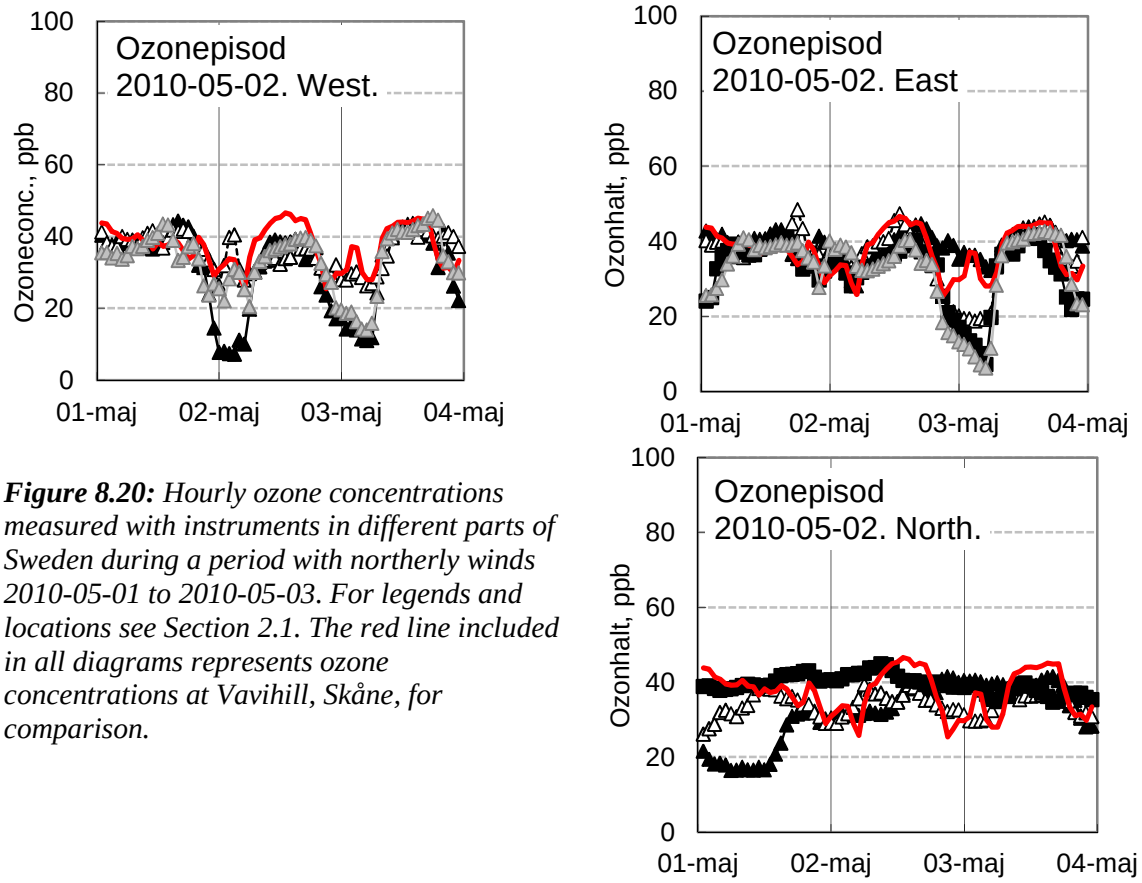

Figure 8.20: *Hourly ozone concentrations measured with instruments in different parts of Sweden during a period with northerly winds 2010-05-01 to 2010-05-03. For legends and locations see Section 2.1. The red line included in all diagrams represents ozone concentrations at Vavihill, Skåne, for comparison.*

Trajectory analysis made by NILU with the FLEXTRA model indicated that the air arriving at all sites across Sweden originated from far northern latitudes, except for Vavihill and Aspvreten which during the first day received air from the Atlantic across northern UK (Figure 8.21).

Vavihill 2010-05-01 18:00

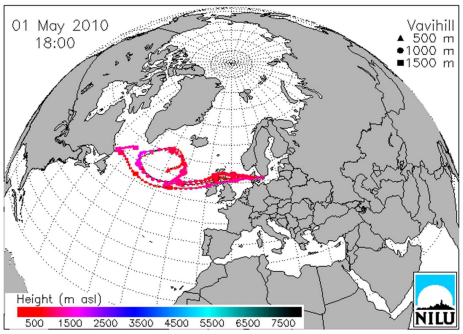

Vavihill 2010-05-03 18:00

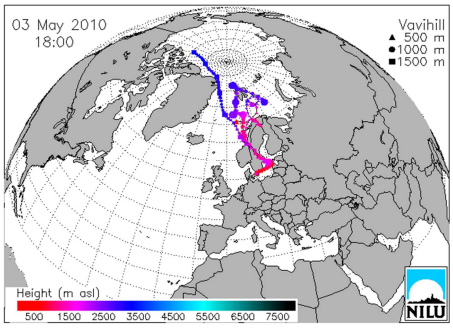

Råö 2010-05-01 18:00.

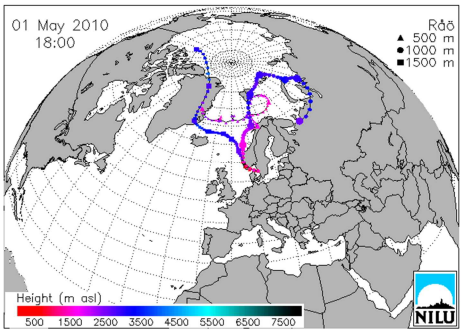

Råö 2010-05-03.

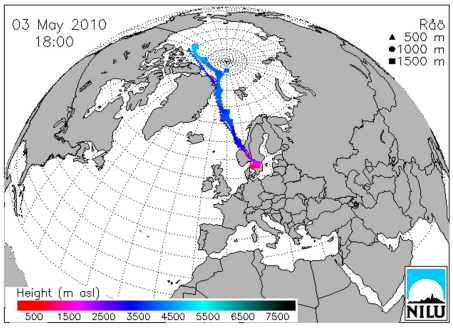

Aspvreten 2010-05-01 18:00.

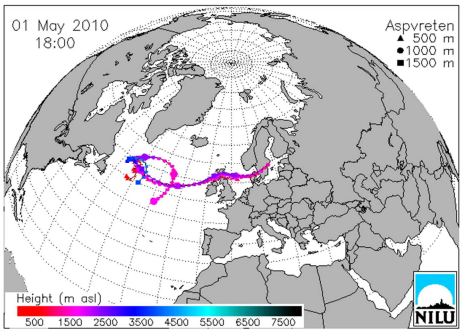

Aspvreten 2010-05-03.

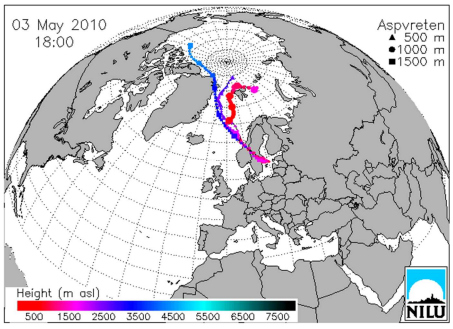

Vindeln 2010-05-01 18:00.

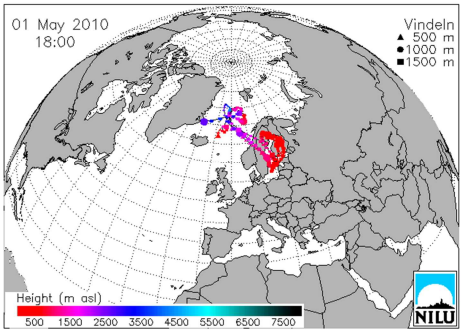

Vindeln 2010-05-03.

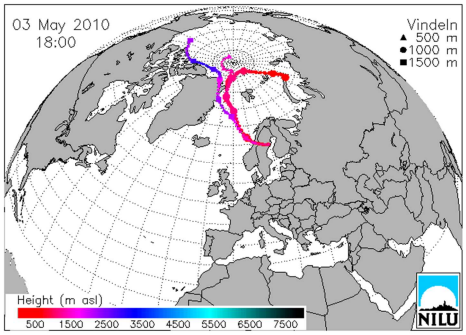

Figure 8.21: *Trajectories for air masses arriving at Vavihill, Råö, Aspvreten and Vindeln during the case of 2010-05-01 to 2010-05-03, as estimated with the FLEXTRA model available at NILU. The arrival time is indicated close to each diagram.*

The highest ozone concentration during this period with northern winds was measured at Grimsö in eastern Sweden (48 ppb) in the evening 2010-05-01. The highest ozone concentrations in the western part of southern Sweden and in northern Sweden were 47 ppb and 45 ppb, respectively (Table 8.12).

Table 8.12: *Highest ozone concentrations observed and modelled during the case study of 2010-05-01 to 2010-05-03.*

	West part of southern Sweden	East part of southern Sweden	Northern Sweden
Highest measured one-hour ozone concentration (ppb)	46.7	48.4	44.9
No of days with ozone concentrations >70 ppb			
Air pressure dynamics	Increase from 998 to 1012 mbar over three days		
Local weather	Sunny during days 2 and 3, low vind-speeds, dry air. Day air temp 12-14 C.		
Highest modelled one-hour ozone concentration (ppb)	49.5	46.6	45.6
Ratio modelled vs measured	1.06	0.96	1.02

The MATCH model performed well for this case. Thus the MATCH model seems to be able to simulate ozone concentrations over Sweden during these rather special conditions during spring. While MATCH captures only a part of the troposphere (see also Section 2.2) it is initialized with a climatological distribution of ozone, prescribing higher values at the upper boundary of the model domain, allowing for the simulation of vertical transport of ozone in analogy to the ozone transport encountered during stratospheric intrusions.

8.3 Additional material for the high-resolution simulation for 2010

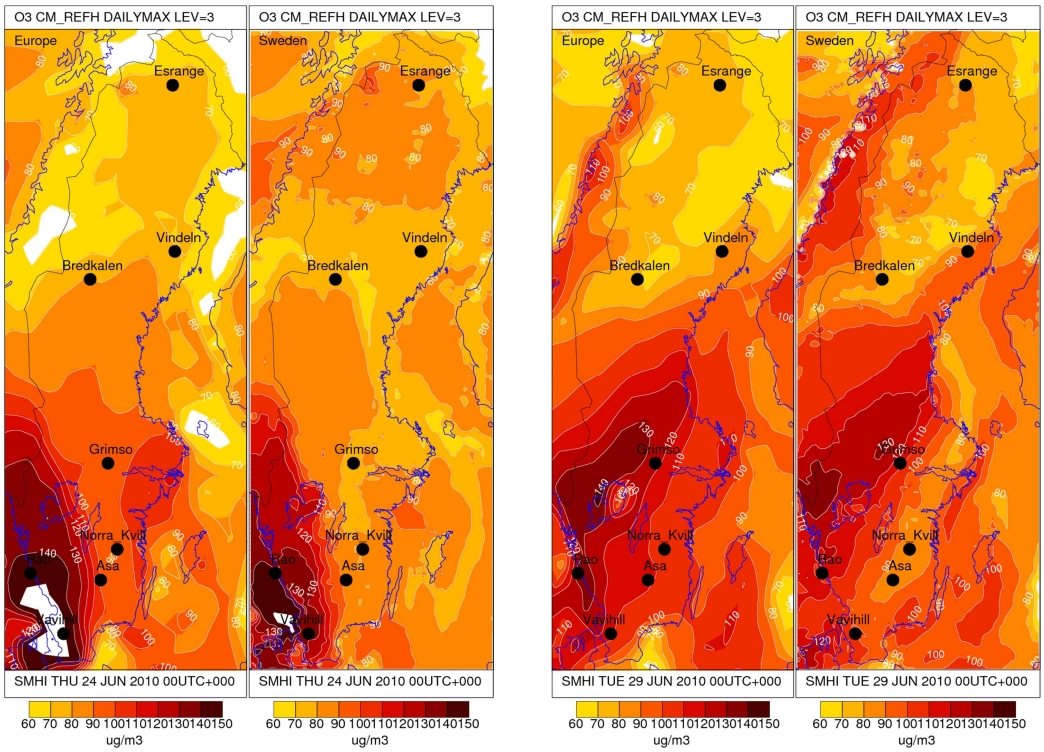

Figure 8.22: *Daily maximum near-surface ozone concentration in the European-scale (left panels) and high-resolution Swedish-scale (right panels) MATCH setup. Left pair is 24 June 2010; right pair is 29 June 2010.*

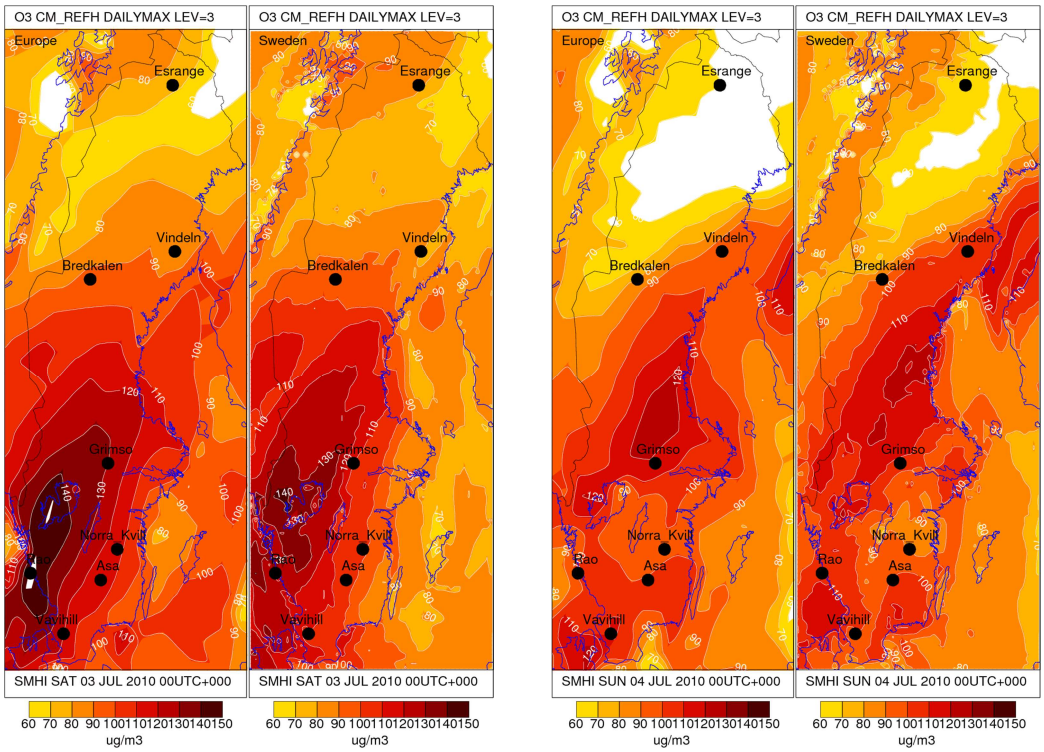

Figure 8.23: *Daily maximum near-surface ozone concentration in the European-scale (left panels) and high-resolution Swedish-scale (right panels) MATCH setup. Left pair is 3 July 2010; right pair is 4 July 2010.*

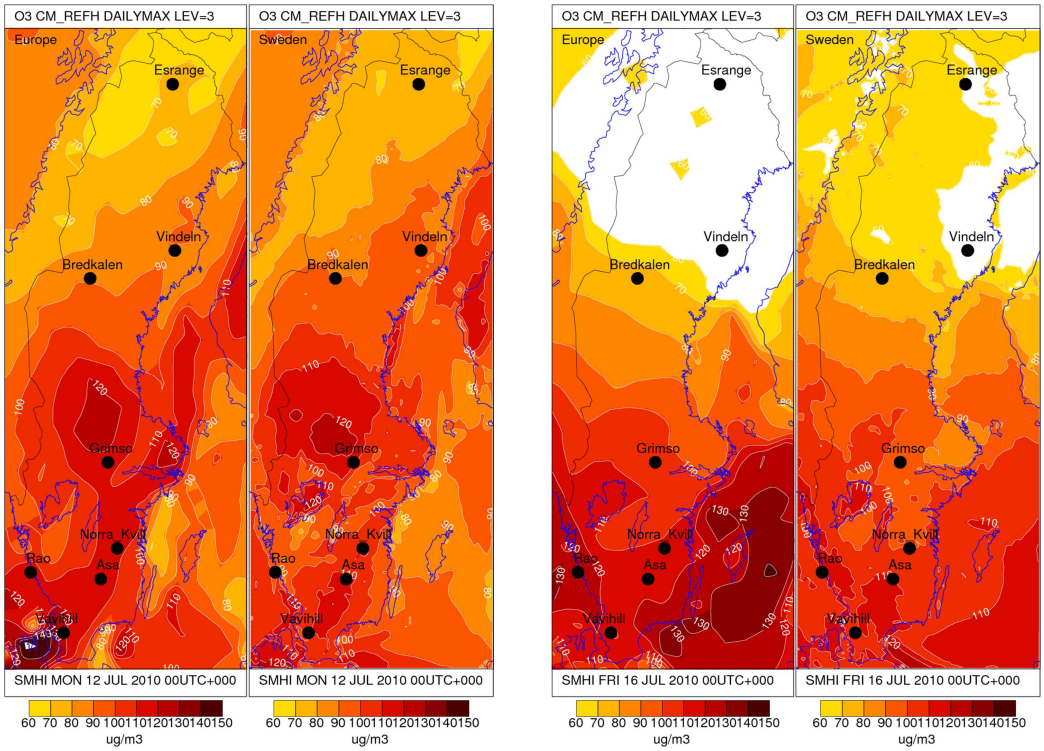

Figure 8.24: *Daily maximum near-surface ozone concentration in the European-scale (left panels) and high-resolution Swedish-scale (right panels) MATCH setup. Left pair is 12 July 2010; right pair is 16 July 2010.*

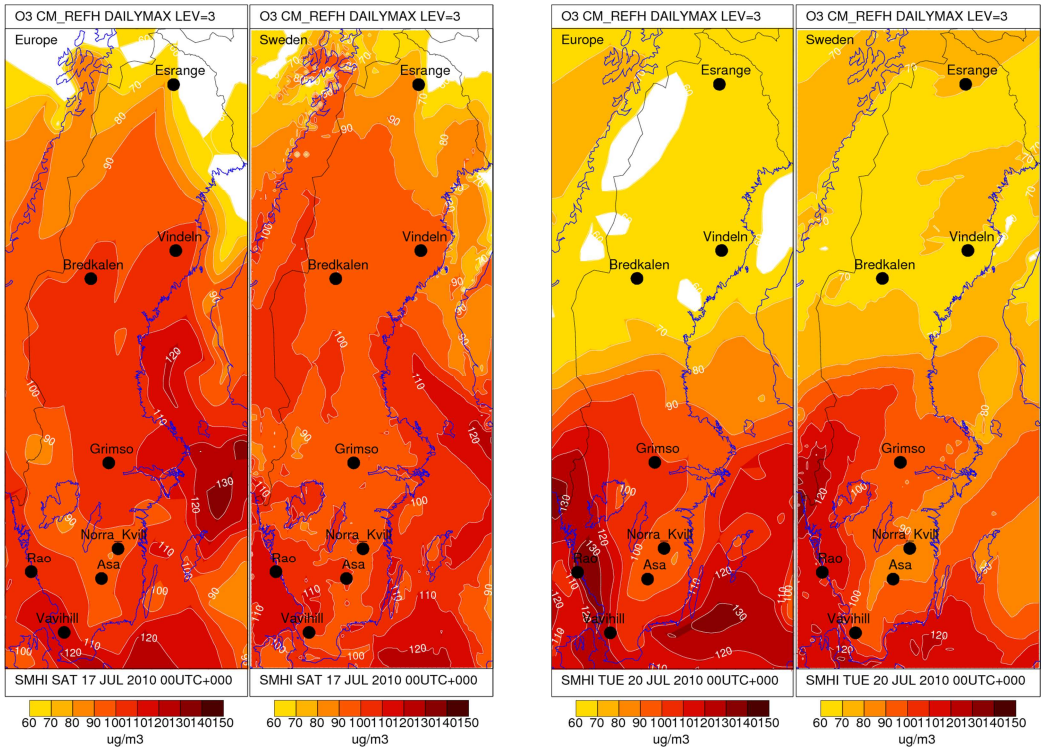

Figure 8.25: *Daily maximum near-surface ozone concentration in the European-scale (left panels) and high-resolution Swedish-scale (right panels) MATCH setup. Left pair is 17 July 2010; right pair is 20 July 2010.*

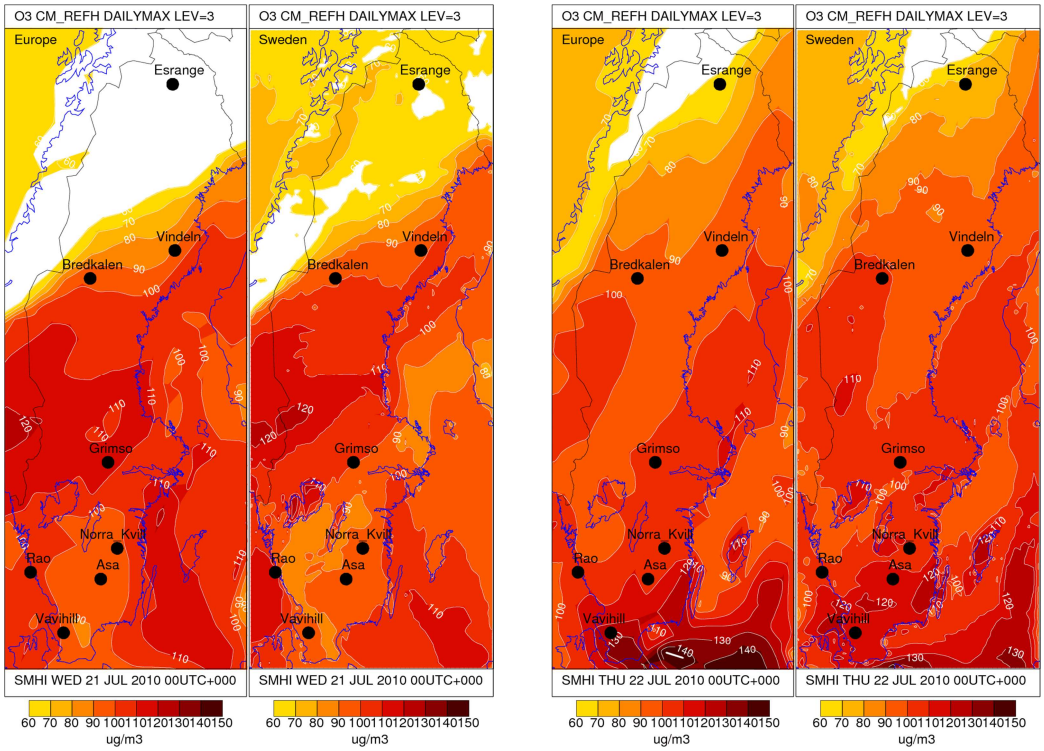

Figure 8.26: *Daily maximum near-surface ozone concentration in the European-scale (left panels) and high-resolution Swedish-scale (right panels) MATCH setup. Left pair is 21 July 2010; right pair is 22 July 2010.*

SMHI Publications

SMHI publishes seven report series. Three of these, the R-series, are intended for international readers and are in most cases written in English. For the others the Swedish language is used.

Name of the series	**Published since**
RMK (Report Meteorology and Climatology)	1974
RH (Report Hydrology)	1990
RO (Report Oceanography)	1986
METEOROLOGI	1985
HYDROLOGI	1985
OCEANOGRAFI	1985
KLIMATOLOGI	2009

Earlier issues published in serie RMK

1 Thompson, T., Udin, I. and Omstedt, A. (1974)
Sea surface temperatures in waters surrounding Sweden.

2 Bodin, S. (1974)
Development on an unsteady atmospheric boundary layer model.

3 Moen, L. (1975)
A multi-level quasi-geostrophic model for short range weather predictions.

4 Holmström, I. (1976)
Optimization of atmospheric models.

5 Collins, W.G. (1976)
A parameterization model for calculation of vertical fluxes of momentum due to terrain induced gravity waves.

6 Nyberg, A. (1976)
On transport of sulphur over the North Atlantic.

7 Lundqvist, J.-E. and Udin, I. (1977)
Ice accretion on ships with special emphasis on Baltic conditions.

8 Eriksson, B. (1977)
Den dagliga och årliga variationen av temperatur, fuktighet och vindhastighet vid några orter i Sverige.

9 Holmström, I., and Stokes, J. (1978)
Statistical forecasting of sea level changes in the Baltic.

10 Omstedt, A. and Sahlberg, J. (1978)
Some results from a joint Swedish-Finnish sea ice experiment, March, 1977.

11 Haag, T. (1978)
Byggnadsindustrins väderberoende, seminarieuppsats i företagsekonomi, B-nivå.

12 Eriksson, B. (1978)
Vegetationsperioden i Sverige beräknad från temperaturobservationer.

13 Bodin, S. (1979)
En numerisk prognosmodell för det atmosfäriska gränsskiktet, grundad på den turbulenta energiekvationen.

14 Eriksson, B. (1979)
Temperaturfluktuationer under senaste 100 åren.

15 Udin, I. och Mattisson, I. (1979)
Havsis- och snöinformation ur datorbearbetade satellitdata - en modellstudie.

16 Eriksson, B. (1979)
Statistisk analys av nederbördsdata. Del I. Arealnederbörd.

17 Eriksson, B. (1980)
Statistisk analys av nederbördsdata. Del II. Frekvensanalys av månadsnederbörd.

18 Eriksson, B. (1980)
Årsmedelvärden (1931-60) av nederbörd, avdunstning och avrinning.

19 Omstedt, A. (1980)
A sensitivity analysis of steady, free floating ice.

20 Persson, C. och Omstedt, G. (1980)
En modell för beräkning av luftföroreningars spridning och deposition på mesoskala.

21 Jansson, D. (1980)
Studier av temperaturinversioner och vertikal vindskjuvning vid Sundsvall-Härnösands flygplats.

22 Sahlberg, J. and Törnevik, H. (1980)
A study of large scale cooling in the Bay of Bothnia.

23 Ericson, K. and Hårsmar, P.-O. (1980)
Boundary layer measurements at Klockrike. Oct. 1977.

24 Bringfelt, B. (1980)
A comparison of forest evapotranspiration determined by some independent methods.

25 Bodin, S. and Fredriksson, U. (1980)
Uncertainty in wind forecasting for wind power networks.

26 Eriksson, B. (1980)
Graddagsstatistik för Sverige.

27 Eriksson, B.(1981)
Statistisk analys av nederbördsdata. Del III. 200-åriga nederbördsserier.

28 Eriksson, B. (1981)
Den "potentiella" evapotranspirationen i Sverige.

29 Pershagen, H. (1981)
Maximisnödjup i Sverige (perioden 1905-70).

30 Lönnqvist, O. (1981)
Nederbördsstatistik med praktiska tillämpningar.
(Precipitation statistics with practical applications.)

31 Melgarejo, J.W. (1981)
Similarity theory and resistance laws for the atmospheric boundary layer.

32 Liljas, E. (1981)
Analys av moln och nederbörd genom automatisk klassning av AVHRR-data.

33 Ericson, K. (1982)
Atmospheric boundary layer field experiment in Sweden 1980, GOTEX II, part I.

34 Schoeffler, P. (1982)
Dissipation, dispersion and stability of numerical schemes for advection and diffusion.

35 Undén, P. (1982)
The Swedish Limited Area Model. Part A. Formulation.

36 Bringfelt, B. (1982)
A forest evapotranspiration model using synoptic data.

37 Omstedt, G. (1982)
Spridning av luftförorening från skorsten i konvektiva gränsskikt.

38 Törnevik, H. (1982)
An aerobiological model for operational forecasts of pollen concentration in the air.

39 Eriksson, B. (1982)
Data rörande Sveriges temperaturklimat.

40 Omstedt, G. (1984)
An operational air pollution model using routine meteorological data.

41 Persson, C. and Funkquist, L. (1984)
Local scale plume model for nitrogen oxides. Model description.

42 Gollvik, S. (1984)
Estimation of orographic precipitation by dynamical interpretation of synoptic model data.

43 Lönnqvist, O. (1984)
Congression - A fast regression technique with a great number of functions of all predictors.

44 Laurin, S. (1984)
Population exposure to SO and NO_x from different sources in Stockholm.

45 Svensson, J. (1985)
Remote sensing of atmospheric temperature profiles by TIROS Operational Vertical Sounder.

46 Eriksson, B. (1986)
Nederbörds- och humiditetsklimat i Sverige under vegetationsperioden.

47 Taesler, R. (1986)
Köldperioden av olika längd och förekomst.

48 Wu Zengmao (1986)
Numerical study of lake-land breeze over Lake Vättern, Sweden.

49 Wu Zengmao (1986)
Numerical analysis of initialization procedure in a two-dimensional lake breeze model.

50 Persson, C. (1986)
Local scale plume model for nitrogen oxides. Verification.

51 Melgarejo, J.W. (1986)
An analytical model of the boundary layer above sloping terrain with an application to observations in Antarctica.

52 Bringfelt, B. (1986)
Test of a forest evapotranspiration model.

53 Josefsson, W. (1986)
Solar ultraviolet radiation in Sweden.

54 Dahlström, B. (1986)
Determination of areal precipitation for the Baltic Sea.

55 Persson, C., Rodhe, H. and De Geer, L.-E. (1986)
The Chernobyl accident - A meteorological analysis of how radionucleides reached Sweden.

56 Persson, C., Robertson, L., Grennfelt, P., Kindbom, K., Lövblad, G. och Svanberg, P.-A. (1987)
Luftföroreningsepisoden över södra Sverige 2 - 4 februari 1987.

57 Omstedt, G. (1988)
An operational air pollution model.

58 Alexandersson, H. and Eriksson, B. (1989)
Climate fluctuations in Sweden 1860 - 1987.

59 Eriksson, B. (1989)
Snödjupsförhållanden i Sverige - Säsongerna 1950/51 - 1979/80.

60 Omstedt, G. and Szegö, J. (1990)
Människors exponering för luftföroreningar.

61 Mueller, L., Robertson, L., Andersson, E. and Gustafsson, N. (1990)
Meso-γ scale objective analysis of near surface temperature, humidity and wind, and its application in air pollution modelling.

62 Andersson, T. and Mattisson, I. (1991)
A field test of thermometer screens.

63 Alexandersson, H., Gollvik, S. and Meuller, L. (1991)
An energy balance model for prediction of surface temperatures.

64 Alexandersson, H. and Dahlström, B. (1992)
Future climate in the Nordic region - survey and synthesis for the next century.

65 Persson, C., Langner, J. and Robertson, L. (1994)
Regional spridningsmodell för Göteborgs och Bohus, Hallands och Älvsborgs län. (A mesoscale air pollution dispersion model for the Swedish west-coast region. In Swedish with captions also in English.)

66 Karlsson, K.-G. (1994)
Satellite-estimated cloudiness from NOAA AVHRR data in the Nordic area during 1993.

67 Karlsson, K-G. (1996)
Cloud classifications with the SCANDIA model.

68 Persson, C. and Ullerstig, A. (1996)
Model calculations of dispersion of lindane over Europe. Pilot study with comparisons to easurements around the Baltic Sea and the Kattegat.

69 Langner, J., Persson, C., Robertson, L. and Ullerstig, A. (1996)
Air pollution Assessment Study Using the MATCH Modelling System. Application to sulfur and nitrogen compounds over Sweden 1994.

70 Robertson, L., Langner, J. and Engardt, M. (1996)
MATCH - Meso-scale Atmosperic Transport and Chemistry modelling system.

71 Josefsson, W. (1996)
Five years of solar UV-radiation monitoring in Sweden.

72 Persson, C., Ullerstig, A., Robertson, L., Kindbom, K. and Sjöberg, K. (1996)
The Swedish Precipitation Chemistry Network. Studies in network design using the MATCH modelling system and statistical methods.

73 Robertson, L. (1996)
Modelling of anthropogenic sulfur deposition to the African and South American continents.

74 Josefsson, W. (1996)
Solar UV-radiation monitoring 1996.

75 Häggmark, L. Ivarsson, K.-I. and Olofsson, P.-O. (1997)
MESAN - Mesoskalig analys.

76 Bringfelt, B., Backström, H., Kindell, S., Omstedt, G., Persson, C. and Ullerstig, A. (1997)
Calculations of PM-10 concentrations in Swedish cities- Modelling of inhalable particles

77 Gollvik, S. (1997)
The Teleflood project, estimation of precipitation over drainage basins.

78 Persson, C. and Ullerstig, A. (1997)
Regional luftmiljöanalys för Västmanlands län baserad på MATCH modell-beräkningar och mätdata - Analys av 1994 års data

79 Josefsson, W. and Karlsson, J.-E. (1997)
Measurements of total ozone 1994-1996.

80 Rummukainen, M. (1997)
Methods for statistical downscaling of GCM simulations.

81 Persson, T. (1997)
Solar irradiance modelling using satellite retrieved cloudiness - A pilot study

82 Langner, J., Bergström, R. and Pleijel, K. (1998)
European scale modelling of sulfur, oxidized nitrogen and photochemical oxidants. Model development and evaluation for the 1994 growing season.

83 Rummukainen, M., Räisänen, J., Ullerstig, A., Bringfelt, B., Hansson, U., Graham, P. and Willén, U. (1998)
RCA - Rossby Centre regional Atmospheric climate model: model description and results from the first multi-year simulation.

84 Räisänen, J. and Döscher, R. (1998)
Simulation of present-day climate in Northen Europé in the HadCM2 OAGCM.

85 Räisänen, J., Rummukainen, M., Ullerstig, A., Bringfelt, B., Hansson, U. and Willén, U. (1999)
The First Rossby Centre Regional Climate Scenario - Dynamical Downscaling of CO_2-induced Climate Change in the HadCM2 GCM.

86 Rummukainen, M. (1999)
On the Climate Change debate

87 Räisänen, J. (2000)
CO_2-induced climate change in northern Europé: comparison of 12 CMIP2 experiments.

88 Engardt, M. (2000)
Sulphur simulations for East Asia using the MATCH model with meteorological data from ECMWF.

89 Persson, T. (2000)
Measurements of Solar Radiation in Sweden 1983-1998

90 Michelson, D. B., Andersson, T., Koistinen, J., Collier, C. G., Riedl, J., Szturc, J., Gjertsen, U., Nielsen, A. and Overgaard, S., (2000)
BALTEX Radar Data Centre Products and their Methodologies

91 Josefsson, W. (2000)
Measurements of total ozone 1997 – 1999

92 Andersson, T. (2000)
Boundary clear air echos in southern Sweden

93 Andersson, T. (2000)
Using the Sun to check some weather radar parameters

94 Rummukainen, M., Bergström, S., Källén, E., Moen, L., Rodhe, J. and Tjernström, M. (2000)
SWECLIM – The First Three Years

95 Meier, H. E. M. (2001)
The first Rossby Centre regional climate scenario for the Baltic Sea using a 3D coupled ice-ocean model

96 Landelius, T., Josefsson, W. and Persson, T. (2001)
A system for modelling solar radiation parameters with mesoscale spatial resolution

97 Karlsson, K.-G. (2001)
A NOAA AVHRR cloud climatology over Scandinavia covering the period 1991-2000

98 Bringfelt, B., Räisänen, J., Gollvik, S., Lindström, G., Graham, P. and Ullerstig, A., (2001)
The land surface treatment for the Rossby Centre Regional Atmospheric Climate Model - version 2 (RCA2)

99 Kauker, F. and Meier, H. E. M., (2002)
Reconstructing atmospheric surface data for the period 1902-1998 to force a coupled
ocean-sea ice model of the Baltic Sea.

100 Klein, T., Bergström, R. and Persson, C. (2002)
Parameterization of dry deposition in MATCH

101 Räisänen, J., Hansson, U., Ullerstig A., Döscher, R., Graham, L. P., Jones, C., Meier, M., Samuelsson, P.and Willén, U. (2003)
GCM driven simulations of recent and future climate with the Rossby Centre coupled atmosphere - Baltic Sea regional climate model RCAO

102 Tjernström, M., Rummukainen, M., Bergström, S., Rodhe, J. och Persson, G., (2003)
Klimatmodellering och klimatscenarier ur SWECLIMs perspektiv.

103 Segersson, D. (2003)
Numerical Quantification of Driving Rain on Buildings

104 Rummukainen, M. and the SWECLIM participants (2003)
The Swedish regional climate modeling program 1996-2003. Final report.

105 Robertson, L. (2004)
Extended back-trajectories by means of adjoint equations

106 Rummukainen, M., Bergström S., Persson G., Ressner, E (2005)
Anpassningar till klimatförändringar

107 Will not be published

108 Kjellström, E., Bärring, L., Gollvik, S., Hansson, U., Jones, C., Samuelsson, P., Rummukainen, M., Ullerstig, A., Willén, U., Wyser, K., (2005)
A 140-year simulation of European climate with the new version of the Rossby Centre regional atmospheric climate model (RCA3).

109 Meier, H.E.M., Andréasson, J., Broman, B., Graham, L. P., Kjellström, E., Persson, G., and Viehhauser, M., (2006)
Climate change scenario simulations of wind, sea level, and river discharge in the Baltic Sea and Lake Mälaren region – a dynamical downscaling approach from global to local scales.

110 Wyser, K., Rummukainen, M., Strandberg, G., (2006)
Nordic regionalisation of a greenhouse-gas stabilisation scenario

111 Persson, G., Bärring, L., Kjellström, E., Strandberg G., Rummukainen, M., (2007).
Climate indices for vulnerability assessments

112 Jansson, A., Persson, Ch., Strandberg, G., (2007)
2D meso-scale re-analysis of precipitation, temperature and wind over Europe - ERAMESAN

113 Lind, P., Kjellström, E., (2008)
Temperature and Precipitation changes in Sweden; a wide range of model-based projections for the 21st century

Empty page

SMHI

Swedish Meteorological and Hydrological Institute
SE 601 76 NORRKÖPING
Phone +46 11-495 80 00 Telefax +46 11-495 80 01

ISSN 0347-2116